How periosteum is involved in long bone growth

Please check the document version of this publication:

• A submitted manuscript is the version of the article upon submission and before peer-review. There can be important differences between the submitted version and the official published version of record. People interested in the research are advised to contact the author for the final version of the publication, or visit the DOI to the publisher's website.
• The final author version and the galley proof are versions of the publication after peer review.
• The final published version features the final layout of the paper including the volume, issue and page numbers.

Link to publication

How Periosteum

is Involved in

Long Bone Growth

How Periosteum

is Involved in

Long Bone Growth

PROEFSCHRIFT

ter verkrijging van de graad van doctor aan de
Technische Universiteit Eindhoven, op gezag van de
rector magnificus, prof.dr.ir. C.J. van Duijn, voor een
commissie aangewezen door het College voor
Promoties in het openbaar te verdedigen
op woensdag 16 december 2009 om 16.00 uur

door

Jasper Foolen

geboren te Vught

Dit proefschrift is goedgekeurd door de promotoren:

prof.dr.ir. K. Ito
en
prof.dr.ir. H.W.J. Huiskes

Copromotor:
dr. C.C. van Donkelaar

Summary

How periosteum is involved in long bone growth

Skeletal growth is a tightly controlled phenomenon. In general, it is difficult to correct for skeletal malformations that develop during growth. One of the tissues that is proposed to be of major importance in regulating long bone growth is the periosteum. Previously, it was proposed that periosteum regulates growth via a direct mechanical feedback mechanism where pressure in growing cartilage, balanced by tension in the periosteum, modulates growth processes of chondrocytes. The presence of this tension is attributed to the periosteal collagen. We support the existence of a load-dependent feedback mechanism between cartilage pressure and periosteum tension by showing that the global orientation of collagen in perichondrium and periosteum concurs with the assessed growth directions of cartilage. Nevertheless, the absolute magnitude of periosteum tension determines the extent to which regulation by this mechanical feedback mechanism is present. From measurements described in this thesis, it is concluded that residual periosteum force does not directly dominate modulation of cartilage growth. Hence, a mechano-biological feedback mechanism must prevail. We demonstrate this mechano-biological feedback mechanism between growing cartilage and tension in the periosteum, whereby the expression of soluble growth-inhibiting factors by periosteum cells is dependent on intracellular tension. Because cartilage growth lengthens the periosteum at a very high rate, a mechanism of fibrous tissue adaptation that preserves low periosteum tension is required. We show that this mechanism is through adaptation towards a state of equilibrium, characterized by a residual tissue strain that corresponds to the strain in between the pliant and stiffer region of the force-strain curve. This process is cell-mediated and involves a structural reorganization of the collagen network, determining tissue stiffness, which is not directly coupled to collagen content or HP crosslink density. This thesis takes us closer towards understanding the regulation of bone growth, by not only demonstrating the critical involvement of the periosteum, but also by exposing mechanisms for the interaction between periosteum and growing cartilage, and for periosteum adaptation.

VI

Contents

VIII

Chapter 1

General Introduction

Long bones are the supporting structures of the skeleton. A developing long bone consists of a diaphysis, metaphyses, and epiphyses (figure 1.1). These regions develop during the embryonic stage and go through proportional changes in size until skeletal maturity (Forriol and Shapiro, 2005). During early growth, the bone extremities are composed of cartilage where the diaphysis is mainly composed of a mineralized bone shaft. The epiphyses are responsible for the transverse and spherical growth of the bone extremities and the shaping of the articular surfaces (Forriol and Shapiro, 2005).
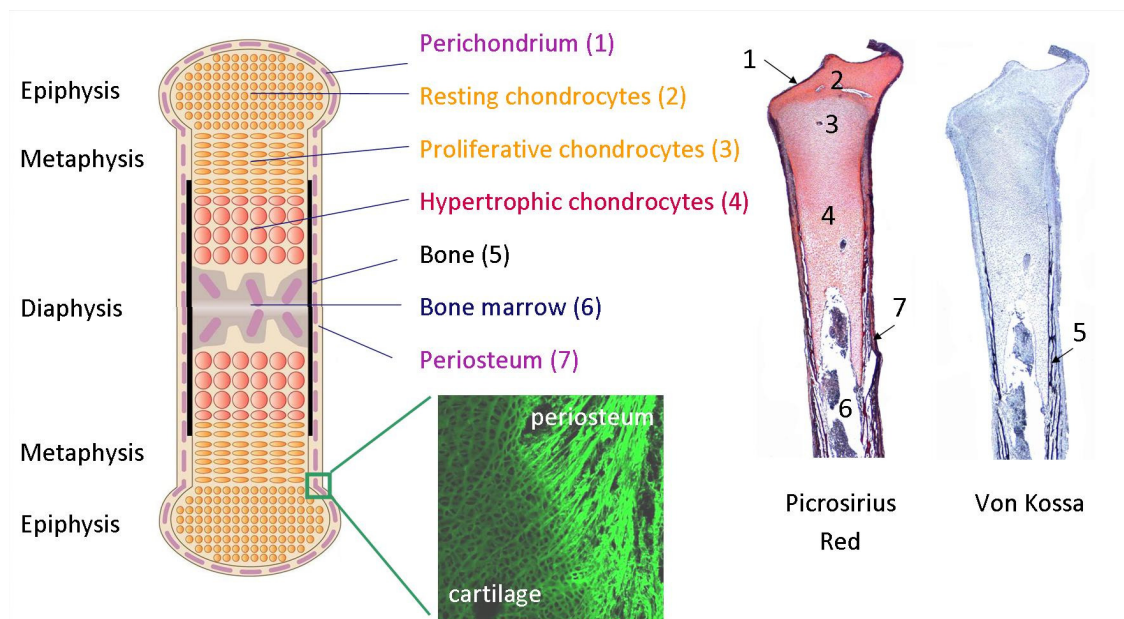
Figure 1.1: On the left, a schematic representation of the structure of a long bone. Image adapted from Kronenberg (Kronenberg, 2003). The fluorescent microscopy image represents the attachment of the periosteum collagen fibers to the cartilage of the epiphyseal base (origin of the image is indicated with a green square in the left image). On the right, histology of the tibiotarsus of an e13 chick embryo, in which the different tissue types are indicated.

Longitudinal growth predominantly results from chondrocytic proliferation and hypertrophy in the metaphyses (Noonan et al., 1998). The diaphysis and metaphyses of long bones are surrounded by periosteum, a fibrous tissue that spans the bone extremities. It attaches to the epiphyseal base, beyond the proliferating metaphyseal cartilage (figure 1.1). Periosteum increases radial growth of the diaphysis and parts of the metaphyses by direct apposition of cortical bone (Forriol and Shapiro, 2005).

Perichondrium surrounds the epiphyseal cartilage and increases cartilage transverse diameter by interstitial growth (Shapiro et al., 1977). Both the periosteum and perichondrium are composed of an inner cambium layer, involved in the apposition of new tissue and biochemical regulation of growth processes (Alvarez et al., 2002; Kronenberg, 2003); and a fibrous outer layer, associated with mechanical modulation of cartilage growth (Crilly, 1972; Forriol and Shapiro, 2005; Moss, 1972).

Periosteum is proposed to interfere with a mechanical feedback mechanism that exists between pressure in growing cartilage and tension in the periosteum (Crilly, 1972; Moss, 1972) (figure 1.2). Extracellular matrix formation, and chondrocytic proliferation and hypertrophy in the growth plate result in elongation of the bone and movement of the epiphysis away from the mid-diaphysis, thereby stretching and thus tensioning the periosteum. Consequently, growth plate cartilage is statically compressed, which is known to inhibit chondrocyte activity. Triggered by the tensioning, periosteum cells synthesize matrix allowing the periosteum to grow, whereby the compressive force on the cartilage is released and further bone lengthening becomes possible.

The hypothesis of a mechanical feedback mechanism is supported by the observation that extracellular matrix production, and chondrocytic proliferation and hypertrophy are stimulated by mechanical tension and retarded by compression (Bonnel et al., 1983; Stokes et al., 2006; Stokes et al., 2007). Morphogenesis of developing long bones may therefore be influenced by tensile and compressive forces exerted on cartilage via insertion of periosteum, tendons, ligaments and muscle contractions (Henderson and Carter, 2002), in combination with localized variations in mechanical restraint of perichondrium (Wolpert, 1981).

The potential of growth modulation by the perichondrium and periosteum was shown both *in vitro* and *in vivo* in different species. Removal of the perichondrium from a stage 32 chick ulna *in vitro* results in an overall increase in rudiment length (Rooney and Archer, 1992), proposed to be a direct effect of the elimination of mechanical perichondrium restraint (Henderson and Carter, 2002). Cutting the perichondrium in an arbitrary direction results in protrusions containing typical cartilage cells (Wolpert, 1981). Circumferentially cutting the periosteum or completely stripping the tissue

results in increased longitudinal growth rates (Bertram et al., 1991; Chan and Hodgson, 1970; Crilly, 1972; Dimitriou et al., 1988; Hernandez et al., 1995; Houghton and Rooker, 1979; Jenkins et al., 1975; Lynch and Taylor, 1987; Sola et al., 1963; Taillard, 1959; Taylor et al., 1987; Warrell and Taylor, 1979; Wilde and Baker, 1987). Contrary, longitudinal incision of the periosteum has no effect on growth (Crilly, 1972; Dimitriou et al., 1988; Houghton and Rooker, 1979; Warrell and Taylor, 1979). Therefore, it is likely that a structural component with morphological anisotropy, such as collagen, is responsible for the modulation of growth.
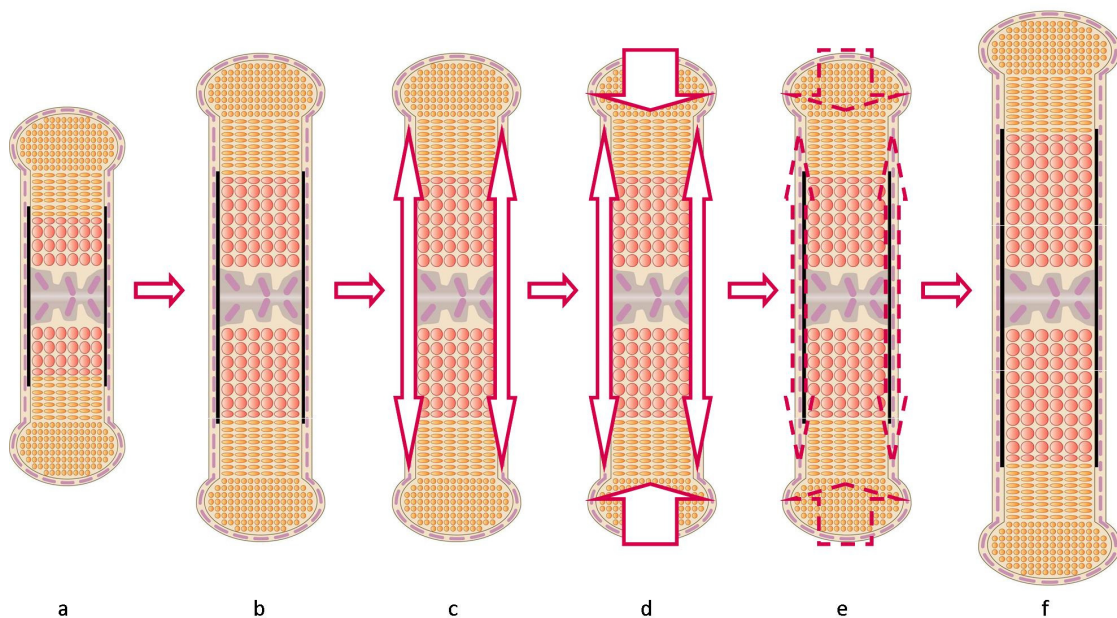
Figure 1.2: Proposed mechanical feedback mechanism that exists between pressure in growing cartilage and tension in the periosteum (Crilly, 1972; Moss, 1972). (a) to (b) Extracellular matrix formation, and chondrocytic proliferation and hypertrophy in the growth plate are postulated to result in movement of the epiphyses away from the mid-diaphysis, (c) thereby stretching and thus tensioning the periosteum. (d) Consequently, growth plate cartilage is statically compressed, which inhibits chondrocyte activity. (e) Triggered by the tensioning, periosteum cells synthesize matrix allowing the periosteum to grow, whereby the compressive force on the cartilage is released and (f) further bone lengthening becomes possible. Image adapted from Kronenberg (Kronenberg, 2003).

Consider the case where perichondrium and periosteum forces are substantial enough to modulate cartilage growth mechanically. Then, the direction of increased growth upon disruption of perichondrium or periosteum is expected to coincide with the

direction in which the tissue is stiffest, i.e. with the orientation of collagen. Hence, for a load-dependent feedback mechanism to exist between the growing cartilage and perichondrium and/or periosteum, their global collagen orientation should match long bone growth directions (this thesis: chapter 2). As longitudinal bone growth is only affected upon circumferential division, and not upon longitudinal incision of the periosteum (Crilly, 1972; Warrell and Taylor, 1979), the periosteal collagen network is expected to be primarily in the longitudinal direction. Perichondrium however, is expected to contain a random organization of collagen fibers, as developing protrusions were observed after incision in an arbitrary direction (Wolpert, 1981). Demonstrating these relationships is a first step in validating the concept that a load-dependent feedback mechanism prevails between different tissue types in growing bones.

The hypothesis by both Moss (Moss, 1972) and Crilly (Crilly, 1972), states that cartilage expansion results in moving the epiphyses away from the mid-diaphysis. Thereby, periosteum tension is induced that compresses the growing cartilage, which decreases cartilage growth rates. Indeed compressive stresses have been shown to decrease cartilage growth rates (Bonnel et al., 1983; Stokes et al., 2005; Wilson-MacDonald et al., 1990). The linear relationship found between cartilage growth rate and imposed stress (Bonnel et al., 1983; Stokes et al., 2006) implies that that any residual periosteum tension, present during long bone development, modulates cartilage growth rates. However, the magnitude of periosteum tension determines the extent to which regulation by this mechanical feedback mechanism, hypothesized by both Moss (Moss, 1972) and Crilly (Crilly, 1972), is present. More specifically, the increase in cartilage growth rate measured upon circumferential periosteum cutting should be equivalent to the amount of cartilage growth rate suppression, originating from compressive stresses induced by periosteum tension (this thesis: chapter 3). If periosteum tension is high enough to explain the magnitude of increased growth rates upon circumferential periosteum cutting, it is likely that periosteum growth is a key regulator of longitudinal long bone growth. However, if periosteum force is too low to decrease cartilage growth rates, it seems plausible that cartilage expansion triggers periosteum growth. The latter postulate is supported by the observation that periosteum in adolescent chicks is loaded even below its elastic region *in vivo* (Bertram et al., 1991).

If low periosteum tension is preserved, while cartilage growth lengthens the periosteum at a very high rate, a fast tissue adaptation mechanism is required (this thesis: chapter 5). As periosteum growth is homogenous over its complete length (Warwick and Wiles, 1934) and adhesion properties to the underlying bone in the diaphyseal region are absent (Bertram et al., 1998), the adaptive response likely applies to the periosteum tissue as a whole. In search of an adaptation mechanism of periosteum and fibrous tissues in general, the embedded contractile cells appear to play a crucial role. Tensional homeostasis is driving these cells to increase contraction upon decreased external loading, and reduce contraction upon increased external loading (Brown et al., 1998; Petroll et al., 2004; Tomasek et al., 1992). This property is essential for the ability of fibrous tissues to adapt to their mechanical environment (Bell et al., 1979; Eastwood et al., 1996; Grinnell and Lamke, 1984; Guidry and Grinnell, 1985).

This tensional homeostasis of contractile cells has been shown to be involved in fibrous tissue adaptation. Increased tissue load is dissipated via cell-mediated active translation and reorientation of existing collagen fibers with respect to each other and the (proteoglycan) matrix they are embedded in (Brown et al., 1998; Grinnell and Lamke, 1984; Guidry and Grinnell, 1985; Harris et al., 1981; Meshel et al., 2005; Sawhney and Howard, 2002; Stopak and Harris, 1982). Furthermore, dissipation of increased load results from viscous properties of collagen fibers and reorientation of these fibers in their matrix (Puxkandl et al., 2002; Sawhney and Howard, 2002). Additional collagen is synthesized and dispersed in the matrix by the cells, in a load-dependent manner (Curwin et al., 1988; Kim et al., 2002; Parsons et al., 1999; Wang et al., 2003; Yang et al., 2004), to meet the new demands.

Decreased tissue strain is restored via cell-mediated tissue contraction (Brown et al., 1998; Petroll et al., 2004; Tomasek et al., 1992), preferential cleavage of unstrained fibers (Ellsmere et al., 1999; Huang and Yannas, 1977; Nabeshima et al., 1996; Ruberti and Hallab, 2005), and tissue compaction via the presence of residual strain (Bertram et al., 1998; Popowics et al., 2002).

The adverse response of fibrous tissues to imposed load suggests that adaptation of periosteum, and likely fibrous tissues in general, might therefore be driven towards specific load equilibrium (this thesis: chapter 5). If such equilibrium is found, more

insight would be gained in the adaptation mechanism of fibrous tissues upon changes in applied load.

The question that emerges when periosteum tension is not the dominant mechanism for the modulation of cartilage, obviously is: 'then what is?' (this thesis: chapter 4). In absence of a direct mechanical effect, biochemical pathways might be involved. It has been shown that a large amount of growth factors from perichondrium and periosteum can modulate growth plate behavior (Alvarez et al., 2001; Alvarez et al., 2002; Hinoi et al., 2006; Kronenberg, 2003; Long and Linsenmayer, 1998; Serra et al., 1999; Simon et al., 2003). More specifically, increased growth after periosteum stripping can be counteracted precisely when the correct concentration of TGF-β1 is supplied to the medium (Crochiere et al., 2008). Also, extended growth upon periosteum removal could be counteracted when conditioned medium was added either from a mixed population of cells from perichondrium and periosteum or from cells at the border region of periosteum and perichondrium (Di Nino et al., 2001). Not surprisingly, the border region of perichondrium and periosteum covers the growing cartilage in which chondrocytes proliferate and differentiate into hypertrophic cells. This can explain how increased growth, observed after periosteum removal (Hernandez et al., 1995; Jenkins et al., 1975; Lynch and Taylor, 1987; Warrell and Taylor, 1979), is regulated. However, increased growth is also observed after circumferential periosteum cutting (Bertram et al., 1991; Crilly, 1972; Lynch and Taylor, 1987; Warrell and Taylor, 1979), when the cells are not removed. It can therefore be questioned if decreased intracellular tension in periosteum cells is the key mechanism in the modulation of longitudinal bone growth? Presence of intracellular tension might regulate production of a specific growth factor pool, in a mechanobiological manner. The ability of cells to generate intracellular tension is dependent on the properties of the substrate, on which they are cultured. Cells cultured on stiff substrates generally display more spreading (Engler et al., 2004), express more focal adhesions (Engler et al., 2006), and contain a more developed actin filament network (Discher et al., 2005; Engler et al., 2004; Engler et al., 2006; Schwarz and Bischofs, 2005). Expression of the actin filament network has been qualitatively related to generation of force (Nekouzadeh et al., 2008). It should be noted that conditioned medium in the study by Di Nino and coworkers (Di Nino et al., 2001) originates from cells cultured on well plates, i.e. stiff substrates on which the cells are

able to attach and generate intracellular tension. Culturing these cells on substrates with lower stiffness might result in an altered potential to modulate bone growth (this thesis: chapter 4). If intracellular tension is the key regulator, the underlying mechanobiological pathway could be exposed and responsible growth factors identified.

This introduction has highlighted questions, which will be dealt with in the following chapters of this thesis.

Chapter 2:   Does periosteum and perichondrium fiber orientation match directions of growth?

Chapter 3:   Can periosteum tension create stresses in embryonic chick cartilage of the magnitude demonstrated to have a direct effect on cartilage growth?

Chapter 4:   Does the magnitude of intracellular tension in perichondrium and periosteum regulate cartilage growth?

Chapter 5:   Does a growing fibrous tissue attain a specific mechanical state and is that equilibrium restored upon disturbance via cell-mediated adaptive processes?

Answering these questions will result in a more comprehensive insight in the way bone morphogenesis is regulated, and how the periosteum is involved in this process. This thesis attempts to fill these knowledge gaps and discuss the future prospective related to our understanding of long bone growth regulation.

Chapter 2

Collagen Orientation in Periosteum and Perichondrium is Aligned With Predominant Directions of Tissue Growth

2.1 Abstract

A feedback mechanism between different tissues in a growing bone is hypothesized to determine the bone's morphogenesis. Cartilage growth strains the surrounding tissues, eliciting alterations of its matrix, which in turn, creates anisotropic stresses, guiding directionality of cartilage growth. The purpose of this study was to evaluate this hypothesis by determining whether collagen fiber directions in the perichondrium and periosteum align with the predominant directions of long bone growth. Tibiotarsi from chick embryos across developmental stages were scanned using optical projection tomography to assess predominant directions of growth at characteristic sites in perichondrium and periosteum. Quantified morphometric data were compared with multiphoton microscopy images of the three-dimensional collagen network in these fibrous tissues. The diaphyseal periosteum contained longitudinally oriented collagen fibers that aligned with the predominant growth direction. Longitudinal growth at both metaphyses was twice the circumferential growth. This concurred with well-developed circumferential fibers, which covered and were partly interwoven with a dominant network of longitudinally oriented fibers in the outer layer of the perichondrium/periosteum at the metaphysis. Toward both articulations, the collagen network of the epiphyseal surface was randomly oriented, and growth was approximately biaxial. These findings support the hypothesis that the anisotropic architecture of the collagen network, detected in periosteum and perichondrium, concurs with the assessed growth directions.

2.2 Introduction

Morphogenesis of developing long bones is the result of cartilage growth. The growing bone is enclosed by the perichondrium in the epiphyses and by the periosteum in metaphyses and diaphysis. The anisotropy in growth, determining its shape, is believed to be due to the influence of the surrounding tissues, which continuously adapt to the changing mechanical environment. This concept was formulated in the so-called 'direction dilation' theory (Wolpert, 1981) according to which bone morphogenesis results from the combination of pressure-induced tissue dilation and spatial variations in the resistance against deformation. Ample evidence exists to support this theory. In developing porcine femora, radial expansion only occurs until a perichondrium is formed. From this point longitudinal elongation predominates (Carey, 1922). In embryonic chicks, the best organized perichondrium is co-localized with the narrowest parts of the developing bone (Rooney and Archer, 1992). Disruption of the epiphyseal perichondrium by incision or collagenase treatment results in the development of small protrusions and increased epiphyseal width, respectively (Rooney, 1984; Wolpert, 1981). The 'direction dilation' theory also seems applicable to the periosteum, which spans the metaphyseal and diaphyseal cartilage. Circumferentially cutting the periosteum, just below the epiphysis, enhances longitudinal growth (Crilly, 1972; Rooney and Archer, 1992) and reduces the force (by 80%) needed for epiphysiolysis (Shapiro, 2001). Likewise, a hemi-circumferential cut induces longitudinal overgrowth at the incised side (Dimitriou et al., 1988).

During growth, the volume of cartilage increases, resulting in 'growth-generated strains and stresses' in the enclosing tissues (Henderson and Carter, 2002). Hence, the cells and extracellular matrix of the perichondrium and periosteum are strained. In turn, because of this external restraint to epiphyseal growth by perichondrium and periosteum, hydrostatic pressure is maintained in the epiphyseal cartilage. Hydrostatic pressure is known to modulate the development of cartilage, through stimulation or inhibition of proliferation and proteoglycan synthesis, depending on the nature of the pressure (Hall et al., 1991; Hansen et al., 2001; Parkkinen et al., 1993).

If the enclosing tissues would not adapt to the elongation during growth, they would be elongated beyond failure strain. Hence, to allow growth, adaptation of the collagen network in the enclosing tissues is required. The mechanical environment controls fibrous tissue remodeling by regulating the expression and synthesis of collagen (Kim et al., 2002; Parsons et al., 1999; Yang et al., 2004), the production of proteases (Prajapati et al., 2000), and the alignment of cells and collagen parallel to the strain direction (Henshaw et al., 2006). Additionally, the susceptibility of collagen fibers to enzymatic degradation by collagenase is strain-dependent. At an optimal stretch of 4%, collagen degradation is minimized (Huang and Yannas, 1977). The diffusion rate of collagenase is not significantly different in 4% strained samples, compared to unloaded controls. Therefore, it is suggested that the degradation pattern depends on altered kinetics of the collagenase-matrix interaction (Nabeshima et al., 1996). In favor of this suggestion, it is found that collagen fibrils, perpendicular to the direction of tensile loading, degrade more easily compared to fibrils aligned with the loading direction. This phenomenon is called 'strain-stabilization' (Ruberti and Hallab, 2005). The direction of the load can therefore influence the anisotropy of a collagen network by synthesizing new collagen and degrading existing collagen in a strain-dependent manner. Hereby, a tissue adapts its mechanical properties to the load it experiences (Feng et al., 2006b).

These mechanisms can explain the alignment of collagen to the direction in which a tissue is strained, which is known to occur in dynamically loaded fibrous tissues. However, it is unknown whether the quasi-static growth-generated strain can also modulate the direction of a collagen network. Hence, our aims were to determine the three-dimensional collagen orientation in periosteum and perichondrium of embryonic chick tibiotarsi from developmental stages 39 to 40, and to determine whether they are aligned with the directions of growth from stage 38 to 41. This is the first step in validating the concept that a load-dependent feedback mechanism prevails between periosteum and growing cartilage.

2.3 Materials and methods

2.3.1 Animals

Fertilized eggs of White Leghorn chickens ('t Anker, Ochten, The Netherlands) were placed in a polyhatch incubator (Brisnea, Sandfort, UK). After a 12 to 15 day period of incubation, chick embryos were removed from the eggs and euthanized by decapitation. This incubation period corresponded to embryos ranging from Hamburger and Hamilton stage 38 to 41 (Hamburger and Hamilton, 1992). Tibiotarsi were carefully dissected, without damaging periosteum or perichondrium.

2.3.2 Growth by Optical Projection Tomography

For whole-mount staining, 28 chick tibiotarsi from embryonic day e12 to e15 were fixed immediately upon dissection in 95% ethanol for 4 days at 4^0C. The tissue was cleared in 1% potassium hydroxide and stained for 8 hours with 0.1 % Alcian Blue (Sigma, St. Louis, MO, USA) for cartilage and for 3 hours with 0.014 % Alizarin Red (Fluka, USA) for bone, consecutively. After staining, the tissue was embedded in 1% low melting point agarose (Invitrogen, Breda, The Netherlands). Embedded samples were dehydrated in 100% methanol and cleared in a solution of benzyl benzoate and benzyl alcohol (2:1; Sigma). Samples were scanned using Optical Projection Tomography (OPT), as described by Sharpe and coworkers (Sharpe et al., 2002), using a prototype OPT scanning device, constructed at the Medical Research Council Human Genetics Unit (Edinburgh, UK) and installed in the Zoology Department, Trinity College Dublin. A 3-dimensional (3D) computer representation of each bone rudiment was produced by integrating 400 serial visible light transmission images from each scanned specimen (Sharpe et al., 2002). The 3D representations could be virtually sectioned in any orientation and comparable sections were used to measure a total of 10 morphometric parameters, i.e. lengths, for each specimen (figure 2.1). Data for each parameter were pooled per embryonic age. A linear regression fit between length and age was taken as the quantitative growth rate in mm/day.
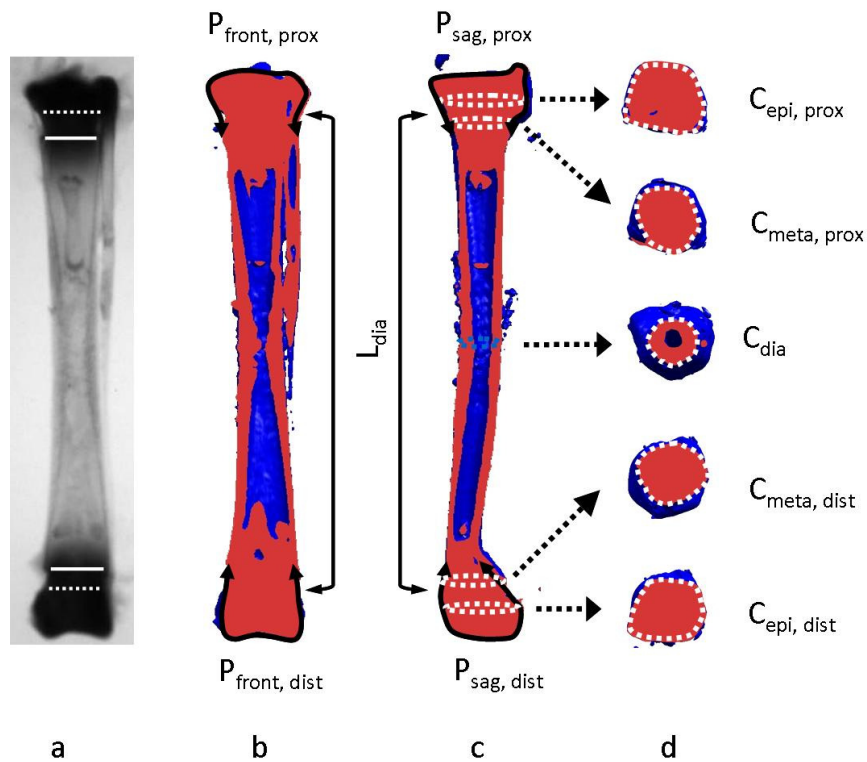
Figure 2.1: Morphometric parameters from OPT data. (a) Raw OPT image of an e14 chick tibiotarsus. Continuous lines represent the end of the bone shaft where the perichondrium begins, visible in the raw data. Dashed lines represent periosteum attachments to the epiphyses, at the location where the epiphysis widens. (b) Mid-frontal and (c) mid-sagittal sections through the bone, in which perimeter dimensions (P_x) represent the length of the perichondrium in the sagittal and frontal sections, indicated by arrowed continuous lines. (d) Transverse sections through locations indicated in (c). Circumferential dimensions (C_x) represent the circumference of the perichondrium or periosteum in transverse sections. Red areas represent the cut-planes of the section and blue represents adjacent tissue, located in deeper planes. The longitudinal dimension (L_{dia}) was measured between attachments of the periosteum to the epiphyses (indicated by dashed lines in (a)). Circumference of the diaphysis (C_{dia}) was measured at the midshaft. Circumference of the distal ($C_{meta,dist}$) and proximal metaphysis ($C_{meta,prox}$) were measured in between the bone shaft and periosteum attachment. Circumference at the distal ($C_{epi,dist}$) and proximal epiphysis ($C_{epi,prox}$) were measured near the largest transverse section. Perimeters of the perichondrium at the proximal epiphysis in the sagittal ($P_{sag,prox}$) and frontal ($P_{front,prox}$) section were measured from the medial to the lateral end of the bone shaft. Corresponding parameters in the distal epiphysis ($P_{sag,dist}$ and $P_{front,dist}$) were measured similarly.

2.3.3 Collagen orientation by Multiphoton Microscopy

Chick tibiotarsi from embryonic day 13 to 14 (n=16) were used for visualization of the perichondrial and periosteal collagen network. Upon dissection, tibiotarsi were incubated in phosphate buffered saline (PBS), supplemented with a collagen probe (2.5 µM) (Krahn et al., 2006) for one hour at 37^0C, 5% CO_2. The CNA35 protein is known to have a high affinity for collagen I relative to other collagen types and shows very little cross reactivity with noncollagenous extracellular matrix proteins. Conjugation of this protein to a fluorescent dye yields the formation of a highly specific probe for collagen imaging (Krahn et al., 2006). After incubation, samples were washed in PBS to remove excessive dye and kept in PBS for the remainder of the experiment. During visualization, tibiotarsi were immersed in PBS and put in a chambered coverglass (Lab-Tek II, Nunc, Roskilde, Denmark). Both the proximal and distal sides of the bones were examined, using a multiphoton microscope (Zeiss LSM 510 META NLO, Darmstadt, Germany) in Two-Photon-LSM (TPLSM) mode. The excitation source was a Coherent Chameleon Ultra Ti:Sapphire laser, tuned and mode-locked at 763 nm. This wavelength resulted in the highest intensity profile for the collagen probe. Laser light was focused on the tissue with a Plan-Apochromat 20x/0.8 numerical aperture (NA) objective or C-Apochromat 63x/1.2 NA water objective, connected to a Zeiss Axiovert 200M. The pinhole of the photo-multiplier was fully opened. The photo-multiplier accepted a wavelength region of 500 – 530 nm. All single images shown in this chapter were obtained from Z-stacks, taken through the perichondrium or periosteum. No additional image processing was performed.

2.3.4 Statistics

Two-Way ANOVA was used to determine the effect of the selected independent variable (embryonic day, which is taken as an ordinal variable referring to the selected embryonic stage) and its interaction with the morphometric dimensions (L_{dia}, C_{dia}, $C_{meta, dist}$ and $C_{meta, prox}$; $C_{epi, dist}$, $P_{sag,dist}$ and $P_{front,dist}$; $C_{epi, prox}$, $P_{sag,prox}$ and $P_{front,prox}$) of the tibiotarsi. If an interaction was found, Two-Way ANOVA was repeated for individual parameters and the p-value was corrected with the Bonferroni criterion. P-values < 0.05 were considered statistically significant.

2.4 Results

2.4.1 Growth

Growth in the epiphyseal perichondrium is shown in figure 2.2. The linear regressions had R-squared values that ranged from 0.86 to 0.93. Statistically significant differences were assessed for growth rates in the distal and proximal epiphyses separately. A significant difference was found in the comparison between the slopes (table 2.1) of the circumferential parameters ($C_{epi, dist}$ and $C_{epi, prox}$) and the perimeters ($P_{sag, dist}$, $P_{sag, prox}$, $P_{front, dist}$ and $P_{front, prox}$). At both extremities, circumferential growth exceeded growth of the perimeter. The ratio between them ranged from 1.54 – 1.97 (table 2.2). Perimeter growth in both epiphyses ($P_{sag, dist}$ and $P_{front, dist}$; $P_{front, prox}$ and $P_{sag, prox}$) was not different. Growth in the metaphysis and diaphysis is shown in figure 2.3. The linear regressions had R-squared values that ranged from 0.92 to 0.96. A significant difference was found in the comparison between the slopes (table 2.1) of the longitudinal parameter (L_{dia}) and all circumferential parameters (C_{dia}, $C_{meta, dist}$, $C_{meta, prox}$) as well as circumferential growth at both metaphyses ($C_{meta, dist}$, $C_{meta, prox}$) with circumferential growth at the diaphysis (C_{dia}). At the metaphyses, circumferential growth was approximately half the longitudinal growth, whereas at the diaphysis this ratio was one to four (table 2.2).
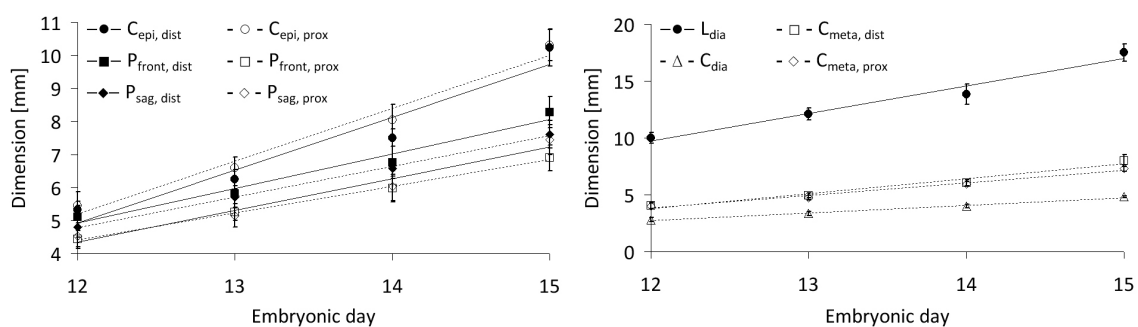
Figure 2.2. Growth in the epiphysis. Circumferential ($C_{epi, prox}$ and $C_{epi, dist}$) and perimeter dimensions in the frontal and sagittal sections ($P_{sag, dist}$, $P_{sag, prox}$, $P_{front, dist}$ and $P_{front, prox}$) against embryonic age (n=28).

Figure 2.3: Growth in the metaphysis and diaphysis. Circumferential ($C_{meta, dist}$, $C_{meta, prox}$ and C_{dia}) and longitudinal dimension (L_{dia}) against embryonic age (n=28).

Table 2.1: Growth rates in the diaphysis, metaphysis and epiphysis. n=28. Values represent the slopes of the linear regression lines depicted in figure 2.1 and 2.2.
*Statistical differences, p < 0.05.

	Growth rate ± S.D. [mm/day]	R^2
Diaphysis / Metaphysis		
L_{dia}	2.42 ± 0.14	0.92
C_{dia}	0.67 ± 0.03	0.96
$C_{meta,dist}$	1.30 ± 0.07	0.93
$C_{meta,prox}$	1.12 ± 0.05	0.95
Epiphysis distal		
$C_{epi,dist}$	1.60 ± 0.10	0.91
$P_{front,dist}$	1.04 ± 0.08	0.87
$P_{sag,dist}$	0.96 ± 0.08	0.86
Epiphysis proximal		
$C_{epi,prox}$	1.60 ± 0.09	0.93
$P_{front,prox}$	0.81 ± 0.05	0.90
$P_{sag,prox}$	0.93 ± 0.05	0.92

Table 2.2: Growth ratios between growth rates (table 2.1) in the diaphysis, metaphysis and epiphysis (n=28).

	Growth ratio [-]
Diaphysis / Metaphysis	
$C_{meta,dist} / L_{dia}$	0.54
$C_{meta,prox} / L_{dia}$	0.46
C_{dia} / L_{dia}	0.28
Epiphysis distal	
$C_{epi,dist} / P_{front,dist}$	1.54
$C_{epi,dist} / P_{sag,dist}$	1.67
$P_{sag,dist} / P_{front,dist}$	0.92
Epiphysis proximal	
$C_{epi,prox} / P_{front,prox}$	1.97
$C_{epi,prox} / P_{sag,prox}$	1.72
$P_{front,prox} / P_{sag,prox}$	0.87

2.4.2 Collagen fiber orientation

At the diaphysis, the outer layer of the periosteum (figure 2.4b) contained some random oriented collagen fibers. Deeper into the tissue (figure 2.4c & d) the orientation was highly anisotropic with almost all oriented longitudinally. In the metaphysis, the outer layer of the perichondrium was composed of a thin, random fiber network (indicated by arrows in figure 2.4f & g). Underneath this layer, thicker circumferential fibers (dashed circles in figures 2.4f – h), presumably originating from the perichondrium, were entangled with longitudinal fibers. The latter fibers (asterisks in figures 2.4g & h) comprising the inner fibrous layer, were continuous with the well-developed longitudinal fibers in the diaphyseal periosteum. The collagen network in the perichondrium covering the epiphyses had no predominant orientation (figure 2.4j – l), and was therefore considered random. Sporadically, locations were identified where groups of fibers ran in parallel (asterisk in figure 2.4l). No differences in collagen orientation were observed between the examined tibiotarsi.
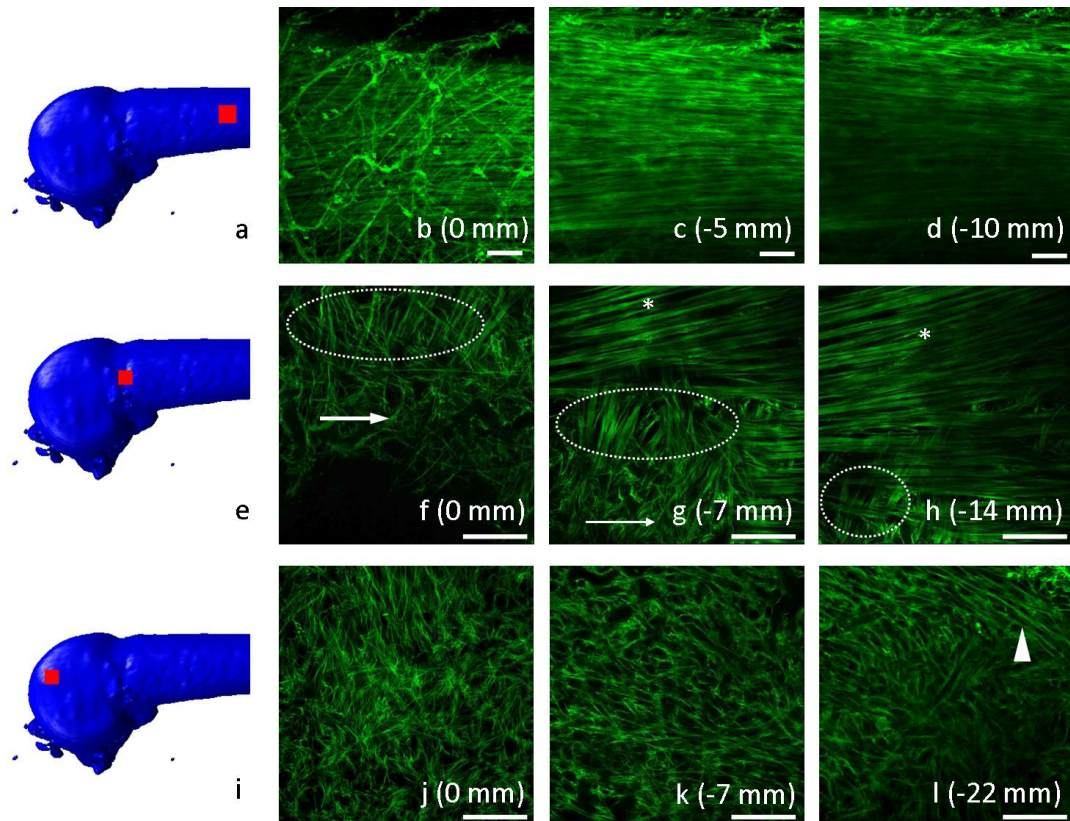
Figure 2.4: TPLSM images of collagen in the perichondrium and periosteum of an e13 chick tibiotarsus. Red squares indicate the location of the z-stack in (a) the diaphyseal periosteum, (e) metaphyseal periosteum/perichondrium and (i) epiphyseal perichondrium. (b – d) Fiber orientation in the diaphyseal periosteum. (b) A thin layer of collagen without a preferential orientation covers (c) longitudinal collagen fibers. (f – h) Fiber orientation in the metaphyseal periosteum/perichondrium. Asterisk: longitudinal periosteal fibers extending from the diaphysis. Dashed circles: circumferential fibers interwoven with the longitudinally organized deeper network. Arrows: random fiber orientation in the outer layer. (j – l) Fiber orientation in the epiphyseal perichondrium is random. Arrowhead: sparse areas with few parallel fibers. (b – d): Objective 20x, NA 0.8. (f – h & j – l): Objective 63x, NA 1.2. Scale bars: 50 μm. Image depth is indicated on images.

An overview of the results is depicted in figure 2.5. (diaphysis) Longitudinal periosteum fibers spanned the diaphysis and the metaphyses, and attached to the epiphyseal base. Growth in the diaphysis was predominantly in the longitudinal direction (ratio 4:1) and all periosteum fibers aligned with that direction. (metaphysis) The outer layer of the perichondrium/periosteum contained well-developed circumferential fibers which covered, and were partly interwoven with, a dominant network of longitudinally-oriented fibers. Longitudinal metaphyseal growth was twice the circumferential growth. (epiphysis) Towards the articulations, the collagen network of the epiphyseal surface was randomly oriented and growth was approximately equibiaxial at both the distal and proximal sides.
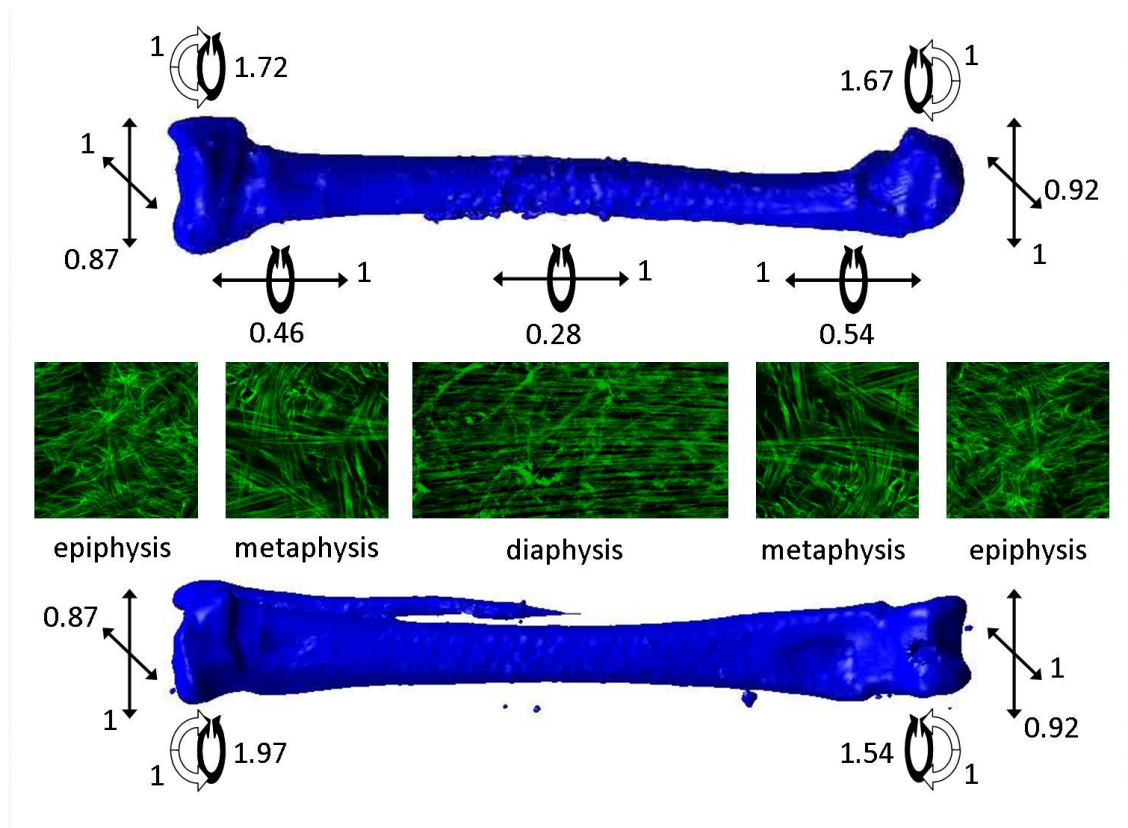
Figure 2.5: Overview of normalized growth ratios (see table 2.2) and corresponding collagen orientation in the diaphysis, metaphysis and epiphysis of the developing tibiotarsus (e13-e14). Sagittal view on top, frontal view below. Proximal left, distal right.

2.5 Discussion

The 3D collagen orientation in embryonic chick tibiotarsi periosteum and perichondrium were compared to the directions of tibiotarsi growth. The results (figure 2.5) revealed that epiphyseal growth was isotropic at the bone-extremity surfaces, whereas at the epiphyseal center, circumferential growth dominated. This corresponded to a random collagen network in the epiphyseal perichondrium. Longitudinal periosteum fibers spanned the metaphysis and diaphysis, and aligned with the dominant longitudinal growth in the diaphysis. Circumferential growth was larger at the metaphysis compared to the diaphysis, which concurred with the finding that longitudinal fibers were covered by a layer of circumferentially-oriented fibers at the metaphysis, but not at the diaphysis. The biaxial collagen network of the metaphysis was found to originate from the dominant longitudinally-oriented periosteal fibers at the diaphysis. These fibers were continuous with fibers at both metaphyses and were fixed at the epiphyseal base only. Adhesion of the periosteum to the underlying cartilage and bone at other locations was poor (Bertram et al., 1998). The longitudinal fibers spanned the complete metaphysis and diaphysis and were loaded in this direction. Their insertions are unfavorable for acting against circumferential growth, therefore another sheet of fibers was found perpendicular to the longitudinal direction. These finding support our hypothesis that predominant directions of growth, generate strain in corresponding directions, which aligns collagen fibers in the perichondrium and periosteum. Hence, growth is proposed to trigger collagen-fiber orientation.

We compared growth at characteristic sites to local orientations of collagen at corresponding sites. A limitation to this study is that the exact location of the TPLSM scans cannot be assessed. It remains experimentally challenging to compare detailed quantified growth at a small scale with collagen orientations at matching locations.

This study shows that collagen orientation coincides with the ratio between different directions of absolute growth (in mm/day). However, growth is defined as a combination of tissue strain and remodeling. The actual strain the collagen fibers experience, which is the genuine trigger for collagen alignment, may differ from the growth rate. Knowledge of such would provide additional insight in the mechanism of collagen turnover by mechanical stimulation. One preliminary study (Chen et al., 2007)

estimated residual strain in mid-diaphyseal periosteum of similarly aged chicks as high as 105% in the longitudinal direction and 10% in the circumferential direction.

In 7- to 8-week-old rabbit metatarsals, collagen orientation in the periosteum/perichondrium is predominantly longitudinal, with some distinct groups of fibers lying in a circumferential orientation or oblique to the long axis (Speer, 1982). The periosteum of the rabbit femur also displayed longitudinally-oriented collagen fibers (Dejonge, 1983). In ribs of 5-months-old rabbits, collagen is oriented parallel to the longitudinal axis of the rib, while in the outer zone of the cartilage, collagen layers are mostly arranged circumferentially (Bairati et al., 1996). The observations in these studies are in agreement with fiber orientations found in the present study. In a crossbreed of New Hampshire and Barred Rock chickens, growth in length and diaphyseal diameter of tibias is linear during the first 3 weeks after fertilization (Church and Johnson, 1964). All corresponding growth dimensions in this crossbreed exceed those of the White-Leghorn chickens from this study by a factor of approximately 2. However, the linear increase of the bone dimensions during the second week after fertilization is in agreement with this study. To the knowledge of the authors, collagen orientation has never been related to growth-directions in developing tissues.

Many studies (Caruso and Dunn, 2004; Ellsmere et al., 1999; Guidry and Grinnell, 1985; Henshaw et al., 2006; Huang and Yannas, 1977; Nabeshima et al., 1996; Ruberti and Hallab, 2005; Sawhney and Howard, 2002; Wang et al., 2003) relate mechanical load to direction dependent degradation and alignment of collagen. The orientation of collagen has been assessed in fibroblast-seeded collagen gels, subjected to different loading regimes. Unloaded gels display a disorganized collagen distribution (Henshaw et al., 2006). Uniaxially constrained gels develop high degrees of fiber alignment and mechanical anisotropy, while collagen gels constrained biaxially remain mechanically isotropic with randomly-distributed collagen fibers (Henshaw et al., 2006; Thomopoulos et al., 2005). Using the same set-up, static uniaxial load induces greater ultimate stress and material modulus compared to dynamic load (Feng et al., 2006b). Differences in collagen alignment between statically and dynamically loaded samples have not been reported. Compaction force of the tethered collagen samples increased immediately, reaching a maximum after 2 days of culturing (Feng et al., 2006a). These

studies all suggest a relationship between strain and collagen orientation; however, they do not indicate what the relationship implies.

Driessen and coworkers (Driessen et al., 2004) hypothesized that collagen fibers align with the direction in between the principal tensile strains, dependent on the strain magnitudes. Predicted collagen architectures with this theory concur with the collagen orientation in various dynamically loaded tissues, including heart valves (Driessen et al., 2005), blood vessels (Driessen et al., 2004), and articular cartilage (Wilson et al., 2006). The present chapter shows that collagen orientations in the perichondrium and periosteum align with the directions of growth. Growth is a combination of mechanical tissue strain and the synthesis of new tissue matrix. Exactly how growth relates to mechanical tissue strain is yet unknown. Hence, it is difficult to correlate the measured collagen orientation in periosteum and perichondrium to predictions by these theories. Possibly, the mechanism for collagen orientation is different in growing tissues that are quasi-statically loaded, compared to dynamically loaded tissues.

We conclude that the local anisotropy in the periosteum and perichondrium concurs with predominant growth directions. This agrees with the concept that a load-dependent feed-back mechanism prevails between different tissue types in growing bones.

2.6 Acknowledgement

Chapter 3

Residual Periosteum Tension is Insufficient to Directly Modulate Bone Growth

3.1 Abstract

Periosteal division is one of the less severe interventions used to correct mild long bone growth pathologies. The mechanism responsible for this growth modulation is still unclear. A generally adopted hypothesis is that division releases compressive force created by tensioned periosteum. We set out to evaluate the feasibility of this hypothesis by quantifying the stress level imposed on cartilage by periosteum tension in the rapid growth phase of chick embryos and evaluating if tension release could be responsible for modulating growth. Residual force in embryonic periosteum was measured in a tensile tester. A finite element model was developed, based on geometry determined using optical projection tomography in combination with histology. This model was then used to calculate the stress-distribution throughout the cartilage imposed by the periosteum force and to evaluate its possible contribution in modulating growth. Residual periosteal force in e17 chick tibiotarsi resulted in compressive stresses of 6 kPa in the proliferative zone and tensile stresses up to 9 kPa in the epiphyseal cartilage. Based on the literature, these compressive stresses are estimated to reduce growth rates by 1.1% and calculated tensile stresses increase growth rates by 1.7%. However, growth rate modulations between 8% and 28% are reported in the literature upon periosteum release. We therefore conclude that the increased growth, initiated by periosteal division, is unlikely to be predominantly the result of mechanical release of cartilage compression by periosteum tension. However, increased epiphyseal growth rates due to periosteal tension, may contribute to bone morphogenesis by widening the epiphysis.

3.2 Introduction

Skeletal growth is a tightly controlled phenomenon. In general, it is difficult to correct for skeletal malformations that develop during growth. Periosteal division is one of the less severe interventions that have been used to, for instance, correct unilateral long bone growth retardation. It is proposed that it interferes with a mechanical feedback mechanism that exists between pressure in growing cartilage and tension in the periosteum (Crilly, 1972; Moss, 1972). In this feedback mechanism, extracellular matrix formation, and chondrocytic proliferation and hypertrophy in the growth plate are postulated to result in movement of the epiphysis away from the diaphysis, thereby stretching and thus tensioning the periosteum. Consequently, growth plate cartilage is statically compressed. Static compression on growing cartilage is known to inhibit chondrocyte activity. Triggered by the tensioning, periosteum cells synthesize matrix allowing the periosteum to grow, whereby the compressive force on the cartilage is released and further bone lengthening becomes possible.

Extensive data exists to support the hypothesis that mechanics is involved in growth modulation (Arriola et al., 2001; Bonnel et al., 1983; Robling et al., 2001; Stokes et al., 2005; Stokes et al., 2006; Stokes et al., 2007; Wilson-MacDonald et al., 1990). Static compression applied to growth plates decreases longitudinal growth rates (Bonnel et al., 1983; Stokes et al., 2005; Wilson-MacDonald et al., 1990). Consistently, static tension increases longitudinal growth rates (Arriola et al., 2001; Stokes et al., 2006; Stokes et al., 2007; Wilson-MacDonald et al., 1990). The effect of applied stress level is linearly related to the percentage growth modulation (Bonnel et al., 1983; Stokes et al., 2006). Proportional modulation of growth was quantified after compression (100 and 200 kPa) and distraction (100 kPa) of growth plates in the proximal tibia of rabbit (aged 48 and 69 days), rat (aged 45 and 65 days) and calf (aged 55 days). Growth-rate sensitivity to stress (the regression relationship between proportional modulation of growth and actual stress) in tibiae was found to be 18.6% per 100 kPa and did not significantly differ between species or age of animals (Stokes et al., 2006). The effect of mechanical loading on growth was related to alterations in the number of proliferative chondrocytes and chondrocyte height in the hypertrophic zone (Stokes et al., 2007).

Furthermore, it is suggested that the periosteum mechanically modulates cartilage growth. Circumferential periosteal division results in increased longitudinal growth in 28- (Warrell and Taylor, 1979) and 60-day-old rats (Lynch and Taylor, 1987), 16- to 20-day-old fowls (Crilly, 1972), and 14- to 16-day old quails (Bertram et al., 1991). Periosteal stripping also increases longitudinal bone growth in young monkeys, 3- to 4-months-old dogs (Sola et al., 1963), 30- (Hernandez et al., 1995) and 60-day-old rats (Lynch and Taylor, 1987) and 6- to 14-year-old humans (Jenkins et al., 1975; Taillard, 1959). Circumferential division supplemented with stripping in 28-day-old rats produces the greatest increase in tibial length (Warrell and Taylor, 1979). Hemi-circumferential periosteal division produces an increase in valgus deformity, longitudinal overgrowth and an S-shaped tibia (Dimitriou et al., 1988; Houghton and Rooker, 1979). On the contrary, longitudinal periosteal incision, which damages the tissue but does not compromise the physical connection to both epiphyses, has no effect on longitudinal growth (Crilly, 1972; Dimitriou et al., 1988; Houghton and Rooker, 1979; Warrell and Taylor, 1979).

According to the above, it appears that mechanics can modulate growth plate growth rates, and increased growth rates as a result of circumferential periosteal division may act through this mechanism. This concurs with the aforementioned hypothesis of Moss (Moss, 1972) and Crilly (Crilly, 1972). However, the hypothesis has never been tested directly. We therefore set out to answer the question whether periosteum tension can create stresses in embryonic chick cartilage of the magnitude demonstrated to have a direct effect on cartilage growth.

3.3 Materials and Methods

We quantified the stress levels imposed on the cartilage by periosteum tension in the rapid growth phase of chick embryos between embryonic day 15 and 17. Since it is impossible to measure stress levels in growing cartilage experimentally, we adopted a combined experimental-numerical approach. Residual force in fast growing chick periosteum was assessed experimentally, using a setup similar to Bertram and coworkers (Bertram et al., 1998). This residual force served as input for finite element analysis, used to calculate the resulting stress-distribution throughout the cartilage.

Bone geometry and boundary conditions for the finite element analysis were obtained from histology in combination with optical projection tomography (OPT). The stresses in cartilage were then compared to the aforementioned growth rate sensitivity to stress of 18.6% per 100 kPa, assessed by Stokes and coworkers (Stokes et al., 2006). An estimate for growth rate increase upon circumferential periosteum division was hereby obtained, evaluated with respect to increased growth rates from the existing literature.

3.3.1 Mechanical testing: residual force measurement

Fertilized eggs of White Leghorn chickens ('t Anker, Ochten, The Netherlands) were placed in a polyhatch incubator (Brinsea, UK). After a 15-, 16- or 17-day period of incubation, i.e. Hamburger and Hamilton stages 41 to 43 (Hamburger and Hamilton, 1992), chick embryos were removed from the eggs and euthanized by decapitation. A total of 36 tibiotarsi (n=12 each for e15, e16 and e17) were carefully dissected, without damaging the periosteum. All remaining surgical procedures were performed in PBS. A single longitudinal incision through the periosteum along the entire diaphysis was made with a scalpel next to the fibula. The fibula was removed without additional tissue, by cutting the proximal and distal end with scissors. The longitudinal incision was used to guide two suture wires (5.0 Vicryl, Ethicon, Johnson & Johnson Medical, Amersfoort, The Netherlands) in between bone and the periosteum (figure 3.1a). The wire ends were guided through mixing needles without bevel (Terumo Europe, Leuven, Belgium). The tibiotarsus was fixed (figure 3.2) in an ElectroForce LM1 TestBench (Bose Framingham, MA, USA) and grippers were displaced until the 2.5N load cell (Sensotec, Honeywell, Apeldoorn, The Netherlands) indicated an unloaded condition.

With the rudiment held at *in vivo* length, suture wires were moved towards the proximal and distal insertion of the periosteum to the cartilage (figure 3.1b). Subsequently, suture wires were pulled through the mixing needles to cut the proximal (figure 3.1c) and distal (figure 3.1d) metaphyseal cartilage. In this way, bone tissue was extracted through the longitudinal cut with the periosteum held at *in vivo* length (figure 3.1d).
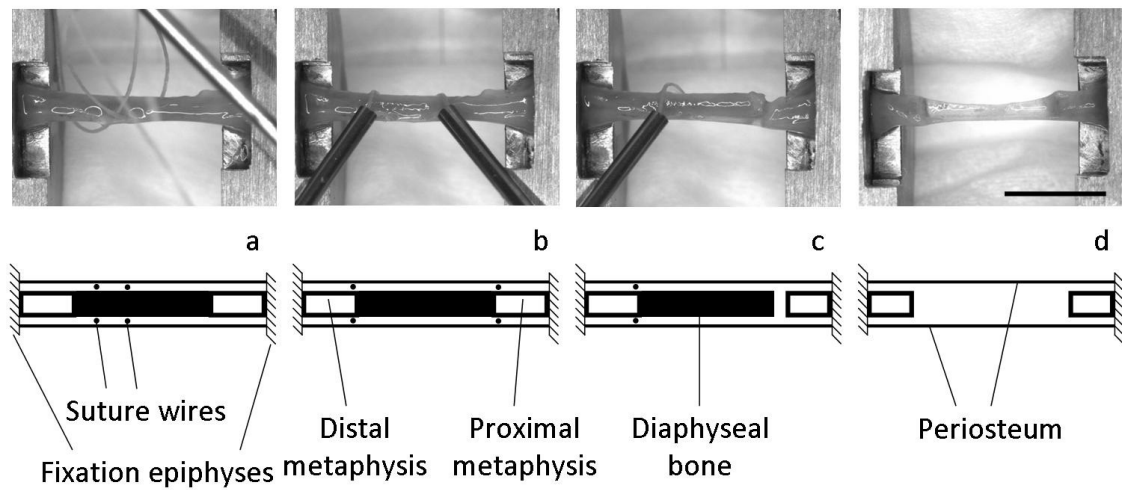
Figure 3.1: Progressive steps in the mechanical test protocol. Digital images (top row) and corresponding illustrations (bottom row). (a) After making a single longitudinal cut with a scalpel alongside the fibula, which was subsequently removed, suture wires were guided in between bone and the periosteum. (b) At *in vivo* length, suture wires were moved proximal and distal. (c) Suture wire has cut the proximal metaphyseal cartilage and (d) bone tissue was removed after cutting through the distal metaphyseal cartilage, with the periosteum held at *in vivo* length. Scale bar represents 10 mm.

With this procedure the recorded contractile force displayed a stepwise increase (i.e. from 0N, where tension in the periosteum is exactly countered by compression in the bone, to periosteum tensile force). This force, staying constant over time, was defined as residual force. Throughout the procedure, the tissue was hydrated with PBS. The complete procedure from dissection to loading spanned approximately 15 minutes.

Figure 3.2: Illustration of bone fixation in the clamps of the tensile tester.
(a) 3D representation. (b) Cross-section of (a).

3.3.2 Statistics

One-Way ANOVA was used to determine if there was a difference in residual force between the different embryonic age groups. For post-hoc testing, the Bonferroni correction was used. For all tests, p-values < 0.05 were considered statistically significant.

3.3.3 Optical Projection Tomography (OPT)

Quantitative morphometric parameters for the periosteum and representative mesh geometry for finite element analysis were obtained from OPT. For whole-mount staining, tibiotarsi from embryonic day e16 and e17 chicks (n=3 for both ages) were used. Procedures are performed exactly as described previously (Foolen et al., 2008), see chapter 2. In short, tibiotarsi were cleared in 1% potassium hydroxide (Sigma, St. Louis, MO, USA) and stained with Alcian Blue (Sigma) for cartilage and Alizarin Red (Fluka, USA) for bone, consecutively. After staining, the tissue was embedded and scanned using OPT, as described by Sharpe and coworkers (Sharpe et al., 2002), using a prototype OPT scanning device, constructed at the Medical Research Council Human Genetics Unit (Edinburgh, UK) and installed in the Zoology Department, Trinity College Dublin. A 3-dimensional (3D) computer representation of each bone rudiment was produced by integrating 400 serial visible light transmission images from each scanned specimen (Sharpe et al., 2002). The 3D representations could be virtually sectioned in any orientation. OTP data for embryonic day e15 (n=7) were adopted from our former study (Foolen et al., 2008), see chapter 2.

3.3.4 Histology

To visualize periosteum attachment to the cartilage, formalin-fixed paraffin-embedded tibiotarsi of e15 to e17 bones (n=3 for all ages) were sectioned at 10 µm. The fluorescent collagen binding protein CNA35 (Krahn et al., 2006) and DAPI staining (Invitrogen, Breda, The Netherlands) were used to visualize collagen and cell nuclei, respectively, in the mid-frontal section. Tile scans were obtained using a multiphoton microscope (Zeiss LSM 510 META NLO, Darmstadt, Germany). The excitation source was a Coherent Chameleon Ultra Ti:Sapphire laser, tuned and mode-locked at 763 nm. Laser light was focused on the tissue with a Plan-Apochromat 20x/0.8 NA objective, connected to a Zeiss Axiovert 200M. Spatial resolution was 1024 x 1024 pixels over a 450µm x 450µm area. The photo-multiplier accepted a wavelength region of 500 – 530 nm for CNA35 and 390 – 465 nm for DAPI visualization.

3.3.5 Finite Element Analysis

The stress-distribution throughout the epiphyseal and metaphyseal cartilage was computed using an axisymmetric finite element model of a proximal e17 tibiotarsus (figure 3.3a). A mid-frontal section from OPT was used to create a representative mesh. Corresponding histology (figure 3.3b & c) was used to determine the location of periosteum attachment to the cartilage, the location of the bone shaft and resting, proliferative, and hypertrophic cartilage zones. Only equilibrium conditions were evaluated and low strains were predicted. Therefore, bone and cartilage zones were described as isotropic, linear elastic materials. The material properties used (table 3.1), were obtained from embryonic mouse bones (Radhakrishnan et al., 2004; Tanck et al., 2000; Tanck et al., 2004) and have been used by others in FE simulations of embryonic avian bone (Nowlan et al., 2008).

The displacements of the nodes on the symmetry axis and the bottom plane of the axisymmetric model were confined in the x-direction and y-direction, respectively (figure 3.3a). Periosteum tension was represented as a surface traction of 4.4 kPa, applied to the epiphyseal cartilage at 14 degrees with respect to the vertical axis (figure 3.3a), which was in accordance with histological analysis (figure 3.3c).

<p align="center">a   b   c</p>
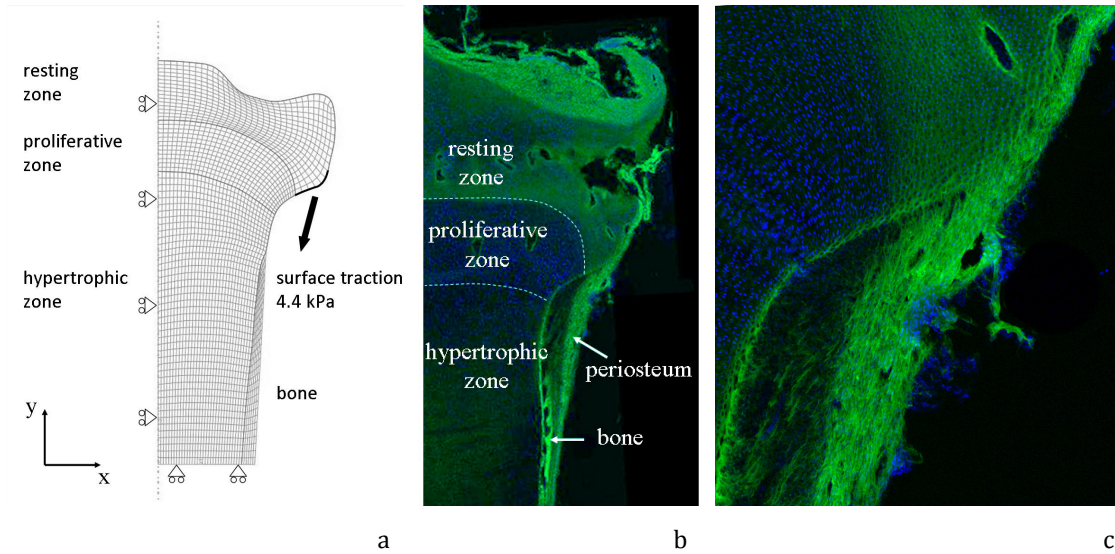
Figure 3.3: (a) Axisymmetric finite element mesh of a proximal e17 chick tibiotarsus. Zone and element distribution, boundary conditions and applied load are indicated in the figure. (b) Histology of a proximal tibiotarsus of an e17 chick embryo stained for collagen (CNA35; green) and cell nuclei (DAPI; blue). (c) Magnification of figure 3.3b showing the attachment of the periosteum to the epiphyseal resting zone, just next to the proliferative zone.

This surface traction equals the residual periosteum force measured in this study (0.032N, see results section), divided by the total area of periosteum attachment (7.2 mm^2) in the finite element model. Periosteum attachment area is determined by revolving the black line from figure 3.3a around the symmetry axis, which corresponds to the periosteal attachment site, as depicted in figure 3.3c. The model was implemented in ABAQUS v6.2 (Hibbitt, Karlsson & Sorensen, Inc., Pawtucket, RI, USA). It consisted of 2482 8-node bi-quadratic axisymmetric elements with reduced integration points (CAX8R).

Table 3.1: Material properties used in the finite element model

	E-modulus [MPa] (Radhakrishnan et al., 2004; Tanck et al., 2004)	Poisson's ratio [-] (Tanck et al., 2000)
Resting zone	0.57	0.25
Proliferative zone	0.71	0.25
Hypertrophic zone	0.88	0.25
Bone	117	0.30

3.4 Results

3.4.1 Residual force measurement

Residual periosteum force was not significantly different between the ages examined (figure 3.4). Although there was no statistically significant difference, the largest residual force (0.032 N) and the corresponding morphology for the e17 tibia was used as input for the numerical model.
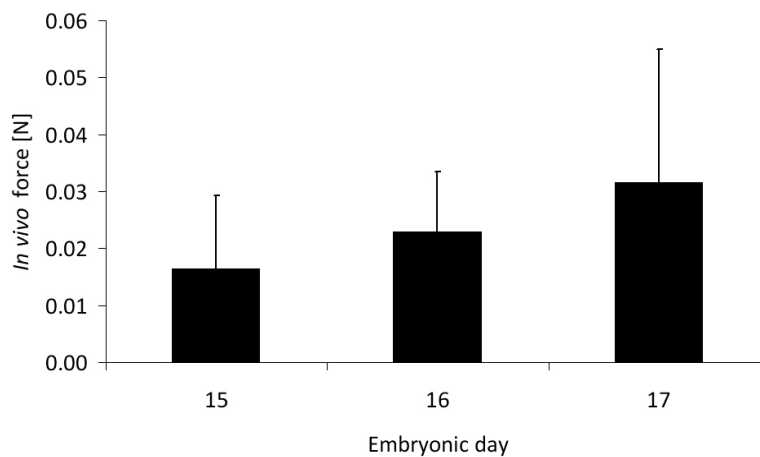
Figure 3.4: Residual periosteum force, determined at three embryonic ages. For all ages, n=12.

3.4.2 Finite element analysis

Finite element analysis of an e17 tibiotarsus calculated stresses in the longitudinal direction (figure 3.5a) near the symmetry axis below 2 kPa in the proliferative zone, and below 3 kPa in the hypertrophic zone. Longitudinal stresses (figure 3.5a) up to 6 kPa were found in the peripheral area of proliferative cartilage with even higher values in the bone shaft. Largest maximal principal stresses were located in the bone shaft and throughout the cartilage resting zone between 1 and 9 kPa (figure 3.5b). These stresses are oriented perpendicular to the symmetry axis and arch over to run parallel to the periosteum insertion as shown by the maximal principal tensile stress vectors (figure 3.5c).
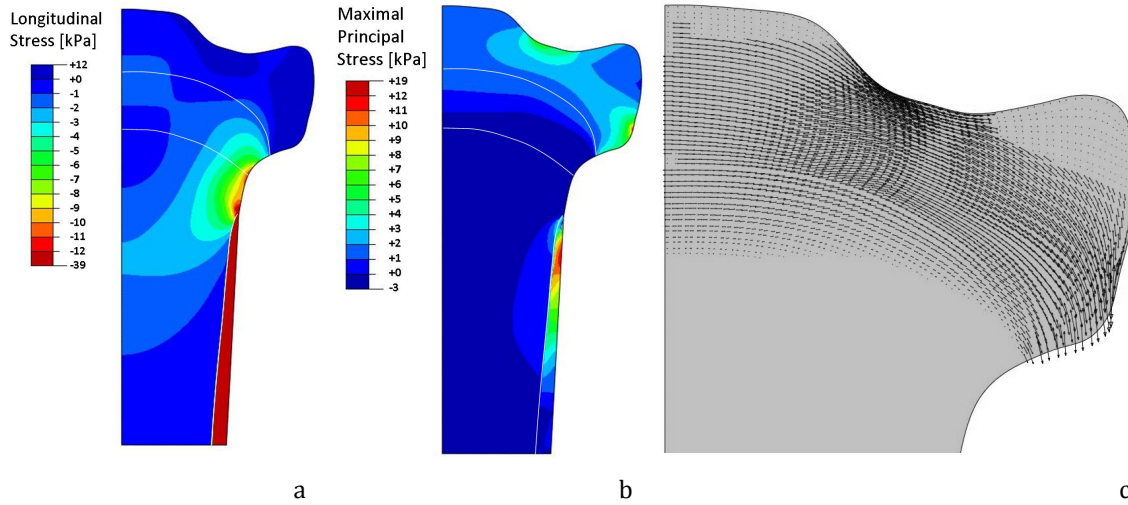
Figure 3.5: Finite element analysis results. (a) Longitudinal stress. (b) Maximal principal stress in an axisymmetric representation of the proximal part of an e17 tibiotarsus. Stresses are presented in kPa. White lines represent zonal boundaries (similar to figure 3.3a). (c) Maximal principal tensile stress vectors in the epiphysis. Compressive stress vectors not shown.

3.5 Discussion

The question was addressed whether periosteum tension can create stress in embryonic chick cartilage of the magnitude demonstrated to have a direct effect on cartilage growth. In the metaphysis, longitudinal compressive stresses did not exceed 6 kPa (figure 3.5a). Given the 18.6% growth rate change per 100 kPa (Stokes et al., 2006), these compressive stresses would evoke an estimated decrease in growth rate of approximately 1.1%, i.e. circumferential periosteum release would theoretically result in a 1.1% increased growth rate. However, increased growth rates (defined as percentage increase in growth rate of the experimental bone over the control) of 11.9% - 15.2% were reported after periosteum division in tibiotarsi and 9.9% - 17.5% in radii of quail, depending on the time after surgery (Bertram et al., 1991), and 27.5% upon proximal division, 8.2% upon distal division, and 18.7% upon periosteum stripping in Wistar rats, 21 days after surgery (Lynch and Taylor, 1987). Growth rate modulations from the latter study were calculated from the raw data supplied. Our estimate of the direct mechanical effect of periosteum release on increased longitudinal growth rates attains magnitudes far below the effect described in the literature. Hence, we postulate

that in addition to a minor mechanical effect, the influence of periosteum release may be predominantly indirect. It has been postulated that alterations in growth may be caused by indirect effects of periosteum division, mediated by a release of growth-modulating factors (Bertram et al., 1998). This concurs with the finding that extended growth caused by mechanical removal of the perichondrium and periosteum can be inhibited when tibiotarsi are cultured in medium conditioned by cells of the region bordering both the perichondrium and the periosteum (Di Nino et al., 2001).

In contrast to metaphyseal growth, maximal principal stresses in the epiphyseal cartilage attained values of 1 to 9 kPa (figure 3.5b). According to the growth rate sensitivity estimate, these tensile stresses could evoke a continuously increased growth rate of 0.2 to 1.7%. The orientation of these stresses, in the radial direction as depicted in figure 3.5c, stimulates additional cartilage growth in the corresponding direction. We therefore hypothesize that these stresses contribute to widening the epiphysis relative to the metaphysis during growth.

Increased growth upon periosteum division has been observed at several locations in a variety of species (Bertram et al., 1991; Crilly, 1972; Dimitriou et al., 1988; Hernandez et al., 1995; Houghton and Rooker, 1979; Jenkins et al., 1975; Lynch and Taylor, 1987; Taylor et al., 1987; Warrell and Taylor, 1979), including domestic fowl from different age groups (Crilly, 1972). All these data originate from animals or humans in the age range from 14 days to 14 years. To our knowledge, no *in vivo* data exists for the embryonic stage. However, in an *in vitro* setup, increased longitudinal growth rates are reported after stripping the periosteum of e12 chick tibiotarsi (Di Nino et al., 2001), similar to postnatal *in vivo* observations. We chose to use embryonic chick growth plates between e15 to e17 because these show the highest incremental growth rate (Church and Johnson, 1964). As we expect periosteum tension to be dependent on growth rate and not on external loads, we assumed that chicks of the breed and age used in the current study respond similarly to periosteal interventions. Yet, it cannot be excluded that additional age or load-related factors alter the growth response upon periosteum dissection *in vivo*.

The growth rate sensitivity to stress values that we used were obtained from Stokes and coworkers (Stokes et al., 2006). These are determined in adolescent rat, rabbit and calf and showed little variation between species and age, ranging from 9.2% to 23.9% per

100kPa. Even when the highest growth rate sensitivity to stress value would have been used in the present study, our conclusion would not have changed. Unfortunately, such quantitative data are not available for chick. Therefore, we cannot exclude the possibility that embryonic chick growth plates respond differently to stress. Yet, although embryonic chicks exist in a mechanical environment different than that of the weight bearing young animals used for comparison, it is unlikely that environmental forces would have changed the stress in the periosteum, because this is predominantly determined by the growth of the long bone, rather than by externally applied forces.

Periosteum attachment to the growing cartilage may be determinative for its growth-modulating potential. The adhesion force of the periosteum in 4-week-old chicks was absent over the diaphysis, more substantial over the metaphyseal region and largest in the epiphysis (Bertram et al., 1998). This is in agreement with the observation that a loose matrix containing very thin Sharpey's fibers exists in between the periosteum and the metaphyseal cartilage (Ellender et al., 1989; Tenenbaum et al., 1986). This concurs with our observations that the periosteum attaches to the epiphysis beyond the proliferative zone with Sharpey's fibers near the metaphysis (figure 3.3c). To maximize the estimated growth-modulating potential of the periosteum, we assumed that all fibers contributing to tension imposed on the cartilage are attached to the epiphyseal base. Hence, in the finite element analysis, the physiological *in vivo* condition was represented by applying periosteum tension to the epiphysis only. By removing this tension in the numerical model, both circumferential division and periosteal stripping are simulated.

The fibula could always be removed without additionally attached periosteum tissue, after making a single longitudinal incision in the periosteum. Since this coincides with the predominant direction of the collagen fibers (Foolen et al., 2008), the damage to the reinforcing collagen in the periosteum is minimal. Therefore, we assume this has no substantial effect on our results. Also, we assume that the influence of removal of the fibula is negligible. It has been shown that fibula dissection does not affect valgus angulation of the developing tibia (Houghton and Rooker, 1979).

Parametric sensitivity of the finite element model was evaluated with respect to tissue moduli and loading input. Changing the elastic modulus of cartilage zones or bone by a factor of 10 did not influence interpretation of the results. Using the highest residual

force measured for calculation of the surface traction (input value for the model), resulted in calculated stresses in the proliferative zone up to 12 kPa, which does not affect our conclusions. Obtaining compressive stresses in the range that could explain reported growth modulations upon periosteum division would require forces two orders of magnitude higher as an input value for the finite element analysis. In this paper, only the stresses at e17 were evaluated and it could be argued that the smaller size tibia at e15 or e16 could result in higher stresses. However, the periosteal residual force is also proportionally smaller at these ages. Finally, periosteum residual force has been determined previously in tibiotarsi and radii of Japanese quails, 14 to 28 days post-hatching (Bertram et al., 1991), which resulted in an estimated 9.3 kPa compressive stress imposed on the cross-sectional area of the growth plate. This magnitude of imposed stress is in agreement with the current study.

In summary, the low periosteum force measured resulted in stress distributions that theoretically retards growth not more than 1.1% percent. We therefore conclude that the compression imposed on the cartilage by periosteum tension affects growth on a scale far below that described in the literature as a consequence of periosteal division. Therefore, we propose that the influence of periosteum release on growth modulation is not directly mechanical. In the resting zone cartilage, increased growth rates are expected as a consequence of periosteal tension. We postulate that these are likely to significantly contribute to bone morphogenesis by widening the epiphysis.

3.6 Acknowledgements

Chapter 4

Perichondrium/Periosteum Intracellular Tension Regulates Long Bone Growth

4.1 Abstract

Perichondrium and periosteum are involved in regulation of long bone growth. Long bones grow faster after removal or circumferential division of periosteum, and this can be countered by culturing these bones in conditioned medium from cells, originating from the border region of the perichondrium and periosteum (perichondrium/periosteum). Because both complete removal and circumferential division are effective, we hypothesize that perichondrium/periosteum cells require an intact environment to release the appropriate soluble factors. More specifically, we propose that this release depends on the ability of the perichondrium/periosteum cells to generate intracellular tension. This hypothesis is explored by modulating the ability of perichondrium/periosteum cells to generate intracellular tension, and monitoring the effect thereof on long bone growth. Perichondrium/periosteum intracellular tension generated via actin filaments was modulated by culturing the cells on substrates with different stiffness. The medium produced by these cultures was added to embryonic chick tibiotarsi from which perichondrium/periosteum was either stripped or left intact. After 3 culture days, long bone growth was proportionally related to the stiffness of the substrate, on which perichondrium/periosteum cells were grown while they produced conditioned medium. A second set of experiments proved that the effect occurred through expression of a growth-inhibiting factor, rather than through the reduction of a stimulatory factor. Finally, evidence for the importance of intracellular tension was obtained by showing that the inhibitory effect was abolished when perichondrium/periosteum cells were treated with cytochalasin D, which disrupts the actin filament network. Thus, we conclude that modulation of long bone growth occurs through release of soluble inhibiting factors by perichondrium/periosteum cells, and that the ability of cells to develop intracellular tension through their actin filaments is at the base of this mechano-regulated control pathway.

4.2 Introduction

Longitudinal bone growth occurs by cartilage expansion via extracellular matrix production, and chondrocytic proliferation and hypertrophy. This growth is partly regulated by the perichondrium and periosteum (Alvarez et al., 2001; Di Nino et al., 2001; Hartmann and Tabin, 2000; Long and Linsenmayer, 1998; Vortkamp et al., 1996), which are fibrous connective tissue sheets that surround long bones. Dissection or circumferential division of periosteum increases cartilage growth rates *in vitro* (Di Nino et al., 2001; Di Nino et al., 2002; Long and Linsenmayer, 1998) and clinically (Chan and Hodgson, 1970; Jenkins et al., 1975; Taillard, 1959; Wilde and Baker, 1987). Moss (Moss, 1972) and Crilly (Crilly, 1972) proposed that periosteum regulates growth via a direct mechanical feedback mechanism where pressure in growing cartilage, balanced by tension in the periosteum, modulates growth processes of chondrocytes. This proposed feedback mechanism was based on the Hueter-Volkmann law, which describes an inverse relationship between compressive forces to cartilage and its rate of growth. However, even though periosteum structure appears optimized for this task (Foolen et al., 2008), see chapter 2, we recently demonstrated that periosteal mechanical tension is of insufficient magnitude to have such direct effects on growth (Foolen et al., 2009), see chapter 3. Bertram and coworkers (Bertram et al., 1998) proposed that cartilage growth acceleration after circumferential periosteal division is mediated by soluble factors. Indeed, conditioned medium from a mixed population of perichondrial and periosteal cells negatively regulates cartilage growth (Di Nino et al., 2001; Di Nino et al., 2002) and counteracts acceleration of growth after periosteum dissection (Di Nino et al., 2001).

Because growth is also accelerated after circumferential division, i.e. in presence of periosteum cells, we hypothesize that loss of intracellular tension is a critical aspect in the control system. More specific, we hypothesize that the ability of the periosteum/perichondrium cells to carry intracellular tension through their actin filament network is at the base of the signaling cascade, eventually resulting in the expression of soluble factors that modulate cartilage growth. Whether these cells can sustain intracellular tension depends either on the mechanical stiffness of their environment (Lo et al., 2000; Wang et al., 2000), or cell-matrix binding to transduce

tensile stresses in the matrix. The conditioned medium used in previous studies (Di Nino et al., 2001; Di Nino et al., 2002) was obtained from periosteum/perichondrium cells cultured on stiff glass substrates, allowing the cells to generate intracellular tension. Here, we question whether the expression of these soluble factors is dependent on the amount of intracellular tension. Second, we aim to evaluate whether the involvement of periosteum cells in controlling cartilage growth is through the release of inhibiting factors, or through a reduced expression of stimulatory factors. Finally, we set out to confirm our hypothesis in an experiment where we eliminated periosteum intracellular tension.

We approached these research questions by culturing periosteum/perichondrium cells on substrates with various stiffnesses, which allow cells to generate various magnitudes of intracellular tension or in the presence of cytochalasin D, which disrupts the actin filament network. Subsequently, the potential of these cells to modulate cartilage growth was evaluated by adding this conditioned medium to cultures of intact embryonic tibiotarsi, or tibiotarsi from which the periosteum was stripped. Pair-wise comparison of cartilage growth between left and right tibiotarsi, which were subjected to different conditions, elucidated a mechano-regulated feedback mechanism transduced through intracellular tension in which periosteum cells control long bone growth through expression of inhibitory factors.

4.3 Materials & Method

4.3.1 Preparation of glass cover slips

Glass cover slips (34 mm in diameter, Menzel, Braunschweig, Germany) were degreased with a Bunsen burner. Surface of the cover slips was covered with a 0.1 M NaOH solution, which was allowed to evaporate overnight. 3-Aminopropyltrimethoxysilane (Sigma, St. Louis, MO, USA) was applied for 5 minutes, after which the cover slips were thoroughly rinsed with de-ionized water. The cover slips were placed in a 6-well plate (Greiner Bio One, Alphen a/d Rijn, The Netherlands) and a 0.5% solution of glutaraldehyde (Sigma) was added for 30 minutes. The glass cover slips were subsequently rinsed six times with de-ionized water and air dried.

4.3.2 Preparation of polyacrylamide gels

Polyacrylamide gel solutions were prepared (table 4.1) to obtain the preferred stiffness, as previously described (Boonen et al., 2009). These stiffnesses were chosen for they span the range from soft to hard biological tissue (Engler et al., 2006). If a stiffness-dependent effect would be present, it will likely be expressed within this stiffness range. To polymerize the mixture of acrylamide (Fluka, USA) and bisacrylamide (Fluka), TEMED (Merck, Germany) and ammonium persulfate (APS, Thermo Fisher Scientific) were added with the appropriate amount of de-ionized water.

Table 4.1: Gel content in volumetric percentages of the 5 different stiffness levels.

Gel stiffness	3 kPa	14 kPa	21 kPa	48 kPa	80 kPa
Acrylamide	12.5%	25%	12.5%	25%	25%
Bisacrylamide	1.5%	1.5%	15%	6.5%	13%
10% APS	0.5%	0.5%	0.5%	0.5%	0.5%
TEMED	0.05%	0.05%	0.05%	0.05%	0.05%
De-ionized water	85.45%	72.95%	71.95%	67.95%	61.45%
Total	100%	100%	100%	100%	100%

After thoroughly stirring the solution, 250 µL was pipetted onto a Teflon plate. The activated side of the cover slip was carefully placed on top of the polyacrylamide droplet. Polymerization was complete in 30 minutes and the cover slip glass, containing a thin layer of attached gel, was carefully removed from the plate. The cover slip glass, put in a 6-well plate with the attached polyacrylamide gel facing upwards, was immersed in 50 mM HEPES (Greiner Bio One), pH 8.5.

4.3.3 Crosslinking of adhesion proteins

Sulfo-SANPAH (sulfosuccinimidyl6(4'-azido-2'-nitrophenyl-amino)hexanoate, Thermo Scientific Pierce, no. 22589) was added to the gels to crosslink extracellular matrix molecules onto its surface. Sulfo-SANPAH was freshly prepared by dissolving it in 0.5% DMSO and 50 mM HEPES (Greiner Bio One), pH 8.5. Photolysis of Sulfo-SANPAH was accomplished by placing the polyacrylamide gel under an ultraviolet lamp and

irradiation for 5 minutes. The discolored solution was removed and the procedure was repeated. The cover slips were placed in a 6-well plate and washed twice with 50 mM HEPES (Greiner Bio One), pH 8.5. HEPES (Greiner Bio One) was removed and a 2 mL Matrigel solution (200 µg/ml; 100 µl growth factor-reduced Matrigel (BD Biosciences, VWR, Amsterdam, The Netherlands) in 16mL 50 mM HEPES (Greiner Bio One), pH 8.5) was added to the well. The well plates, housing the gels, were incubated for 5 hours at 4°C. Cover slips were sterilized for 10 minutes under an ultraviolet lamp. The glasses were transferred to well plates and washed twice with sterile PBS. Culture medium was added 30 minutes before cells were seeded on the gels.

4.3.4 Perichondrial/periosteal cell cultures and collection of conditioned media

The border region of the perichondrium and periosteum (perichondrium/periosteum) was dissected from e12 tibiotarsi, chick embryos Hamburger and Hamilton stage 38 (Hamburger and Hamilton, 1992). Cells from this border region are known for their growth modulating potential, in contrast to cells from perichondrium or periosteum alone, which do not exhibit this potential (Di Nino et al., 2001). Tissue explants, supplemented with DMEM (Gibco, Invitrogen, Breda, The Netherlands), 10% fetal bovine serum (Greiner Bio-One) and penicillin and streptomycin (Lonza, Walkersville, USA), were cultured in 6-well plates at 37°C, 5% CO_2. Cells migrated from the explants and were thus obtained without enzymatic digestion. After 6 days, cells attached to the plate were dissociated by trypsinization. Complete medium was added to inactivate the trypsin, and cells were collected by centrifugation and passaged. Cell cultures were grown to multilayer confluency in complete medium in approximately 6 days, and rudiments of tissue explants were removed from the cultures. The cells were again dissociated by trypsinization and seeded onto the coated polyacrylamide gels with varying stiffness, supplied with complete medium. After 24 hours, complete medium was removed and the cultures were washed twice with PBS. For cultures treated with cytochalasin D (CD, Sigma), 6 µM cytochalasin D in DMEM (with penicillin and streptomycin) was added. After 30 minutes of incubation, medium containing cytochalasin D was removed and cells were washed twice with PBS. Subsequently, 4mL

serum-free DMEM (with penicillin and streptomycin) was added. Cultures not treated with cytochalasin D were handled identically with the exception of the cytochalasin D incubation step. After 24 h, conditioned medium was pooled per treatment condition and collected into 50 ml tubes (Falcon, BD Biosciences), centrifuged to remove floating cells and added to e12 tibiotarsi explants that were freshly harvested that same day.

4.3.5 Tibiotarsus dissection

Tibiotarsi were dissected from chicks, embryonic day e12, and the surrounding tissue was removed. From the 'stripped' tibiotarsi, perichondrium and periosteum was removed by circumferentially cutting the diaphyseal periosteum and stripping both tissues from the underlying bone and cartilage with forceps. Articular perichondrium was not removed, as this would damage the underlying cartilage.

4.3.6 Experimental design

Tibiotarsi from each embryo were always maintained as an "experimental pair" and cultured for 3 days (37°C; 5% CO_2) in conditioned or unconditioned medium (an overview is given in table 4.2). Three different sets of experiments were conducted. The first set consisted of experimental pairs of which one was stripped and other left intact, both supplied with the same unconditioned medium (DMEM with penicillin/streptomycin, Lonza) or conditioned medium from cells cultured on gels (stiffness ranging from 3 kPa to 80 kPa) or glass substrates (>> 80 kPa). In the second set, experimental pairs were either both stripped or both left intact, yet supplied with conditioned medium from 3 kPa or 80 kPa substrates. In the third set, experimental pairs were either both stripped or both left intact, yet supplied with different types of conditioned medium. Type of conditioned medium originated from cells cultured on gels with a stiffness of 3 kPa, 80 kPa or 80 kPa in presence of cytochalasin D for 30 minutes.

Table 4.2: Overview of the experiments performed. (set 1) Experimental pairs consisted of a stripped versus intact tibiotarsi. Medium added to the tibiotarsi consisted of either unconditioned medium (DMEM with penicillin/streptomycin) or conditioned medium from varying gel stiffness (# kPa indicates gel stiffness) or glass substrate. (set 2) Experimental pairs were both stripped or both left intact and supplied with conditioned medium from 3 kPa gels or 80 kPa gels. (set 3) Experimental pairs were both stripped or both left intact and supplied with conditioned medium from 3 kPa gels, 80 kPa gels, or 80 kPa CD (gels where cells were treated with cytochalasin D for 30 minutes). For all groups, n = 4.

Set	stripped vs intact tibiotarsi						
1	unconditioned	3 kPa	14 kPa	21 kPa	48 kPa	80 kPa	glass

Set	both tibiotarsi stripped	both tibiotarsi intact
2	3 kPa vs 80 kPa	

Set	both tibiotarsi stripped		both tibiotarsi intact	
3	3 kPa vs 80 kPa CD	80 kPa vs 80 kPa CD	3 kPa vs 80 kPa CD	80 kPa vs 80 kPa CD

4.3.7 Analysis of cultured tibiotarsi

Whole mount staining

To distinguish clearly the border between the growing cartilage and the boney shaft, tibiotarsi were fixed immediately upon culture in 95% ethanol for 3 days at 4^0C. The tibiotarsi were cleared in 2% potassium hydroxide and stained 8 hours with 0.1 % Alcian Blue (Sigma) for cartilage and for 3 hours with 0.014 % Alizarin Red (Fluka) for bone, consecutively. Tibiotarsi were fixed overnight in 10% formalin and stored in PBS with 1% sodiumazide until image collection.

Measurements of cartilage growth

All measurements were made of the distal cartilage of the long-bone rudiment. This cartilage has a uniform shape, whereas the shape of the proximal cartilage is irregular. For image collection, an Evolution VF digital color camera (Media Cybernetics, Bethesda,

USA) attached to a stereomicroscope (Zeiss, Darmstadt, Germany) was used. Distal cartilage length was determined along the midline of the cartilage, starting at the midpoint of the tarsal curve and ending at the midpoint of the border between the cartilage and the boney shaft. Thus, the line of measurement was kept at the midline of the cartilage at all points connecting the two ends (figure 4.1). So, if the cartilage curved, the midline also curved. This procedure is similar to the study of Di Nino and coworkers (Di Nino et al., 2001). The absolute values for the lengths of the midlines were determined and recorded using a Matlab routine (the MathWorks, Eindhoven, The Netherlands), calibrated to the same magnification as the images. Each separate measurement was conducted by two persons in blinded fashion.
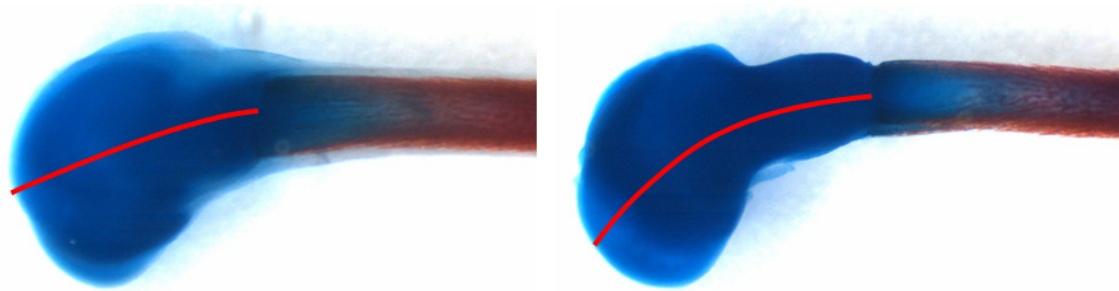
Figure 4.1: Tibiotarsi stained for cartilage (Alcian Blue, Sigma) and bone (Alizarin Red, Fluka). Red lines represent cartilage length of the distal epiphysis of an intact (left) and stripped tibiotarsus (right), after 3 days of culture.

4.3.8 Multiphoton microscopy

After extraction of conditioned medium, cells were fixed in 10% formalin for 30 minutes and permeabilized for 30 minutes in 0.5% Triton-X in PBS. Cells were incubated with FITC-conjugated phalloidin (1:500, P1951, Sigma) and DAPI (100ng/ml, Invitrogen, Breda, The Netherlands) for 20 minutes at room temperature for visualizing F-actin and cell nuclei, respectively. Cells were washed 4 times for 5 minutes with PBS and embedded in mowiol. Images were taken with a multiphoton microscope (Zeiss LSM 510 META NLO) in Two-Photon-LSM mode. The excitation source was a Coherent Chameleon Ultra Ti:Sapphire laser, tuned and mode-locked at 752 nm. This wavelength resulted in the highest intensity profile for the FITC label. Laser light was focused on the cells with a Plan-Apochromat 20x/0.8 NA objective, connected to a Zeiss Axiovert 200M.

The pinhole of the photo-multiplier was fully opened. Photo-multipliers accepted wavelength regions of 435-485 nm and 500–550 nm for DAPI and FITC, respectively. No additional image processing was performed.

4.3.9 Statistics

Paired sample comparison (t-test) was used to determine significant differences in procedure between experimental pairs within a group. Experimental groups are marked with an asterisk if a significant difference is detected between the experimental pairs. Linear regression analysis was used to determine the relationship between gel stiffness and length ratio between the stripped and intact tibiotarsi. P-values < 0.05 were considered statistically significant for all tests.

4.4 Results

The first set of experiments addressed the question whether and how the stiffness of the environment of periosteum/perichondrium cells would influence the expression of growth modulating factors by these cells (table 4.2: set 1). Conditioned medium from isolated e12 chick periosteum/perichondrium cells had different effects on growth of e12 tibiotarsi, depending on the stiffness of the substrate. Comparison between growth of the paired (same chick) tibiotarsi distal cartilage, one stripped and the other left intact, revealed that after 3 days of culture, distal cartilage length was significantly longer in stripped versus intact tibiotarsi in unconditioned medium, and in conditioned medium obtained from periosteum/perichondrium cell cultures on 3, 14, 21 and 48 kPa stiff substrates (paired t-test; figure 4.2). The difference in distal length between the stripped and intact tibiotarsus decreased with increasing stiffness of the substrate, and was no longer significant on 80 kPa gels and on glass (paired t-test; figure 4.2). This resulted in a significant relationship between substrate stiffness (3 to 80 kPa) and length ratio between the experimental pairs (linear regression analysis, p=0.01, R^2=0.30, figure 4.2b).

a   b
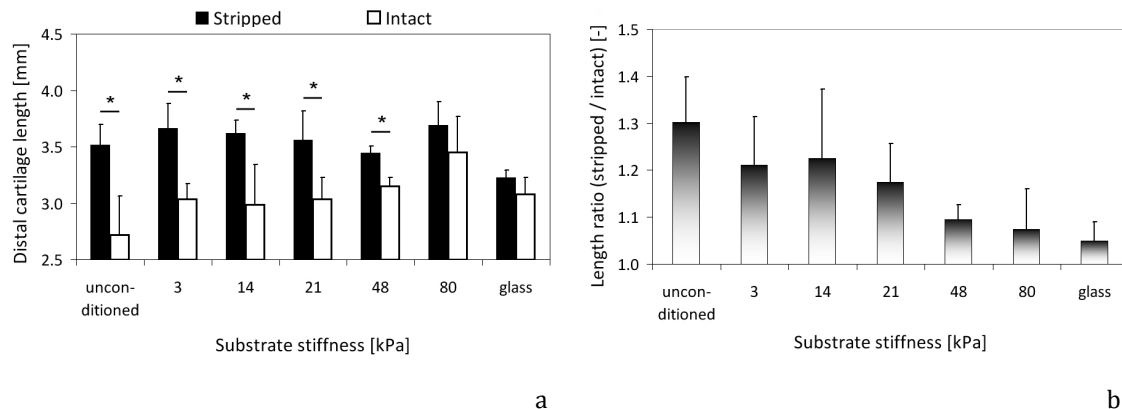
Figure 4.2: Length measurements for set 1. (a) Distal cartilage length. A significant difference (indicated by an asterisk) between stripped and intact tibiotarsi (paired t-test) was found in unconditioned medium (DMEM) and conditioned medium from substrates up to 48 kPa (b) Length ratio of the experimental pairs. A significant relationship was found between substrate stiffness and length ratio (linear regression analysis, p=0.01, R^2 = 0.30; 'unconditioned' and 'glass' are excluded from this analysis). For all groups, n = 4.

Different explanations are possible for the observation that with increasing substrate stiffness, the difference in cartilage length between stripped and intact bones decreased (figure 4.2b). Conditioned medium from stiffer substrates may stimulate growth of intact bones, it may decrease the enhanced growth in stripped bones, or both intact and stripped bones might show changed growth rates, one more than the other. Because of the variability in absolute growth rates between similarly aged embryos (Lovitch and Christianson, 1997), one can only draw conclusions from experiments in which contralateral bones are compared in a pair-wise fashion, i.e. it is not possible to interpret the slopes of the lines through the dark and open bars in figure 4.2a.

Therefore, a second set of experiments was performed (table 4.2: set 2). This second set showed that cartilage length of stripped bones, cultured in conditioned medium from 3 kPa substrates, was significantly longer compared to stripped bones cultured in medium from 80 kPa substrates (figure 4.3). Intact bones cultured in the same two media did not grow at different rates (figure 4.3). Hence, we concluded that periosteum/perichondrium cells can inhibit cartilage growth through the expression of a soluble factor, and that the expression of this factor is dependent on the stiffness of the environment of the periosteum cells.

a   b

Figure 4.3: Length measurements for set 2. (a) Distal cartilage length. (b) Length ratio of the experimental pairs. A significant difference (indicated by an asterisk) was detected in cartilage length between stripped bones cultured in conditioned medium from cells grown on 3 kPa and 80 kPa substrates (paired t-test). This significant difference was absent when tibiotarsi were left intact. For both groups, n = 4.

An independent set of experiments (table 4.2: set 3) was performed to show that indeed the expression of the growth-inhibiting factor by periosteum/perichondrium cells depended on the ability of these cells to develop intracellular tension. The difference in cartilage length between stripped bones exposed to conditioned medium from periosteum/perichondrium cells cultured on 3 kPa or 80 kPa substrates, was absent when the cells were exposed to cytochalasin D prior to the 24 hours of culture during which they generate conditioned medium (figure 4.4). In addition, a significant difference in distal cartilage length was observed between stripped bones cultured in conditioned medium from 80 kPa substrates or 80 kPa substrates treated with cytochalasin D. Finally, no significant differences were detected in the corresponding group where periosteum was left intact (figure 4.4).

Microscopic observations of fluorescently labeled F-actin in the periosteum/perichondrium cells at different time points of culture proved that our approach with the cytochalasin D treatment was appropriate. The cells showed a disorganized actin filament network after 30 minutes of cytochalasin D treatment, and the microfilaments were unable to recover in the subsequent 24 hours culturing period without cytochalasin D, during which they produced the conditioned medium. At the

end of this period the cells contained small aggregates of F-actin and weakly organized stress fibers compared to untreated cells (figure 4.5).
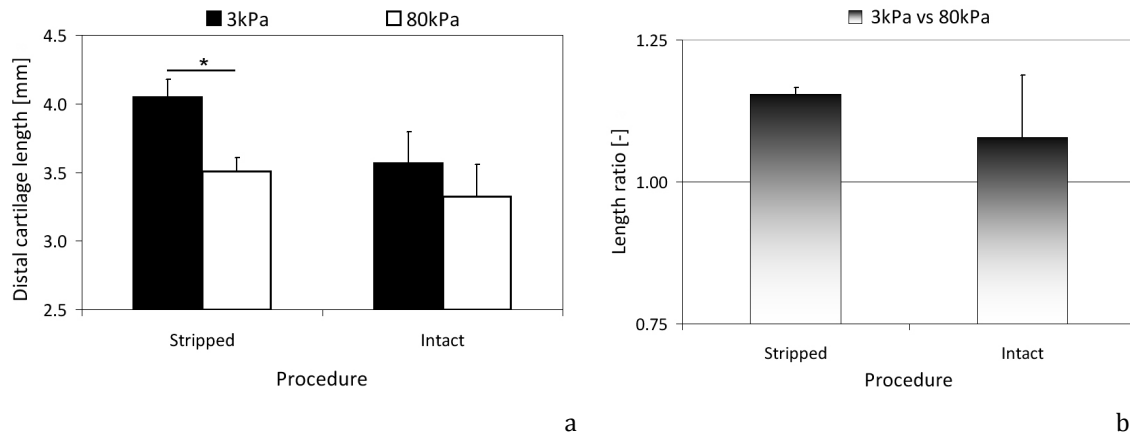

a   b
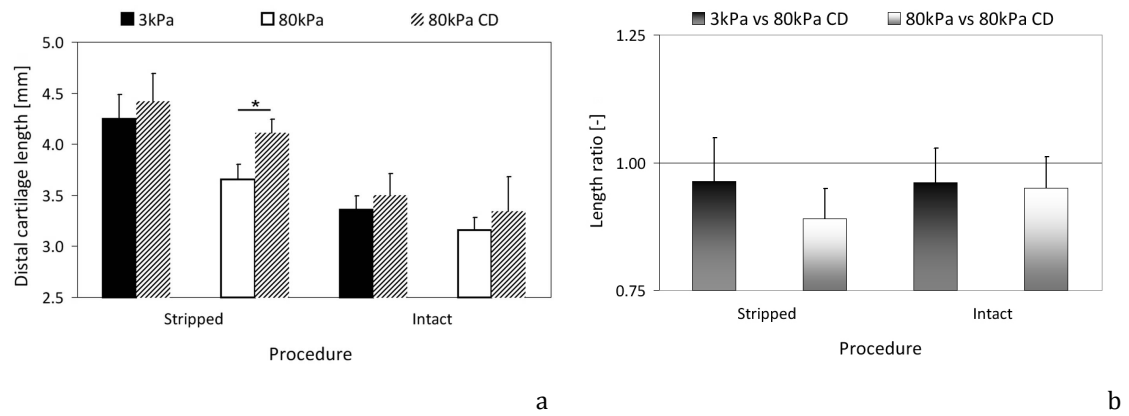
Figure 4.4: Length measurements for set 3. (a) Distal cartilage length. (b) Length ratio of the experimental pairs supplied with the indicated conditioned medium. A significant difference (indicated by an asterisk, paired t-test) was detected in cartilage length between stripped bones cultured in conditioned medium from cells cultured on 80 kPa and 80 kPa CD (80 kPa substrates treated with cytochalasin D for 30 minutes). For all groups, n = 4.

a   b
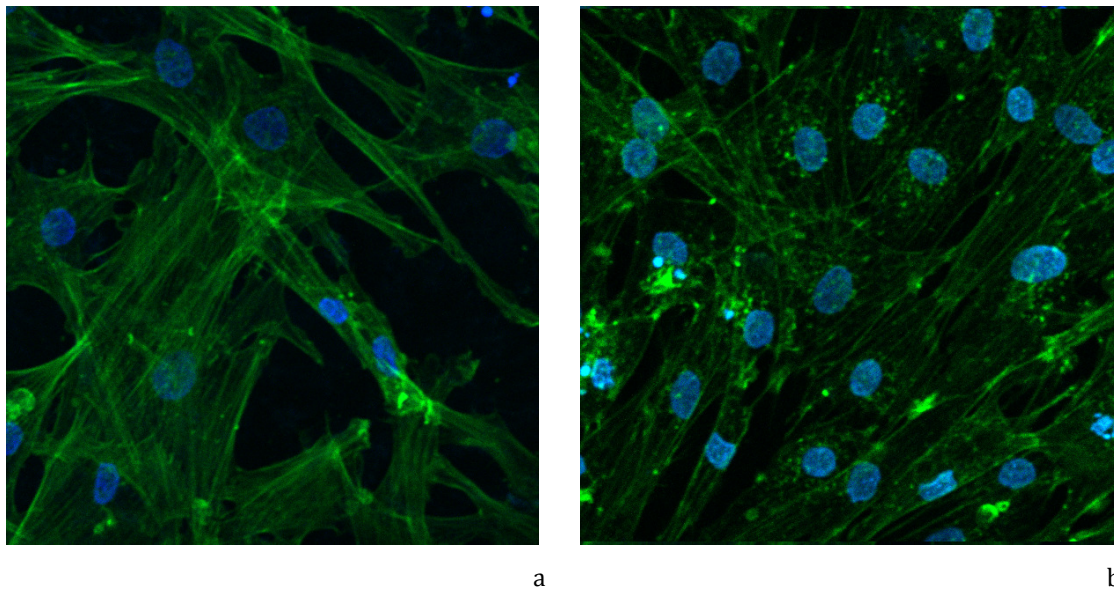
Figure 4.5: Cells cultured on 80 kPa substrates stained for F-actin (FITC-Phalloidin) and nuclei (DAPI). (a) Untreated cells cultured for 24 hours. (b) Cells cultured for 24 hours after 30 minutes of cytochalasin D treatment.

So far, our data indicated that periosteum/perichondrium cells can inhibit cartilage growth through the expression of a growth-modulating soluble, and that the amount of intracellular tension that can be generated via the actin filament network is at the base of this mechanism. The ultimate test to prove this postulated mechano-regulated mechanism was by showing that conditioned medium from periosteum cells cultured on 80 kPa stiff substrates was able to counter all extended growth induced by stripping of the bones. The cartilage in these stripped bones, supplied with 80 kPa conditioned medium, grew at identical rates compared to intact tibiotarsi in the presence of unconditioned medium (figure 4.6).

a   b
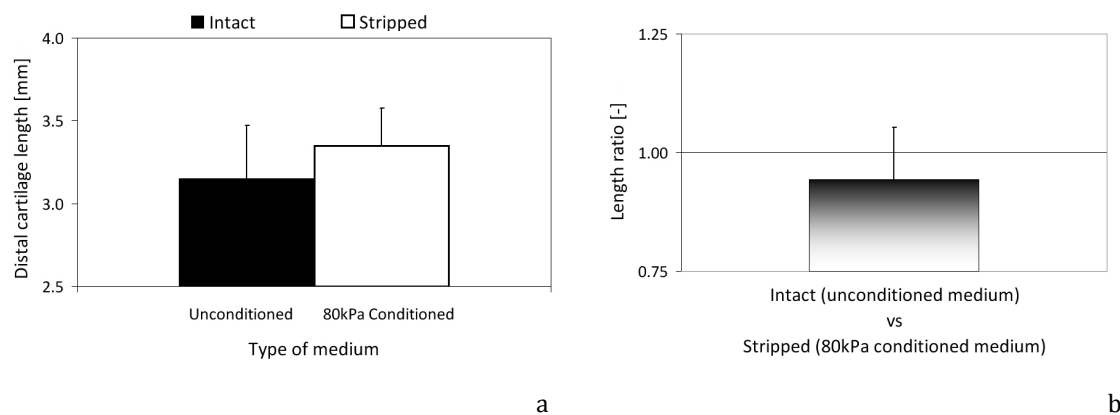
Figure 4.6: Length measurements for paired tibiotarsi: intact in unconditioned medium versus stripped in 80kPa conditioned medium. (a) Distal cartilage length. (b) Length ratio of the experimental pairs. No significant difference was detected in cartilage length between intact bones cultured in unconditioned medium, and stripped bones cultured in conditioned medium from cells seeded on 80 kPa substrates (paired t-test, n = 4).

4.5 Discussion

This study explored the mechanism through which periosteum/perichondrium cells are responsible for modulating cartilage extension in growing bones. Prior research (Di Nino et al., 2001) showed that soluble factors are involved. We followed this by suggesting a mechanism in which the expression of these factors is mechano-regulated, i.e. that they would only be expressed by periosteum/perichondrium cells when these are able to develop sufficient intracellular tension. We explored this hypothesis by

culturing bone rudiments in the presence of unconditioned medium or conditioned medium from periosteum/perichondrium cells that were limited in their ability to develop intracellular tension. Intracellular tension was modulated by varying the stiffness of the substrate on which the cells were grown, or by disrupting their actin filament network. Indeed, the combination of different sets of experiments allowed us to conclude that (1) a mechanism prevails in which periosteum/perichondrium cells are able to modulate bone growth through secreted solutes, (2) that these solutes have an inhibiting effect on cartilage growth, (3) that this mechanism is mechano-regulated, and (4) that the ability of the periosteum/perichondrium cells to develop intracellular tension is at the base of this mechano-regulation pathway.

An elegant mechano-regulated feedback mechanism for physiological bone growth emerges from our observations. When cartilage growth is relatively fast, periosteum becomes tensioned. This could introduce intracellular tension in periosteum cells directly through focal adhesions (elaborated on later) or by stiffening of their environment through collagen alignment and straining. This stimulates them to express growth-inhibiting factors, which subsequently normalize the enhanced cartilage growth rate. Vice versa, the same mechano-regulated control loop would allow recovery of delayed growth, because periosteum tension would drop if cartilage did not expand sufficiently. To establish whether this feedback mechanism also prevails *in vivo*, it remains to be determined whether soluble factors produced by cells in our model system match those produced *in vivo*.

The conclusions in this study were drawn on the response of periosteum/perichondrium cells when their ability to contract was modulated. The first approach to modulate contractility was by altering the stiffness of the substrate they were exposed to. Substrate stiffness is emerging as an important physical factor in the response of many cell types. Compared to soft substrates, cells cultured on stiff substrates produce larger traction forces (Lo et al., 2000; Wang et al., 2000), have more stable (Discher et al., 2005; Pelham, Jr. and Wang, 1997) and larger focal adhesions (Goffin et al., 2006), a more organized actin filament network (Discher et al., 2005; Engler et al., 2004; Schwarz and Bischofs, 2005), and a larger projected cell area (Engler et al., 2004; Lo et al., 2000; Pelham, Jr. and Wang, 1997; Wang et al., 2000; Yeung et al., 2005). Substrate stiffness also affects protein expression (Lee et al., 1984; Pelham, Jr.

and Wang, 1997; Yeung et al., 2005). Many of these aspects have directly or indirectly been shown to hold for fibroblasts, present in periosteum and perichondrium.

The second approach to modulate cell contractility was through addition of cytochalasin D. This inhibits fibroblast contractile properties by disrupting the actin filament network (Bell et al., 1979; Guidry and Grinnell, 1985; Guidry and Grinnell, 1987), which clearly occurred within 30 minutes in our setup. After incubation, the cells were thoroughly washed to ensure that cytochalasin D would not be transferred with the conditioned medium to the tibiotarsi in the organ cultures. Subsequently, cells were cultured 24 hours in serum-free medium, in which the actin network was expected not to recover (Tomasek and Hay, 1984). Small aggregates of actin and less organized stress fibers compared to untreated cells after 24 hours confirmed this theory (figure. 4.5). A 30 minutes incubation period therefore appeared sufficient to achieve the desired effect, and this effect lasted the 24 hours, required for producing conditioned medium.

Both the variation in substrate stiffness and application of cytochalasin D to cells in culture modulated the ability of the perichondrium/periosteum cells to actively develop intracellular tension via their actin filament network. Both approaches affected the expression of growth-modulating factors in ways that were in agreement with our hypothesis. Whether intracellular tension, generated by passively stretching the periosteum cells, would have the same effect is speculative. However, it has been proposed that mechanotransduction, e.g. in focal adhesions, depends on the development of stresses that are generated by a balance of external forces and cell-generated forces, resulting in signaling (Chen, 2008). We assume that *in vivo* it is indifferent to the cells whether the intracellular tension is induced by external tissue straining or by active cell contraction.

Cells were seeded at similar densities onto the gels, 48 hours before collection of conditioned medium (24 hours for proper attachment of the cells to the gels and another 24 hours in serum-free medium). If proliferation or apoptosis would strongly influence the number of cells substrate-stiffness dependently, as was documented for NIH 3T3 cells (Wang et al., 2000), this could confound our data. However, our data provide indirect evidence that cell numbers were not affecting our results. For instance, after treatment with cytochalasin D, cartilage length differed between stripped bones that were both supplied with conditioned medium from 80 kPa. Similarly, we did not

encounter any unexpected differences between the periosteum/perichondrium cell cultures on standard well plates (Greiner Bio One) and the softer matrigel. Although it is known that extracellular matrix composition may change cell behavior (Boonen et al., 2009; Macfelda et al., 2007; Maley et al., 1995), experimental results from both types of substrates are in agreement with our theory.

In conclusion, this study provides experimental support for the hypothesis that modulation of cartilage growth via the release of soluble factors from periosteum/perichondrium cells depends on the amount of intracellular tension the cells can generate. Based on this evidence, we postulate a mechanobiological feedback loop between growing cartilage and tension in the periosteum, whereby the expression of soluble growth-inhibiting factors by periosteum cells is dependent on intracellular tension. This work has significantly improved our understanding of an important feedback system that controls long bone growth. Together with future identification of the involved mechano-sensitive soluble factors, this insight results in increased understanding of bone development and regulation of cartilage growth.

4.6 Acknowledgements

Chapter 5

An Adaptation Mechanism for Fibrous Tissue to Sustained Shortening

5.1 Abstract

The mechanism by which fibrous tissues adapt upon alterations in their mechanical environment remains unresolved. In this chapter, we determine that periosteum in chick embryos resides in an identical mechanical state, irrespective of the developmental stage. This state is characterized by a residual tissue strain that corresponds to the strain in between the pliant and stiffer region of the force-strain curve. We also demonstrate that periosteum is able to regain that equilibrium state *in vitro* within three days upon disturbance of that equilibrium state. This adaptation is not dependent on protein synthesis, because the addition of cycloheximide did not affect the response. However, a functional actin filament network is required, as is illustrated by a lack of adaptation upon tissue shortening in the presence of cytochalasin D. This led us to hypothesize that cells actively reduce collagen fiber crimp after tissue shortening; i.e. that in time the number of recruited fibers is increased via cell contraction. Support for this mechanism is found by visualization of fiber crimp with multi-photon microscopy before the perturbation and at different time points during the adaptive response.

5.2 Introduction

Fibrous tissues have the ability to adapt to their mechanical environment. The direction and magnitude of imposed load can lead to adapting structural and mechanical properties. This is important for proper functioning of all fibrous tissues, especially those with a load-bearing capacity such as tendons, ligaments, and tissue-supporting fibrous sheets. The mechanism by which fibrous tissues adapt to alterations in their mechanical environment remains unresolved. Such knowledge would be helpful to guide repair and engineering of fibrous tissues.

Structural changes of a collagenous matrix subjected to different mechanical environments have been studied under well-controlled *in vitro* conditions in the 'fibroblast-seeded collagen gel' model system. Upon embedding fibroblasts into a collagen gel, contraction will occur via interaction between collagen and embedded cells. Freely contracting collagen gels have inferior ultimate stress and material modulus and larger ultimate strain compared to statically loaded equivalents (Feng et al., 2006b). Additionally, a disorganized distribution of cells (Henshaw et al., 2006; Nakagawa et al., 1989) and absence of collagen alignment is observed in freely contracting constructs (Henshaw et al., 2006) and in biaxially constrained gels that remain mechanically isotropic (Henshaw et al., 2006; Thomopoulos et al., 2005). In contrast, uniaxially constrained gels develop high degrees of cell and fiber alignment and mechanical anisotropy (Henshaw et al., 2006; Huang et al., 1993; Nakagawa et al., 1989; Thomopoulos et al., 2005; Wakatsuki and Elson, 2003). This is accompanied by gel contraction, generating substantial contraction force (Bell et al., 1979; Dodd et al., 1982; Feng et al., 2006a; Grinnell and Lamke, 1984). Gel contraction is cell-mediated, as contraction is absent in cell deprived collagen gels (Bell et al., 1979; Eastwood et al., 1996; Grinnell and Lamke, 1984; Guidry and Grinnell, 1985), and in fibroblast seeded gels in the presence of the actin polymerization inhibitor cytochalasin B (Bell et al., 1979; Guidry and Grinnell, 1985). Observed structural and geometrical changes in these collagen gels can be explained by passive (Mosler et al., 1985; Puxkandl et al., 2002), and by cell-mediated, active reorientation of collagen fibers (Brown et al., 1998;

Grinnell and Lamke, 1984; Guidry and Grinnell, 1985; Harris et al., 1981; Meshel et al., 2005; Sawhney and Howard, 2002; Stopak and Harris, 1982).

The mechanism by which fibroblasts mechanically reorganize collagen matrices strongly depends on the magnitude and direction of applied load. Increased fibroblast contraction is observed upon a decrease in external loading, while a reduction is observed upon increased external loading (Brown et al., 1998; Petroll et al., 2004; Tomasek et al., 1992). This response of fibroblasts to attain tensional homeostasis (Brown et al., 1998) features analogy with the behavior of fibrous tissues. Namely, increased tissue strain is dissipated via the viscous properties of collagen fibers, reorientation of these fibers in the matrix (Puxkandl et al., 2002; Sawhney and Howard, 2002), and mechanical disruption or degradation of overstretched fibers in the long term (Ellsmere et al., 1999; Huang and Yannas, 1977). To meet the new demands, additional collagen is synthesized in response to increased tissue load (Curwin et al., 1988; Kim et al., 2002; Parsons et al., 1999; Wang et al., 2003; Yang et al., 2004) and the diameter of existing fibrils is increased (Michna, 1984; Michna and Hartmann, 1989). Decreased tissue strain is restored via cell-mediated tissue contraction (Brown et al., 1998; Petroll et al., 2004; Tomasek et al., 1992), preferential cleavage of unstrained fibers (Ellsmere et al., 1999; Huang and Yannas, 1977; Nabeshima et al., 1996; Ruberti and Hallab, 2005) and tissue compaction via the presence of residual strain (Bertram et al., 1998; Popowics et al., 2002).

These responses suggest a mechanism by which fibrous tissues adapt towards homeostasis, characterized by a particular mechanical equilibrium. In search of this tissue equilibrium and to propose a mechanism for the adaptation behavior, a step-by-step approach was adopted. (1) Determine whether growing fibrous tissues indeed attain a specific mechanical state *in vivo*, irrespective of its length and developmental stage ('native adaptation'). (2) Evaluate *in vitro* if this specific mechanical state, considered as the preferred mechanical equilibrium, is restored upon disturbance ('stretch-dependent adaptation'). (3) Assess the time-scale at which this equilibrium is recovered ('transient adaptation'). (4) Determine whether adaptation is based on passive tissue behavior, or that protein synthesis and/or cell contractile properties contribute to this adaptation process ('blocking cell-mediated adaptation'). (5) Propose

a mechanism for fibrous tissue adaptation, by visualizing the structure of the collagen network during the adaptation process ('visualization of the collagen network').

By following this approach, we evaluated the hypothesis that fibrous tissues adapt towards homeostasis characterized by a particular mechanical equilibrium; and to propose a mechanism for the adaptive behavior upon geometric changes.

5.3 Materials and method

5.3.1 Tissue preparation

Fertilized eggs of White Leghorn chickens ('t Anker, Ochten, The Netherlands) were placed in a polyhatch incubator (Brisnea, Stanford, UK). After a 15-, 16-, 17- or 18-day period of incubation, i.e. Hamburger and Hamilton stage 41 to 44 (Hamburger and Hamilton, 1992), chick embryos were removed from the eggs and euthanized by decapitation. Tibiotarsi were carefully dissected, without damaging the periosteum. A longitudinal incision through the periosteum over the entire length of the diaphysis was made adjacent to the fibula. The fibula was removed by cutting the proximal and distal end with scissors. The longitudinal incision was used to guide two sutures (5.0 Vicryl, Ethicon, Johnson & Johnson Medical, Amersfoort, The Netherlands) in between bone and the periosteum. The needles connected to the sutures were removed and the sutures were guided through mixing needles without bevel (Terumo Europe, Leuven, Belgium). The tibiotarsus was fixed in an ElectroForce LM1 TestBench (Bose, Framingham, MA, USA) and grippers were displaced until the 2N load cell (Sensotec, Honeywell, Apeldoorn, The Netherlands) indicated a stressless situation. At this *in vivo* length, suture wires were moved towards the proximal and distal insertion of the periosteum to the cartilage. Subsequently, suture wires were pulled through the mixing needles to cut the proximal and distal metaphyseal cartilage. Mineralized bone tissue could then be extracted with the periosteum held at *in vivo* length (method is illustrated in figure 5.1, and previously described (Foolen et al., 2009), see chapter 3). From *in vivo* length, the tissue was subjected to procedures as described in the study design (paragraph 5.3.2).
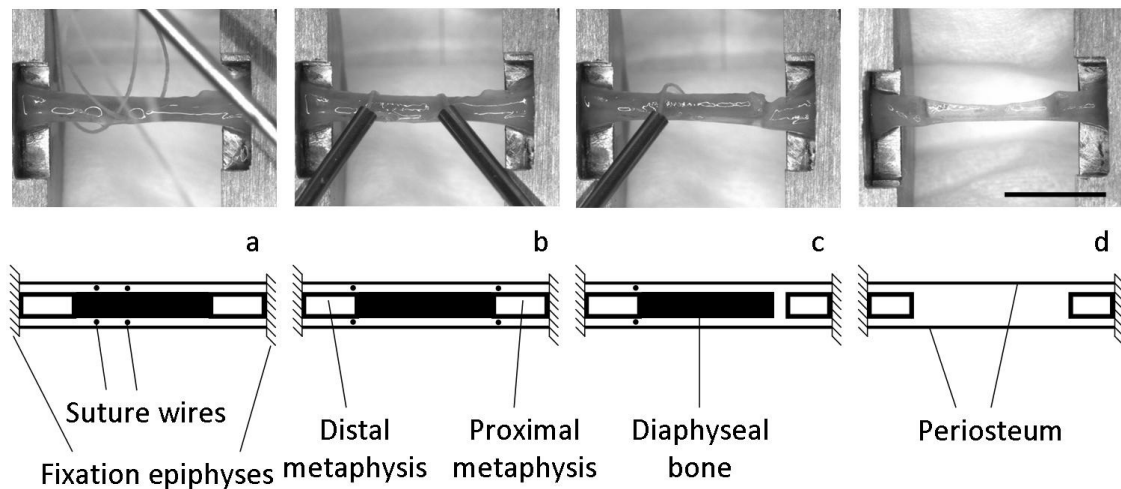
Figure 5.1: Subsequent steps in the mechanical test protocol. Digital images (top row) and corresponding illustrations (bottom row). (a) After making a single longitudinal cut with a scalpel alongside the fibula, which was subsequently removed, suture wires were guided in between bone and the periosteum. (b) At *in vivo* length, suture wires were moved proximal and distal. (c) Suture wire has cut the proximal metaphyseal cartilage and (d) bone tissue was removed after cutting through the distal metaphyseal cartilage, with the periosteum held at *in vivo* length. Scale bar represents 10mm. Figure is adopted from Foolen and coworkers (Foolen et al., 2009), see chapter 3.

5.3.2 Study design

Native adaptation (1)

Immediately after extraction of mineralized tissue from e15 to e18 tibiotarsi in the ElectroForce LM1 TestBench (Bose), the tissue was mechanically characterized (n= 12 per age group). A standardized force-stretch curve was obtained by shortening the periosteum to 0.75 times the *in vivo* length and subsequently straining the tissue to failure at 0.1%/sec. Mechanical adaptation was assessed by determining the transition point between the low and high stiffness of the force-stretch curve. This point was defined as the tangent to the force-stretch curve of 1/8th of the slope in the linear stiffness region (figure 5.2). After mechanical characterization, periosteum was disposed of remaining tissue and stored at -30oC until further analysis.
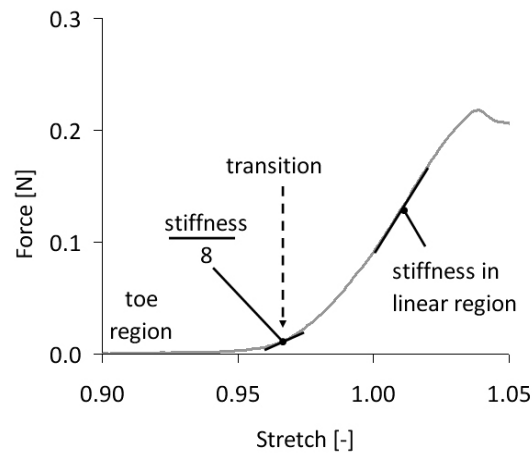
Figure 5.2: Illustration of the transition stretch of an arbitrary force-stretch curve. Transition stretch is defined as the stretch value where the tangent of the force-stretch curve is equal in slope to that in the linear stiffness region divided by 8. The rationale for taking this value is elaborated on in the discussion. 'Stretch' is calculated from the reference value of 1.00, corresponding to *in vivo* length.

Stretch-dependent adaptation (2)

Starting from *in vivo* length, periosteum of e15 tibiotarsi was stretched to 0.85, 0.90, 0.95, 1.00 or 1.05 times *in vivo* length (n=4 for all stretch groups) and subsequently cultured for 3 days while stretch was maintained in the ElectroForce LM1 TestBench. Experiments were performed in complete medium containing DMEM (Gibco, Invitrogen, Breda, The Netherlands), 10% FBS and 1% penicillin/streptomycin (Lonza, Walkersville, USA). The medium was kept at 37.5^0C during culturing, by circulating heated water through submerged tubing, and controlling the temperature of this circulating water based on the medium temperature, monitored close to the sample by a thermocouple. After culturing, the standardized force-stretch curve was obtained, and periosteum was stored at -30^0C until further analysis. An overview of all *in vitro* experiments (study designs 2 to 4) is depicted in table 5.1.

Transient adaptation (3)

Starting from *in vivo* length, periosteum from e15 tibiotarsi was stretched to 0.95 times *in vivo* length and evaluated after 1, 2 and 4 days of culturing (n=4, for each group). Culture conditions were exactly as described in study design (2): 'stretch-dependent

adaptation'. After mechanical evaluation, tissues were stored at -30⁰C until further analysis. Data from the 0.95 stretch group cultured for 3 days, and native e15 (representative for 0 hours in culture at 0.95 stretch) were adopted from study design (1): 'native adaptation' and study design (2): 'stretch-dependent adaptation'.

Blocking cell-mediated adaptation (4)

The setup of this experiment was identical to study design (2): 'stretch-dependent adaptation', however, the complete medium was supplemented with cytochalasin D (10μg/ml, Sigma, St. Louis, MO, USA) and/or cycloheximide (25μg/ml, Sigma). Cytochalasins inhibit matrix contraction by disrupting the actin filament network of the fibroblasts (Bell et al., 1979; Guidry and Grinnell, 1985; Guidry and Grinnell, 1987). Cycloheximide blocks protein synthesis by cells (Guidry and Grinnell, 1985). Cycloheximide treated samples were stretched to 0.95 and 1.05 times *in vivo* length (n=4 for both groups) and cultured for 3 days. Samples treated with both cytochalasin D and cycloheximide were stretched to 0.95 times *in vivo* length and cultured for 3 days. Mechanical evaluation and storage until further analysis were performed as described earlier (study design (1): 'native adaptation'). Data from the 0.95 and 1.05 stretch groups, cultured for 3 days, were adopted from study design (2): 'stretch-dependent adaptation'.

Table 5.1: Overview of *in vitro* experiments. Stretch was applied from 0.85 to 1.05 times *in vivo* length (L_0) and tissue was cultured for 1, 2, 3 or 4 days. CH=cycloheximide was added to complete medium; CD=cytochalasin D was added to complete medium.

Stretch:	$0.85 \cdot L_0$	$0.90 \cdot L_0$	$0.95 \cdot L_0$	$1.00 \cdot L_0$	$1.05 \cdot L_0$
1			n=4		
2			n=4		
3	n=4	n=4	n=4 n=4, CH n=4, CH & CD	n=4	n=4 n=4, CH
4			n=4		

Days of culture
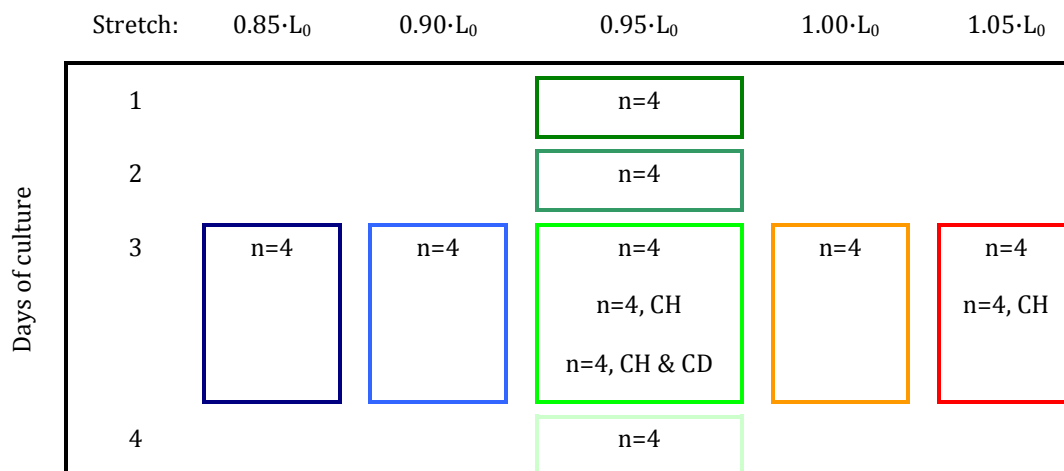
Visualization of the collagen network (5)

After tissue harvesting was performed, as described in paragraph 5.3.1., periosteum was stretched to 0.90 times *in vivo* length in a custom build device that could be mounted on a microscope stage. The central diaphyseal periosteum was scanned before as well as 1 and 72 hours after applying the stretch. During culturing, with or without supplemented cycloheximide and cyctochalasin D, the custom built device was placed in an incubator (37^0C, $5\%CO_2$). Two hours prior to scanning, the medium was supplemented with 3µM Cell Tracker Blue (Molecular Probes, Invitrogen, Breda, The Netherlands), 10µM Propidium Iodide (Molecular Probes) and 25µM CNA35 probe (Krahn et al., 2006) to visualize living cells, dead nuclei, and collagen, respectively. The CNA35 protein is known to have a high affinity for collagen I relative to other collagen types and shows very little cross reactivity with noncollagenous extracellular matrix proteins. Conjugation of this protein to a fluorescent dye yields the formation of a highly specific probe for collagen imaging (Krahn et al., 2006). The custom built stretch device was mounted on a multiphoton microscope (Zeiss LSM 510 META NLO, Darmstadt, Germany) in Two-Photon-LSM mode. The excitation source was a Coherent Chameleon Ultra Ti:Sapphire laser, tuned and mode-locked at 763 nm. This wavelength resulted in the highest intensity profile for the collagen probe. Laser light was focused on the tissue with a Plan-Apochromat 40x/0.8 numerical aperture water objective, connected to a Zeiss Axiovert 200M. The pinhole of the photo-multiplier was fully opened. Photo-multipliers accepted wavelength regions of 435-485, 500–550 and 600-640 nm for Cell Tracker Blue, CNA35, and Propidium Iodide, respectively. All single images were obtained from Z-stacks, taken through the periosteum. No additional image processing was performed.

5.3.3 DNA and GAG content

After lyophilization, samples were digested in papain solution (100 mM phosphate buffer, 5 mM L-cystein, 5 mM EDTA and 125-140 µg papain per ml) overnight at 60°C. After digestion, the samples were centrifuged and the supernatant was used for both DNA and GAG assays. For measuring DNA quantity, the Hoechst dye method (Cesarone

et al., 1979) was used. The supernatant was diluted in TE-buffer (10 mM Tris, 1mM EDTA, pH 8.0) and DNA was labeled using the Hoechst dye (Fluka, Sigma, USA) working solution (10 mM Tris, 1 mM EDTA, 2 M NaCl, pH 7.4 and 2.5 µg Hoechst dye per ml). After incubation in a dark environment for 10 minutes on a plate shaker at room temperature, fluorescence was measured using a plate reader (excitation 360 nm, emission 460 nm, Bio-Tek, Winooski, USA) and DNA quantity was determined from a standard curve prepared from calf thymus DNA (Sigma). The GAG content was determined using a modified version of the protocol described by Farndale and coworkers (Farndale et al., 1986). In short, 40 µl of supernatant was pipetted into a flat bottom 96-well plate in duplicate. To each well 150 µl of DMMB color reagent (46 µM dimethylmethylene blue, 40.5 mM glycin, 40.5 mM NaCl, pH 3.0) was added. Absorbance was measured at 540 nm and 595 nm and the difference calculated. GAG amount was determined from a standard curve prepared from chondroitin sulphate from shark cartilage (Sigma). For native adaptation; n=16, 14, 14 and 12 for embryonic ages 15, 16, 17 and 18, respectively. For all *in vitro* experiments; n=4 for all groups.

5.3.4 Collagen content and HP crosslink density

Lyophilized tissue samples were hydrolyzed in 6M hydrochloric acid (Merck, Germany) and used for amino acid and crosslink analyses. Hydroxyproline residues were measured on the acid hydrolysates using reverse-phase high-performance liquid chromatography after derivatization with 9-fluorenylmethyl chloroformate (Fluka) (Bank et al., 1996). The same hydrolysates were used to measure the number of the mature HP crosslinks, using high-performance liquid chromatography as described previously (Bank et al., 1997; Robins et al., 1996). For native adaptation; n=16, 14, 14 and 12 for embryonic ages 15, 16, 17 and 18 respectively. For all *in vitro* experiments; n=4 for all groups.

5.3.5 Statistics

One-Way ANOVA was used to determine the effect of the selected independent variable (embryonic age, applied stretch, culture time, or addition of blocking agent) and its interaction with a dependent variable (transition stretch, stiffness, amount of GAG, DNA and collagen, and HP crosslink density). The p-value was corrected with the Bonferroni criterion. Linear regression analysis was used to determine the relationship between embryonic age, applied stretch or culture time with transition stretch, tissue stiffness and biochemical composition (GAG, DNA, collagen and HP crosslinks). Paired sample comparison (paired t-test) was performed to determine significant differences in applied stretch and measured transition stretch at each time point in samples stretched to 0.95 times *in vivo* length evaluated after 0, 1, 2, 3 or 4 days. P-values <0.05 were considered statistically significant.

5.4 Results

5.4.1 Native adaptation (1)

At all embryonic ages (e15 – e18), the *in vivo* length of the periosteum (corresponding to 1.00 stretch, figure 5.3a) maintained the tissue at its stiffness transition point, quantified by assessing the corresponding stretch value (figure 5.3b). Hence, although periosteum can grow up to 25%/day between the embryonic ages studied (Foolen et al., 2008), the *in vivo* periosteum length always adapted to maintain the tissue at a similar stiffness transition, indicating adaptation towards a preferred mechanical equilibrium. Tissue stiffness increased significantly with embryonic age (p=0.000, R^2=0.83, figure 5.3c), which can in part be attributed to an increase in circumference of the periosteum with age (Foolen et al., 2008), see chapter 2. In relationship to embryonic age, DNA content decreased (p=0.000, R^2=0.31), while both collagen content and HP crosslink density increased (p=0.002, R^2=0.17 & p=0.000, R^2=0.71, respectively). GAG content showed no relationship with embryonic age (p=0.42, figure 5.3d).

a

b

c

d
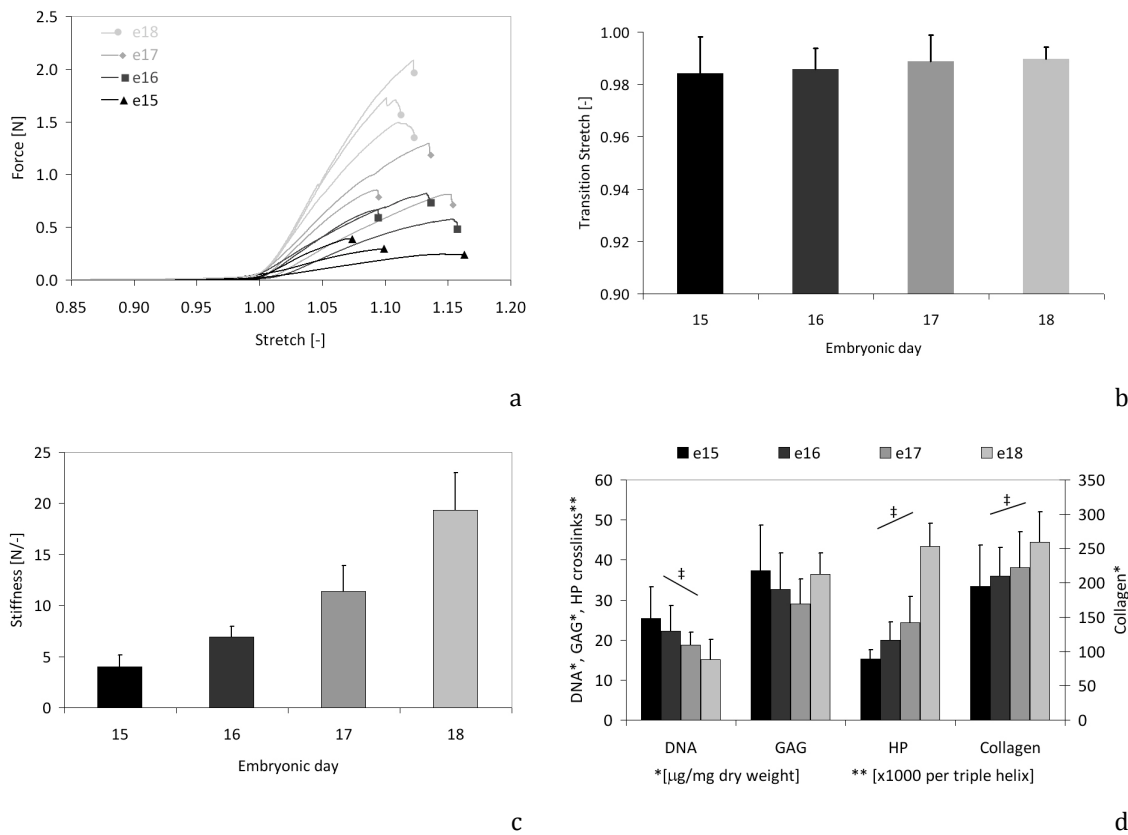
Figure 5.3: Periosteum properties in native adaptation. (a) Representative force-stretch curves of native e15 to e18 chick periosteum. *In vivo* length corresponds to a stretch value of 1.00. For the sake of clarity only 3 curves per embryonic age are shown (n=12). (b) Stretch values matching the stiffness transition of native e15 to e18 chick periosteum, representative for the *in vivo* loading state. (c) Tissue stiffness showed a positive relationship with developmental age (R^2=0.83). (d) DNA, GAG, HP crosslink and collagen content of native periosteum. ‡ indicates a significant relationship with age for DNA (R^2=0.31), HP crosslinks (R^2=0.71) and collagen (R^2=0.17). For all ages, n=12.

5.4.2 Stretch-dependent adaptation (2)

The results of study (1): 'native adaptation', imply that a change in periosteum length triggers adaptation towards a mechanical equilibrium, which is the stiffness transition region. In support of this hypothesis, we showed that after artificially inducing a length change over a range of -10% to +5% in our *in vitro* culture system, the transition stretch approximated the applied stretch after 3 days of culturing (figure 5.4a & b). Only at a length change around -15%, an offset became apparent (figure 5.4b). This shows that upon a change in length, periosteum is able to mechanically adapt by shifting its stiffness transition point to the current length. The shape of the curve also changed, with an increased heel region length towards lower applied stretch values (figure 5.4a). An important finding is that tissue stiffness (figure 5.4c) increased significantly with applied static stretch (p=0.000, R^2=0.73). Hereby, stiffness of the 1.05 stretch group was significantly higher after 3 culture days compared to native e15 periosteum, but all stretch groups had significantly lower stiffness compared to native e18 periosteum (One-Way ANOVA). No relationship was found between applied stretch and DNA or GAG content (figure 5.4d, p=0.78 & p=0.16, respectively). Collagen content and HP crosslink density showed a negative relationship with applied stretch (figure 5.4d, p=0.011, R^2=0.31 & p=0.015, R^2=0.29, respectively). All stretch groups were not significantly different to DNA content of native periosteum at any age between e15 and e18 (One-Way ANOVA). However, DNA content corresponded most to native e18 periosteum. HP crosslink density in all stretch groups after 3 days of culture was significantly higher than native e15, but not different from native e18 periosteum (One-Way ANOVA).
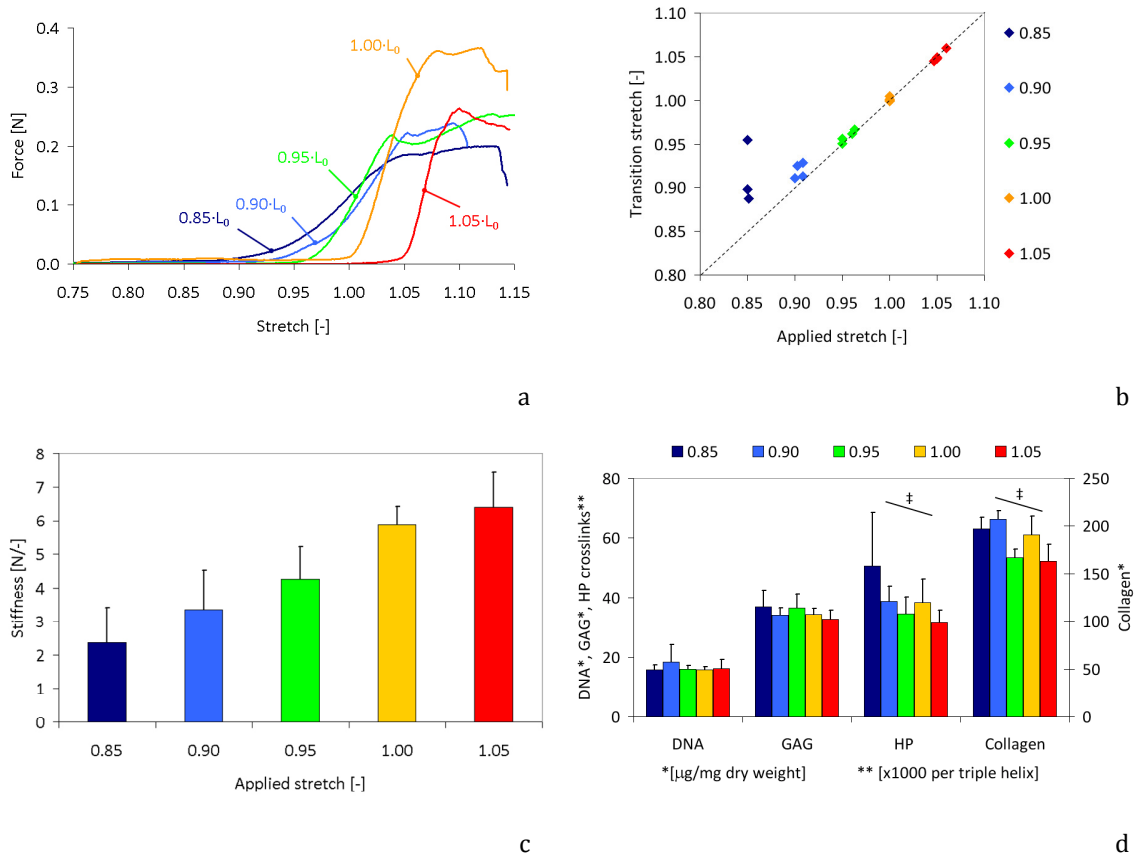
Figure 5.4: Properties of periosteum after stretch-dependent adaptation. (a) Representative force-stretch curves of experimentally stretched periosteum (stretched to 0.85, 0.90, 0.95, 1.00 and 1.05 times L_0, i.e. *in vivo* length. For clarity, only one measurement per group is shown (n=4). (b) Transition stretch versus the stretch applied to experimental samples for 3 days. The dashed line represents a 1:1 ratio and is indicative for complete mechanical adaptation. Each measurement is represented by one diamond, i.e. the graph shows 20 diamonds in total, but some diamonds overlap. (c) Tissue stiffness showed a positive relationship with applied stretch (R^2=0.73). (d) DNA, GAG, HP crosslink and collagen content. ‡ indicates a significant relationship with applied stretch for HP crosslink density (R^2=0.29) and collagen content (R^2=0.31). For all groups, n=4.

5.4.3 Transient adaptation (3)

The shift in transition stretch gradually developed (figure 5.5a & b) and was most dominant during the first two days of culturing (figure 5.5b). No significant difference was detected between applied stretch and measured transition stretch from day 3 (figure 5.5b, paired t-test). A non-significant drop in stiffness was observed after 4 days of culture (figure 5.5c). DNA content showed a negative relationship (p=0.001, R^2=0.31) and HP crosslink density a positive relationship (p=0.000, R^2=0.63) with culture time. From the first culture day on, HP crosslink density was significantly higher compared to native e15 periosteum. Interestingly, the slopes of regression in DNA and HP crosslinks with time were the same *in vivo* and *in vitro* (figures 5.3d and 5.5d compared). GAG and collagen content showed no transient response (figure 5.5d, p=0.58 & 0.17, respectively).
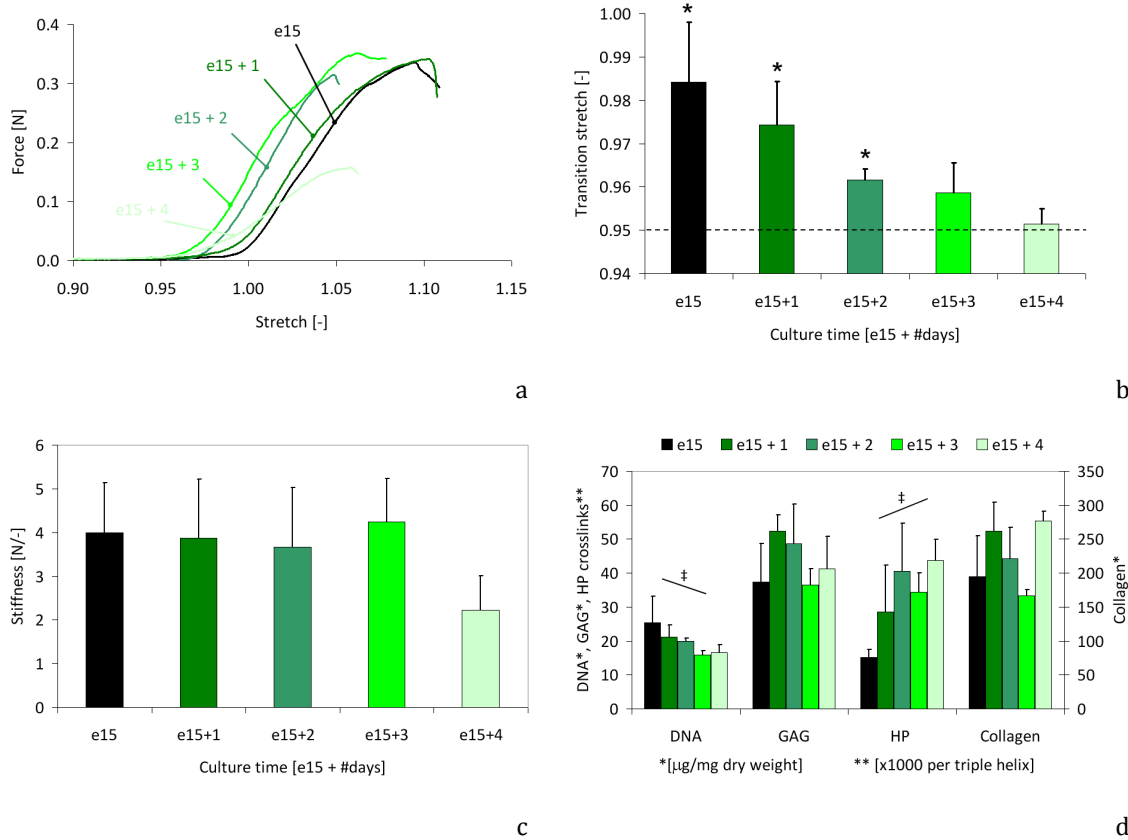
Figure 5.5: Periosteum properties after time-dependent adaptation at 0.95 times *in vivo* length. (a) Representative force-stretch curves of experimentally stretched periosteum cultured up to 4 subsequent days. For clarity, only one measurement per group is shown (n=12 for e15, n=4 for e15 + # of days in culture). (b) Transient response of the transition stretch. Asterisks denote a significant difference between applied stretch and transition stretch (paired t-test). (c) Transient response of the tissue stiffness. A non-significant decrease in stiffness was observed at time point e15+4. (d) DNA, GAG, HP crosslink and collagen content. ‡ indicates a significant relationship with age for DNA (R^2=0.31) and HP crosslink (R^2=0.63). For comparison, the e15 and e15+3 groups were adopted from study (1): 'native adaptation' and study (2): 'stretch-dependent adaptation', respectively. For groups e15+1, 2 & 4, n=4.

5.4.4 Blocking cell-mediated adaptation (4)

Blocking protein synthesis by adding cycloheximide (CH) did not change the shift in transition stretch (figure 5.6a & b). However, blocking the ability of cells to contract by adding cytochalasin D (CD) in addition to CH, abolished the shift in transition stretch (figure 5.6a & b). Tissue stiffness of samples stretched to 0.95 times *in vivo* length treated with CH, was significantly lower compared to samples treated with both CH and CD (figure 5.6c). DNA and GAG content decreased in the presence of CH relative to samples in complete medium, but collagen content increased (figure 5.6d, One-Way ANOVA). Note that this does not mean that collagen is synthesized; selective loss of proteoglycans also induces these results. Addition of blocking agents (CD and/or CH) did not significantly change HP crosslink density.
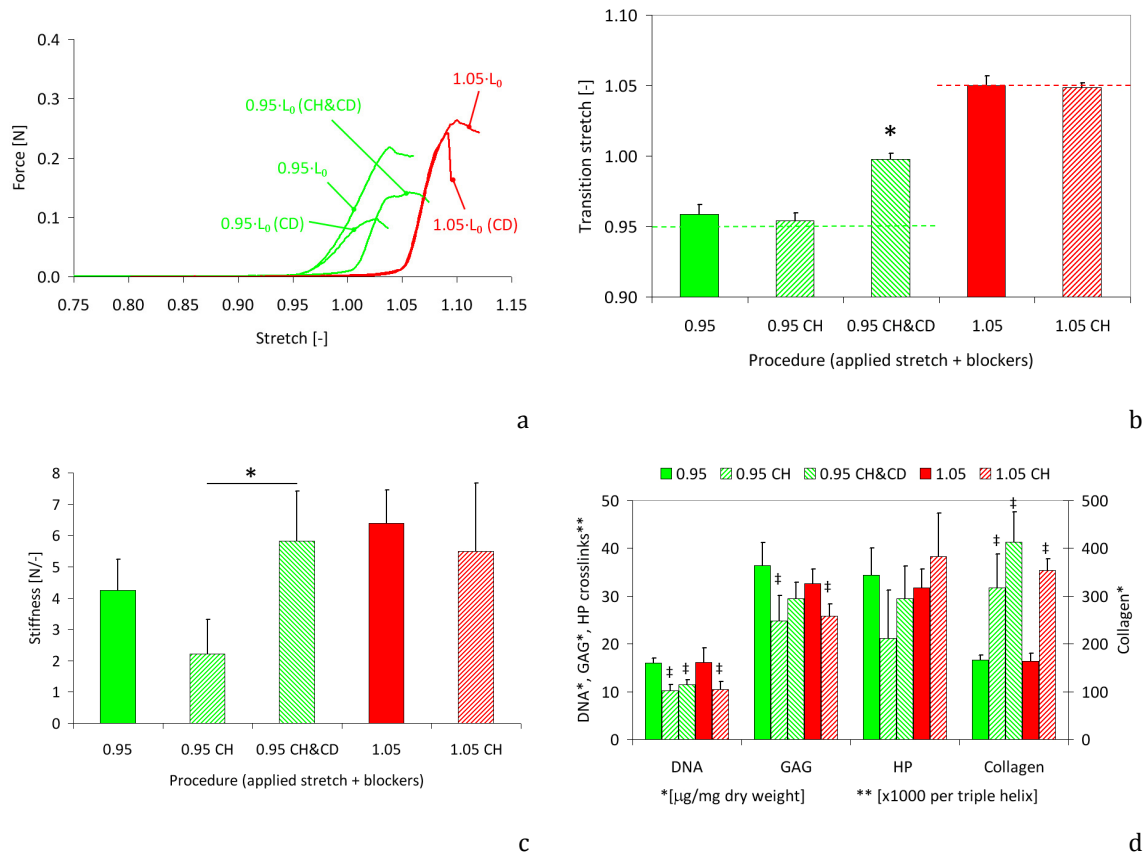
Figure 5.6: Properties of experimentally stretched periosteum, cultured for 3 days in the presence of blockers. (a) Representative force-stretch curves of periosteum (stretched to 0.95 and 1.05 times *in vivo* length), treated with CD and/or CH. For clarity only one measurement per group is shown (n=4). (b) Transition stretch of samples treated with CD and/or CH. Dashed green and red line represent the applied stretch (0.95 and 1.05, respectively). Asterisk denotes a significant difference from the applied stretch (paired t-test). (c) Stiffness of the CH treated group was significantly different from the CH & CD group, both stretched to 0.95 times *in vivo* length (One-Way ANOVA), denoted by the asterisk. (d) DNA, GAG, HP crosslink and collagen content of 3-day stretched samples. ‡ indicates a significant change in biochemical content, caused by the addition of blocking agents, relative to similarly stretched controls (One-Way ANOVA). For comparison, the 0.95 and 1.05 group were adopted from study (2): 'stretch-dependent adaptation'. For all groups, n=4.

5.4.3 Visualization of the collagen network (5)

The proportional relationship between applied stretch and tissue stiffness (figure 5.4c) did not result from increased collagen content or HP crosslink density (figure 5.4d), suggesting that tissue stiffness was dominated by structural changes of the collagen network. Furthermore, blocking protein synthesis alone had no effect on the shift in transition stretch, while disrupting the actin filament network with cytochalasin D prevented this shift (figure 5.6b). This suggests an adaptation mechanism that is independent of matrix protein expression, but highly dependent on the contractile properties of the cells. Evaluation of collagen morphology confirmed that tissue adaptation upon sustained shortening, involved a reorganization of the collagen fiber network, only when the cells had a functional actin filament network.

Native periosteum contains straight collagen fibers, oriented in the longitudinal direction (Foolen et al., 2008), see chapter 2. After mounting periosteum in the custom built stretch device and observing the tissue with multi-photon microscopy, this collagen morphology was confirmed (figure 5.7a & e). Immediately after shortening the tissue to 0.90 times the initial length, all collagen fibers were crimped (figure 5.7b & f). After 72h of culturing at 0.90 times the initial length, the fibers were predominantly straight, although a portion of them still displayed a crimped morphology (figure 5.7c & g). After 72h of culturing in the presence of CH and CD, all collagen fibers remained crimped (figure 5.7d & h). Both with and without CH and CD, cells remained viable over the culture period (figure 5.7i & j).
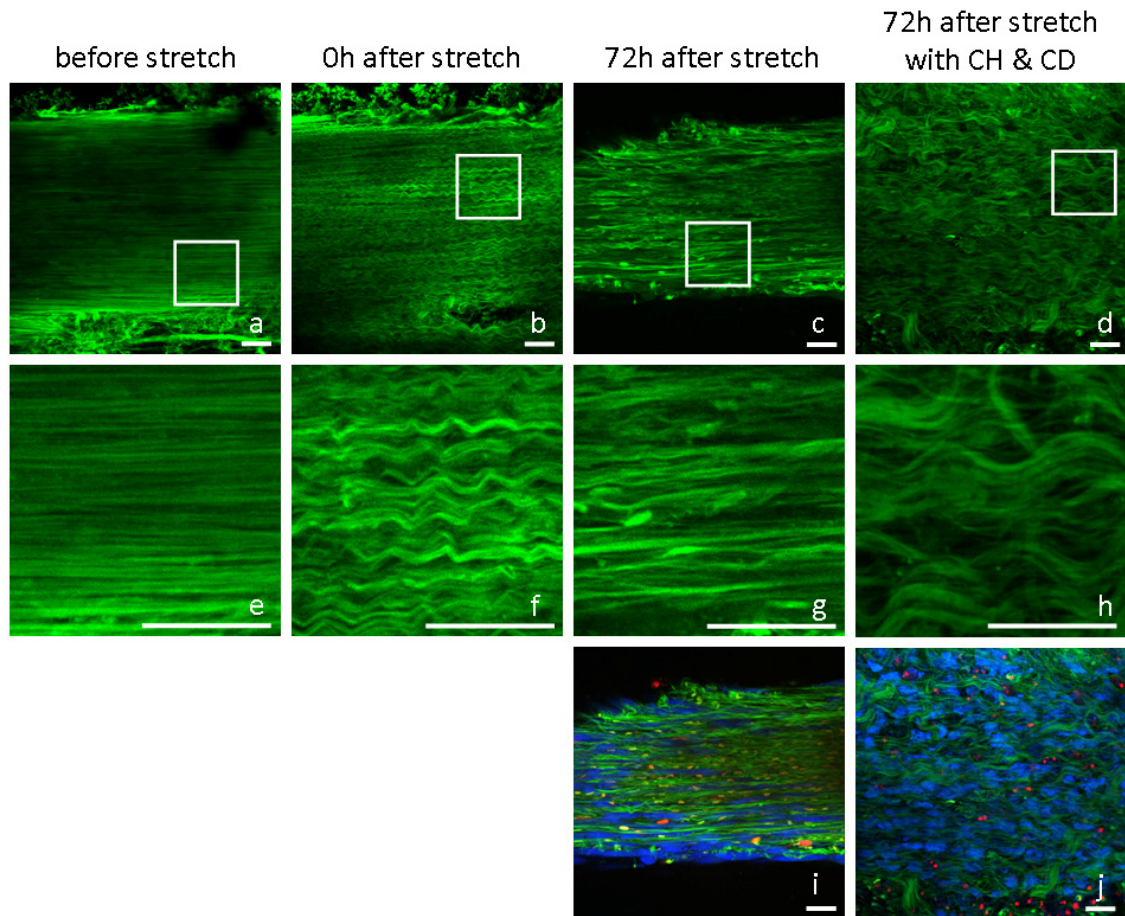
Figure 5.7: TPLSM images of collagen in periosteum of e15 chick tibiotarsi. Collagen morphology was visualized, using the CNA35 probe, before applying stretch as well as 1 and 72 hours (with or without addition of CH and CD) after applying stretch of 0.90 times the initial length. (a-d) Single images from Z-stacks. Procedure and time-point are indicated at the top. (e-h) Magnification of figures (a-d), indicated by the white box. (i & j) Images are identical to figure c & d, but now channels for viable cells (in blue; Cell Tracker Blue) and dead nuclei (in red; Propidium Iodide) are included. Objective 40x, NA 0.8. Scale bars represent 25μm.

5.5 Discussion

We hypothesized that adaptation directs fibrous cellular tissue towards mechanical equilibrium. We set out to test this hypothesis by characterizing this mechanical equilibrium. For this, force-stretch curves of growing native periosteum were evaluated. *In vivo*, the strain state corresponded to that of the heel region of the force stretch curve. Therefore, we postulated that native adaptation would drive periosteum towards a state, in which its stiffness is in the transition from pliant to much stiffer. Subsequently, we studied the involvement of cells in this adaptation process by monitoring *in vitro* the stretch-dependent and transient adaptation. In agreement with our hypothesis, upon induced alterations in tissue length, periosteum adapted by transiently restoring this preferred mechanical state. The underlying mechanism for the adaptive response was exposed by visualization of the collagen morphology upon shortening the tissue to 0.90 times the initial length. The resulting collagen fiber crimp was gradually reduced during three days of culturing. This process was cell-mediated and required a functional actin filament network; reduction of collagen crimp was absent in periosteum cultured in the presence of cycloheximide and cytochalasin D. Interestingly, the structural organization of the collagen network, and not the collagen content or HP crosslink density, determined the stiffness of the tissue. Therefore, we conclude that changes in the force-stretch relationship upon shortening are caused by collagen crimp, while the adaptive response is due to a gradual straightening of the collagen fibers by active cell contraction via the actin filament network.

The consideration to use chick periosteum as a model system originated from the ability to subject the tissue to stretch regimes starting exactly from its very well defined *in vivo* length. Also, the collagen network was known to be well aligned (Foolen et al., 2008), see chapter 2, and periosteum is one of the few quasi-statically loaded tissues. Another advantage is that embryonic chick tibiotarsi have a high incremental growth rate (Church and Johnson, 1964) and therefore adapt at a very high rate. Periosteum can grow up to 25%/day (Foolen et al., 2008), see chapter 2, and still maintain low *in vivo* force (Foolen et al., 2009), see chapter 3.

Periosteum has a potential for osteogenesis (Augustin et al., 2007) and chondrogenesis (Emans et al., 2005; O'Driscoll et al., 1994; Ravetto et al., 2009). However, differentiation was negligible in our experiments, because GAG content did not change and mineralization was not observed. Therefore, extrapolation of the adaptation mechanism to other fibrous tissues remains valid.

In the ElectroForce LM1 TestBench (Bose), mechanical properties were determined by straining the tissues to failure at 0.1%/sec relative to their *in vivo* length. For visco-elastic tissue, stiffness increases with strain rate. Pilot studies showed that at the at low strain rate of 0.1%/sec, strain-rate-dependent effects are minimal. Yet, in fact, the applied strain-rate during failure testing was higher for samples that were adapted to a shorter length during culture. Correction of strain-rate to the newly acquired length would have enhanced the proportional relationship between applied stretch and stiffness, and would therefore have strengthened the relationship that was already determined.

Mechanical adaptation was assessed by determining the transition point between low and high stiffness on the force-stretch curve. For appropriate comparison, this transition point needed to be uniquely defined. We did that as follows. The transition point in unstretched samples (i.e. stretched to 1.00 times *in vivo* length, figure 5.4a & b) after 3 days of culture was considered the reference situation. In the force-stretch curve of these samples, the transition point between low and high stiffness was then defined as the point where stretch equaled 1.00. At this point, the tangent to the force-stretch curve appeared to equal 1/8th of the slope in the linear stiffness region. Subsequently, we used this characteristic to determine the transition point in each of the force-stretch curves for the other experimental conditions. It should be noted that the choice for the condition that exactly defines the transition point is arbitrary. However, an evaluation of our data showed that the results and conclusions are not sensitive to this definition (figure 5.8).
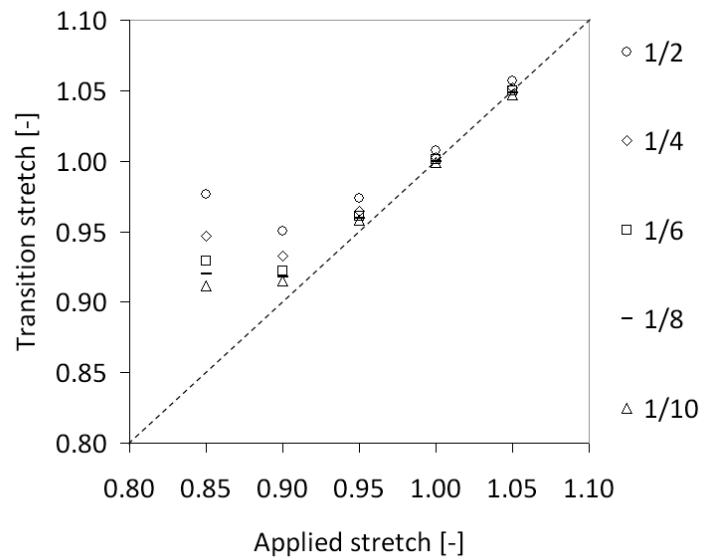
Figure 5.8: Sensitivity analysis on data from study 2: 'stretch-dependent adaptation'. Analysis is performed on the tangent to the force-stretch curve that equals the slope in the linear stiffness region divided by 2, 4, 6, 8 and 10. Each data point represents the average value of the group. At low applied stretch values, the transition stretch values are more sensitive to the chosen slope factor due to the increased length of the heel region. The transition stretch of samples stretched to 1.00 exactly matches *in vivo* length, when the tangent to the force-stretch curve equaled $1/8$th of the slope in the linear stiffness region.

While the TestBench allowed us to mount the tibiotarsus at *in vivo* length using feedback from the force-signal, the custom built stretch device for the microscope did not allow force measurement. A possible effect on initial tissue length is however minimal compared to the induced strains. Also, the fiber structure after mounting in the stretch device (figure 5.7a & e) resembles *in vivo* structure (Foolen et al., 2008), see chapter 2, very well, indicating a proper transfer of the *in vivo* situation to the experimental setup. The CNA35 probe (Krahn et al., 2006) used to visualize periosteal collagen in the custom built stretch device has a drawback of potentially preventing proper collagen fibril formation (Boerboom et al., 2007). We therefore chose to visualize separate samples per time point, instead of one sample at multiple times.

In study (3): 'visualization of the collagen network', we chose to apply a stretch of 0.90 times the initial length. We aimed at relating tissue mechanical properties to structural organization of the collagen network. The stretch-dependent adaptation experiment

revealed that tissue stiffness decreased after 3 culture days at 0.90 times *in vivo* length, while at 0.95 times *in vivo* length, such decrease was not present.

In post-hatched quails the *in vivo* strain state corresponded to that of the heel region of the force stretch curve, i.e. the strain where transition in stiffness from pliant to much stiffer behavior occurs (Bertram et al., 1998). This is in agreement with the *in vivo* loading state of periosteum in the current study.

HP crosslink density significantly increased with development in subchondral bone of newborn foals and tibial bones from male broiler breeder chickens (Rath et al., 2000). In our study, HP crosslink density also increased with developmental age, which may contributed to increased stiffness (Balguid et al., 2007). However, stiffness in the experimentally stretched samples was negatively related to HP crosslink density. We suggest changes in stiffness are dominated by structural reorganization of the collagen network, which conceals the effect of increased HP crosslink density on tissue stiffness.

It was observed that protein synthesis is not a requisite for tissue contraction, as addition of cycloheximide to the medium had no effect on a shift of the transition stretch, compared to untreated equivalents. This agrees with the observation that cycloheximide treated fibroblasts, in the presence of serum-containing medium, contract indistinguishably from untreated fibroblasts (Guidry et al., 1990; Guidry, 1992). Mechanically, removal of fibrous tissue load *in vitro* and *in vivo* results in decreased material modulus (Abreu et al., 2008; Arnoczky et al., 2007; Binkley and Peat, 1986; Feng et al., 2006b; Loitz et al., 1989; Yamamoto et al., 2002; Yamamoto et al., 1993), which agrees with observations in the current study. Biochemically, deprivation of tissue load results in decreased expression of collagen mRNA (Lavagnino and Arnoczky, 2005), levels of procollagen (Grinnell et al., 1999; Nakagawa et al., 1989), amount of cells (Grinnell et al., 1999) and DNA (Mochitate et al., 1991), of which the latter two presumably result from apoptosis (Grinnell et al., 1999; Zhu et al., 2001). However, we observed that collagen content was significantly higher in shortened samples (0.85 & $0.90 \cdot L_0$) compared to stretched samples ($1.05 \cdot L_0$, One-Way ANOVA, data not shown), and although DNA content decreased relative to native e15 periosteum, no relationship with applied stretch was found in our setup.

Stiffness of e18 periosteum was significantly higher than e15 periosteum cultured for 3 days. Part of this difference can be attributed to an increase in circumference of native periosteum, while *in vitro* cultured tissue does not gain width. The metaphyseal cartilage from embryonic age e12 to e17 increases its circumference on average by 20%/day (e12 – e15 data adopted from Foolen and coworkers (Foolen et al., 2008); e16 and e17 data not shown).

Treatment with cytochalasin D and/or cycloheximide resulted in a significant increase in collagen content per tissue dry weight. Since collagen synthesis was restricted by the addition of cycloheximide, the increase can only be explained from a reduction in total dry weight, i.e. loss of cells, GAG's and other proteins, while collagen content remained high because proteolytic enzymes could not be synthesized. Unfortunately, it is not feasible to interpret absolute amounts of tissue components or total dry weight. The isolation of the periosteum tissue for analysis after culture was done manually with a scalpel blade. The total amount of tissue extracted from the bone with this procedure is not sufficiently standardized or reproducible to allow for quantitative comparison of measured total amounts of collagen. Therefore, only measures relative to the total dry weight were presented.

In summary, collagen fibers showed a typical crimped morphology upon tissue shortening. After 3 days of culture, this fiber crimp was reduced and varied between fibers, i.e. a large number of fibers was straight, while others remained crimped. With reduction of tissue length, tissue stiffness decreased, the transition point shifted, and the heel region lengthened. All effects were mediated by cell contraction. Combining these morphological observations and mechanical measurements, resulted in the following adaptive mechanism. In full equilibrium, all fibers are straight. Fibers become crimped when tissue is shortened. This weakened environment unbalances tensional homeostasis of the cells, which therefore start to contract the matrix. During the adaptation process, crimp varies between fibers. Cells pull on individual fibers, which become straight, until a new equilibrium is reached with minimal crimp. With reduction of fiber crimp, the transition point gradually shifts from the old to the new tissue length. When an adapting tissue is subjected to a tensile test, load that is borne by individual fibers depends on the amount of crimp present in the fiber and the stretch value from

where a fiber starts to become recruited. Thereby, a proportional relationship between the applied stretch level and tissue stiffness is obtained, which is accompanied by an increase in length of the heel region in its force-stretch relation. When cells are inactivated by cytochalasin D, they will not remove fiber crimp. Consequently, fiber crimp remains and tissue properties including the transition stretch, length of the heel region and stiffness are unaltered.

5.6 Conclusion

This chapter adds to our current insight in mechanical adaptation of fibrous tissue by showing that (1) periosteum in chick embryos resides in a particular mechanical state, irrespective of the developmental stage. This mechanical state is characterized by a residual tissue strain that corresponds to the strain in between the pliant and the stiffer region of the stress-strain curve. (2) Periosteum is able to regain that mechanical state *in vitro* within three days upon disturbance of that equilibrium. (3) Pursuing the particular mechanical state is cell-contraction mediated. (4) Cell contraction reduces the crimp of slack collagen fibers after tissue shortening, which increases the number of recruited fibers in time.

5.7 Acknowledgements

Chapter 6

General Discussion

6.1 Recapitulation of main findings

The overall scope of this thesis was to study the interaction between periosteum mechanical behavior and cartilage growth. Starting point was the existence of two different hypotheses. The first hypothesis proposes that periosteum tension forms a mechanical feedback mechanism with pressure in growing cartilage (Crilly, 1972; Moss, 1972). This feedback mechanism starts from the fact that extracellular matrix production, and chondrocytic proliferation and hypertrophy in the growth plate result in movement of the epiphysis away from the mid-diaphysis. Thereby, periosteum is stretched and thus tensioned. Periosteum spans the complete diaphysis and both metaphyses and lacks adhesion properties to the underlying bone (Bertram et al., 1998). Consequently, periosteum tension is postulated to statically compress growth plate cartilage, which inhibits chondrocyte activity. Triggered by the tensioning, periosteum cells synthesize matrix allowing the periosteum to grow. Thereby, compressive force on the cartilage is released and further bone lengthening becomes possible (Crilly, 1972; Moss, 1972). The second hypothesis proposes that cartilage growth is mediated by a change in the release of soluble factors from the periosteum (Bertram et al., 1998). In this hypothesis, periosteum tension induced by cartilage growth is assumed to affect periosteal intracellular tension. Variations in intracellular tension are proposed to modulate the expression of soluble factors, involved in the regulation of cartilage growth.

Existence of the mechanical feedback mechanism, proposed by Moss (Moss, 1972) and Crilly (Crilly, 1972), requires causality between periosteum tension and growing cartilage. This is supported by showing that mechanical disruption of periosteum in the circumferential, not the longitudinal direction, resulted in increased growth rates (Bertram et al., 1991; Chan and Hodgson, 1970; Crilly, 1972; Dimitriou et al., 1988; Hernandez et al., 1995; Houghton and Rooker, 1979; Jenkins et al., 1975; Lynch and Taylor, 1987; Sola et al., 1963; Taillard, 1959; Taylor et al., 1987; Warrell and Taylor, 1979; Wilde and Baker, 1987). Also, longitudinal growth rates of growth plates are decreased upon application of static compression (Bonnel et al., 1983; Stokes et al.,

2005; Wilson-MacDonald et al., 1990) and increased upon static tension (Arriola et al., 2001; Stokes et al., 2006; Stokes et al., 2007; Wilson-MacDonald et al., 1990). Both the removal of periosteum and perichondrium (Long and Linsenmayer, 1998) as well as load-induced cartilage growth (Stokes et al., 2007) were associated with alterations in proliferation and hypertrophy of the chondrocytes. We showed that the morphological anisotropy of the collagen fibers in periosteum and perichondrium concurs with predominant directions of growth (chapter 2). Directions and magnitude of cartilage expansion may therefore be related to the amount of restrictive force, present in the collagen network of periosteum and perichondrium.

These findings support the concept that a load-dependent feedback mechanism prevails between cartilage and the fibrous perichondrium and periosteum, as hypothesized by Moss (Moss, 1972) and Crilly (Crilly, 1972). Whether this feedback mechanism between cartilage and periosteum is effective or not, depends on the magnitude of residual periosteum force. Measurements of *in vivo* periosteum tension revealed that its magnitude theoretically induces cartilage compressive stresses that affect growth on a scale far below that described in the literature as a consequence of periosteal division (chapter 3). Thus, release of periosteum tension via division cannot be the dominant mechanism for directly increasing cartilage growth rates (chapter 3). We therefore conclude that the first hypothesis (Crilly, 1972; Moss, 1972) is incorrect.

Now that the first hypothesis (Crilly, 1972; Moss, 1972) was falsified, we explored the second hypothesis, by Bertram and coworkers (Bertram et al., 1998). This second hypothesis (Bertram et al., 1998) was supported by the observation that the cooperative action of soluble factors secreted by both the perichondrium and periosteum negatively regulate cartilage growth (Di Nino et al., 2001; Di Nino et al., 2002). It was shown that the responsible factors are present *in ovo* (Maeda and Noda, 2003). Overgrowth of tibiotarsi from which the perichondrium/periosteum was removed, was prevented when the bones were cultured *in ovo* (placed onto the chorioallantoic membrane of similarly aged eggs) compared to *in vitro* (Maeda and Noda, 2003). Identification of the soluble factors, responsible for modulation of endochondral cartilage growth is in progress (Alvarez et al., 2001; Crochiere et al., 2008; Di Nino and Linsenmayer, 2003; Di Nino et al., 2002). The studies by Di Nino and

coworkers (Di Nino et al., 2001; Di Nino et al., 2002), could however only explain bone overgrowth upon removal of the perichondrium and periosteum, where cells are removed, and not upon circumferential division, when cells are still present. Both phenomena can be explained by the findings from the study in chapter 4: Modulation of long bone growth, via a release of soluble factors by perichondral/periosteal cells, is an effect of the ability of these cells to develop intracellular tension through their actin filament network. The main finding that lead to this conclusion was that increased growth upon removal of perichondrium and periosteum were reduced to normal levels, when conditioned medium was provided, produced by cells from the border region of the perichondrium and periosteum, cultured on sufficiently stiff substrates (chapter 4). Furthermore, disruption of the actin filament network of these cells counteracted their growth-modulating effect completely (chapter 4). We therefore suggest that regulation of growth by periosteum is based on an elegant mechano-regulated feedback loop between cartilage growth in bone rudiments and inhibition thereof by perichondrial/periosteal cells, dependent on intracellular tension.

We also found that the effect is through a growth-inhibiting, rather than a growth-stimulating factor (chapter 4). Not surprisingly, the cells responsible for inhibition of growth rates originate from the perichondrium and periosteum region that covers the cartilage with the highest growth modulating potential, namely the proliferative and pre-hypertrophic zone. Consistent with the hypothesis by Bertram and coworkers (Bertram et al., 1998), the proposed mechano-regulated feedback loop (chapter 4) will act as follows. When cartilage growth is relatively fast, periosteum becomes tensioned. This could introduce intracellular tension in periosteum cells directly through focal adhesions (see below) or by stiffening of their environment through collagen alignment and straining. This stimulates them to express growth-inhibiting factors, which subsequently normalize the enhanced cartilage growth rate. Vice versa, the same mechano-regulated control loop would allow recovery of delayed growth, because periosteum tension would drop if cartilage did not expand sufficiently. To establish whether this feedback mechanism also prevails *in vivo*, it remains to be determined whether soluble factors produced by cells in our model system match those produced *in vivo*.

We falsified the original hypothesis (Crilly, 1972; Moss, 1972) by showing that periosteum tension is too low for directly modulating cartilage growth rates (chapter 3). However, the underlying adaptation mechanism for maintaining low tension remained to be determined. We showed that periosteum tissue resides in a particular mechanical state irrespective of the developmental stage, characterized by low force and residual tissue strain that corresponds to the location on the force-strain curve in between the pliant and stiffer region (chapter 5). Periosteum is able to regain that mechanical state upon disturbance of that equilibrium. Finally, we revealed a mechanism for this adaptation, by showing that pursuing the particular mechanical state is cell-contraction mediated and based on reducing the crimp of slack collagen fibers after tissue shortening, which increases the number of recruited fibers in time (chapter 5). Periosteum cells therefore act via two separate mechanisms to maintain periosteum tension. In case of a reduction in periosteum tension, they actively contract the collagen fiber matrix (chapter 5) and stimulate longitudinal bone growth via diminishing the expression of growth-inhibiting factors (chapter 4). It can be speculated that maintenance of this specific periosteum tension is important for subperiosteal ossification. Increased periosteum tension was shown to enhance bone formation whereas a reduction diminished ossification (Glucksmann, 1942).

The regulation of long bone growth still needs further investigation. However, this thesis provides evidence that involvement of periosteum is critical, which takes us a step closer towards understanding regulation of long bone growth. This may add to the development of methods to solve clinically relevant growth related pathologies.

6.2 Ethical considerations

Although approval by the Animals Ethics Committee is not required for experiments conducted in this thesis, an ethical discussion is appropriate. Several considerations led to the choice for the use of the chick embryo tibiotarsus as a model system, frequently used in studying embryonic bone development (Bertram et al., 1998; Church and Johnson, 1964; Di Nino et al., 2001; Long and Linsenmayer, 1998; Maeda and Noda, 2003; Nowlan et al., 2008; Roach, 1997; Rooney, 1984). Besides advantages such as the

ease of accessibility, low cost and very fast growth, an important ethical consideration was that chick embryos develop outside of their host. Therefore, the amount of animals euthanized for this study, could be limited and every animal served a direct scientific purpose. The amount of discomfort, pain and suffering was minimized by immediate decapitation, without preceding operations. Furthermore, when possible, both the left and right tibiotarsus was used. In fact, some studies required the use of both tibiotarsi as an internal control. Furthermore, the age of the animals was chosen as young as possible, as perception of the embryos increases with age. Hereby, size of the tibiotarsus was the limiting factor in the possibility to adequately execute experimental procedures.

6.3 Future directions

This thesis describes the involvement of periosteum in the regulation of embryonic long bone development. The avian model system was chosen because of fast growth, ethical considerations, and ease of accessibility and availability. However, avian long bone development is different from mammalian growth, in particular endochondral ossification (Roach, 1997). Therefore, extrapolation towards mammalian mechanisms remains to be examined and will provide a better base for extrapolation towards human. Furthermore, conclusions and findings are based on *in vitro* experiments, designed to mimic the *in vivo* environment as closely as possible. *In vitro* experiments provide a tool to study processes that are impossible to study *in vivo*. Still, our explant model system involved dissection of the tibiotarsus from its natural environment, altering mechanical and biochemical influences. Extraction and cultivation of perichondrial/periosteal cells introduced a second change with respect to their natural environment. The discrepancies between the behavior of our model system in the *in vitro* setup compared to *in vivo* remain to be assessed, in order to extrapolate our finding with respect to modulation of long bone growth by signal expression of cells, mediated by intracellular tension. An interesting follow-up experiment, for instance, would therefore be to use conditioned medium obtained from cells in slack or stretched periosteum. Results from such a study could support our conclusion from the study in which perichondrial/periosteal cells were cultured on substrates with a known stiffness (chapter 4). It has been proposed that mechanotransduction, for instance in focal

adhesions, depends on the development of stresses that are generated by a balance of external forces and cell-generated forces, resulting in signaling (Chen, 2008). However, the coupling of externally applied force and intracellular tension requires further investigation. In this study, we assumed that *in vivo* it is indifferent to the cells whether the intracellular tension is induced by external tissue straining or by active cell contraction. Furthermore, it is still unknown whether modulation of growth by conditioned medium is essentially similar for all stiffnesses examined, i.e. that substrate stiffness is related to the concentration and not the composition of the growth factor pool produced by the cells. To verify this, the growth inhibiting potential of conditioned medium from 80kPa substrates should be studied upon decreasing the concentration via dilution with unconditioned medium. Another insight into the regulatory pathways of cartilage growth could be obtained by identifying the responsible mechano-sensitive growth factors expressed by perichondrium and periosteum. Hereby, expression of these growth factors on the transcription level between *in vitro* setups and *in vivo* could be compared. Identifying these growth factors will not only increase our understanding of long bone growth regulation, it might also provide a means for clinical intervention through local drug administration. Furthermore, it will aid in further development of tissue engineered cartilage. In the case of periosteum-derived tissue engineering of cartilage for instance, periosteum tension is proposed to have a significant effect on the development of cartilage (chapter 4).

It has been shown that the periosteum firmly attaches to the epiphyseal base (Bertram et al., 1998) and spans the complete diaphysis and metaphyses. Periosteal collagen fibers align the longitudinal growth direction (chapter 2), which is homogenous throughout the complete periosteum length (Warwick and Wiles, 1934). This describes how tissues grow/adapt at the organ level. However, it is still unknown how fibrous tissues elongate during growth at a molecular level while maintaining structural integrity. It has been proposed that upon extension beyond the elastic limit, the polymers of covalently crosslinked collagen molecules within the fibrils can slip with respect to neighboring polymers as a result of strain-catalyzed hydrolysis of bonds between the polymers (Davison, 1992). We show that *in vivo*, embryonic periosteum tissue is loaded below its elastic region (chapter 5), and that fibrous tissue adapts towards a preferred mechanical state, characterized by low *in vivo* load (chapter 3 & 5).

Therefore, individual fiber strain is not expected to exceed its elastic region, as strain of the tissue is higher than the embedded fibrils (Fratzl et al., 1998; Puxkandl et al., 2002) and collagen molecules (Mosler et al., 1985). Hence, it remains to be explored whether tissue extension during growth at the molecular level is based on the concept of breaking and reformation of the polymers of covalently crosslinked collagen molecules. Real-time matrix visualization during growth processes offers a great opportunity to study this mechanism. Apart from the adaptive response in (quasi)-statically loaded tissues, the adaptive mechanism in dynamically loaded tissues offers another challenging field. Unraveling the adaptive growth mechanism of a loaded tissue at a molecular level would assist in understanding concepts of wound healing and growth related pathologies, and may be useful in tissue engineering principles.

Reference List

Abreu,E.L., Leigh,D., and Derwin,K.A. (2008). Effect of altered mechanical load conditions on the structure and function of cultured tendon fascicles. *J. Orthop. Res.* **26,** 364-373.

Alvarez,J., Horton,J., Sohn,P., and Serra,R. (2001). The perichondrium plays an important role in mediating the effects of TGF-beta1 on endochondral bone formation. *Dev. Dyn.* **221,** 311-321.

Alvarez,J., Sohn,P., Zeng,X., Doetschman,T., Robbins,D.J., and Serra,R. (2002). TGFbeta2 mediates the effects of hedgehog on hypertrophic differentiation and PTHrP expression. *Development* **129,** 1913-1924.

Arnoczky,S.P., Lavagnino,M., Egerbacher,M., Caballero,O., and Gardner,K. (2007). Matrix metalloproteinase inhibitors prevent a decrease in the mechanical properties of stress-deprived tendons: an in vitro experimental study. *Am. J. Sports Med.* **35,** 763-769.

Arriola,F., Forriol,F., and Canadell,J. (2001). Histomorphometric study of growth plate subjected to different mechanical conditions (compression, tension and neutralization): an experimental study in lambs. Mechanical growth plate behavior. *J. Pediatr. Orthop. B* **10,** 334-338.

Augustin,G., Antabak,A., and Davila,S. (2007). The periosteum Part 1: Anatomy, histology and molecular biology. *Injury* **38,** 1115-1130.

Bairati,A., Comazzi,M., and Gioria,M. (1996). A comparative study of perichondrial tissue in mammalian cartilages. *Tissue Cell* **28,** 455-468.

Balguid,A., Rubbens,M.P., Mol,A., Bank,R.A., Bogers,A.J., van Kats,J.P., de Mol,B.A., Baaijens,F.P., and Bouten,C.V. (2007). The role of collagen cross-links in biomechanical behavior of human aortic heart valve leaflets--relevance for tissue engineering. *Tissue Eng* **13,** 1501-1511.

Bank,R.A., Beekman,B., Verzijl,N., de Roos,J.A., Sakkee,A.N., and TeKoppele,J.M. (1997). Sensitive fluorimetric quantitation of pyridinium and pentosidine crosslinks in biological samples in a single high-performance liquid chromatographic run. *J. Chromatogr. B Biomed. Sci. Appl.* **703,** 37-44.

Bank,R.A., Jansen,E.J., Beekman,B., and te Koppele,J.M. (1996). Amino acid analysis by reverse-phase high-performance liquid chromatography: improved derivatization and detection conditions with 9-fluorenylmethyl chloroformate. *Anal. Biochem.* **240,** 167-176.

Bell,E., Ivarsson,B., and Merrill,C. (1979). Production of a tissue-like structure by contraction of collagen lattices by human fibroblasts of different proliferative potential in vitro. *Proc. Natl. Acad Sci. U. S. A* **76,** 1274-1278.

Bertram,J.E., Hall,B.K., and DeMont,M.E. (1991). Does diaphyseal periosteum restrict longitudinal growth in long bones. In *Dixon, A.D., Sarnat, B.G., and Hoyte, D.A.N., Eds. Fundamentals of bone growth: Methodology and Applications.* pp. 363-374. Boca Rotn, FL: CRC.

Bertram,J.E., Polevoy,Y., and Cullinane,D.M. (1998). Mechanics of avian fibrous periosteum: tensile and adhesion properties during growth. *Bone* **22,** 669-675.

Binkley,J.M. and Peat,M. (1986). The effects of immobilization on the ultrastructure and mechanical properties of the medial collateral ligament of rats. *Clin. Orthop. Relat Res.* 301-308.

Boerboom,R.A., Krahn,K.N., Megens,R.T., van Zandvoort,M.A., Merkx,M., and Bouten,C.V. (2007). High resolution imaging of collagen organisation and synthesis using a versatile collagen specific probe. *J. Struct. Biol.* **159,** 392-399.

Bonnel,F., Peruchon,E., Baldet,P., Dimeglio,A., and Rabischong,P. (1983). Effects of compression on growth plates in the rabbit. *Acta Orthop. Scand.* **54,** 730-733.

Boonen,K.J., Rosaria-Chak,K.Y., Baaijens,F.P., van der Schaft,D.W., and Post,M.J. (2009). Essential environmental cues from the satellite cell niche: optimizing proliferation and differentiation. *Am. J. Physiol Cell Physiol* **296,** C1338-C1345.

Brown,R.A., Prajapati,R., McGrouther,D.A., Yannas,I.V., and Eastwood,M. (1998). Tensional homeostasis in dermal fibroblasts: mechanical responses to mechanical loading in three-dimensional substrates. *J. Cell Physiol* **175,** 323-332.

Carey,E.J. (1922). Direct observations on the transformations of the mesenchyme in the thigh of the pig embryo, with especial reference to the genesis of the thigh muscles of the knee and hip joints, and of the primary bone of the femur. *Journal of Morphology and Physiology* **37,** 1-77.

Caruso,A.B. and Dunn,M.G. (2004). Functional evaluation of collagen fiber scaffolds for ACL reconstruction: cyclic loading in proteolytic enzyme solutions. *J. Biomed. Mater. Res. A* **69,** 164-171.

Cesarone,C.F., Bolognesi,C., and Santi,L. (1979). Improved microfluorometric DNA determination in biological material using 33258 Hoechst. *Anal. Biochem.* **100,** 188-197.

Chan,K.P. and Hodgson,A.R. (1970). Physiologic leg lengthening. A preliminary report. *Clin. Orthop. Relat Res.* **68,** 55-62.

Chen,C.S. (2008). Mechanotransduction - a field pulling together? *J. Cell Sci.* **121,** 3285-3292.

Chen,J.C., Zhao,B., Longaker,M.T., Helms,J.A., and Carter,D.R. (2007). Periosteal biaxial residual stresses and strains during chick embryonic bone growth. *53rd annual meeting of the Orthopaedic Research Society, San Diego* abstract number 1333.

Church,L.E. and Johnson,L.C. (1964). Growth of long bones in the chicken. Rates of growth in length and diameter of the humerus, tibia and metatarsus. *Am. J. Anat.* **114,** 521-538.

Crilly,R.G. (1972). Longitudinal overgrowth of chicken radius. *J. Anat.* **112,** 11-18.

Crochiere,M.L., Kubilus,J.K., and Linsenmayer,T.F. (2008). Perichondrial-mediated TGF-beta regulation of cartilage growth in avian long bone development. *Int. J. Dev. Biol.* **52,** 63-70.

Curwin,S.L., Vailas,A.C., and Wood,J. (1988). Immature tendon adaptation to strenuous exercise. *J. Appl. Physiol* **65,** 2297-2301.

Davison,P.F. (1992). The organization of collagen in growing tensile tissues. *Connect. Tissue Res.* **28,** 171-179.

Dejonge,P. (1983). Collagen-fibers in the periosteum of a long bone. *Acta morphologica neerlando-scandinavica* **21,** 173-174.

Di Nino,D.L. and Linsenmayer,T.F. (2003). Positive regulation of endochondral cartilage growth by perichondrial and periosteal calcitonin. *Endocrinology* **144,** 1979-1983.

Di Nino,D.L., Long,F., and Linsenmayer,T.F. (2001). Regulation of endochondral cartilage growth in the developing avian limb: cooperative involvement of perichondrium and periosteum. *Dev. Biol.* **240,** 433-442.

Di Nino,D.L., Crochiere,M.L., and Linsenmayer,T.F. (2002). Multiple mechanisms of perichondrial regulation of cartilage growth. *Dev. Dyn.* **225,** 250-259.

Dimitriou,C.G., Kapetanos,G.A., and Symeonides,P.P. (1988). The effect of partial periosteal division on growth of the long bones. An experimental study in rabbits. *Clin. Orthop. Relat Res.* 265-269.

Discher,D.E., Janmey,P., and Wang,Y.L. (2005). Tissue cells feel and respond to the stiffness of their substrate. *Science* **310,** 1139-1143.

Dodd,N.J., Schor,S.L., and Rushton,G. (1982). The effects of a collagenous extracellular matrix on fibroblast membrane organization. An ESR spin label study. *Exp. Cell Res.* **141,** 421-431.

Driessen,N.J.B., Wilson,W., Bouten,C.V.C., and Baaijens,F.P.T. (2004). A computational model for collagen fibre remodelling in the arterial wall. *J. Theor. Biol.* **226,** 53-64.

Driessen,N.J.B., Bouten,C.V.C., and Baaijens,F.P.T. (2005). Improved prediction of the collagen fiber architecture in the aortic heart valve. *J. Biomech. Eng* **127,** 329-336.

Eastwood,M., Porter,R., Khan,U., McGrouther,G., and Brown,R. (1996). Quantitative analysis of collagen gel contractile forces generated by dermal fibroblasts and the relationship to cell morphology. *J. Cell Physiol* **166,** 33-42.

Ellender,G., Feik,S.A., and Ramm-Anderson,S.M. (1989). Periosteal changes in mechanically stressed rat caudal vertebrae. *J. Anat.* **163,** 83-96.

Ellsmere,J.C., Khanna,R.A., and Lee,J.M. (1999). Mechanical loading of bovine pericardium accelerates enzymatic degradation. *Biomaterials* **20,** 1143-1150.

Emans,P.J., Surtel,D.A., Frings,E.J., Bulstra,S.K., and Kuijer,R. (2005). In vivo generation of cartilage from periosteum. *Tissue Eng* **11,** 369-377.

Engler,A., Bacakova,L., Newman,C., Hategan,A., Griffin,M., and Discher,D. (2004). Substrate compliance versus ligand density in cell on gel responses. *Biophys. J.* **86,** 617-628.

Engler,A.J., Sen,S., Sweeney,H.L., and Discher,D.E. (2006). Matrix elasticity directs stem cell lineage specification. *Cell* **126,** 677-689.

Farndale,R.W., Buttle,D.J., and Barrett,A.J. (1986). Improved quantitation and discrimination of sulphated glycosaminoglycans by use of dimethylmethylene blue. *Biochim. Biophys. Acta* **883,** 173-177.

Feng,Z., Ishibashi,M., Nomura,Y., Kitajima,T., and Nakamura,T. (2006a). Constraint stress, microstructural characteristics, and enhanced mechanical properties of a special fibroblast-embedded collagen construct. *Artif. Organs* **30,** 870-877.

Feng,Z., Tateishi,Y., Nomura,Y., Kitajima,T., and Nakamura,T. (2006b). Construction of fibroblast-collagen gels with orientated fibrils induced by static or dynamic stress: toward the fabrication of small tendon grafts. *J. Artif. Organs* **9,** 220-225.

Foolen,J., van Donkelaar,C.C., Murphy,P., Huiskes,R., and Ito,K. (2009). Residual periosteum tension is insufficient to directly modulate bone growth. *J. Biomech.* **42,** 152-157.

Foolen,J., van Donkelaar,C.C., Nowlan,N., Murphy,P., Huiskes,R., and Ito,K. (2008). Collagen orientation in periosteum and perichondrium is aligned with preferential directions of tissue growth. *J. Orthop. Res.* **26,** 1263-1268.

Forriol,F. and Shapiro,F. (2005). Bone development: interaction of molecular components and biophysical forces. *Clin. Orthop. Relat Res.* 14-33.

Fratzl,P., Misof,K., Zizak,I., Rapp,G., Amenitsch,H., and Bernstorff,S. (1998). Fibrillar structure and mechanical properties of collagen. *J. Struct. Biol.* **122,** 119-122.

Glucksmann,A. (1942). The role of mechanical stresses in bone formation in vitro. *J. Anat.* **76,** 231-239.

Goffin,J.M., Pittet,P., Csucs,G., Lussi,J.W., Meister,J.J., and Hinz,B. (2006). Focal adhesion size controls tension-dependent recruitment of alpha-smooth muscle actin to stress fibers. *J. Cell Biol.* **172,** 259-268.

Grinnell,F. and Lamke,C.R. (1984). Reorganization of hydrated collagen lattices by human skin fibroblasts. *J. Cell Sci.* **66,** 51-63.

Grinnell,F., Zhu,M., Carlson,M.A., and Abrams,J.M. (1999). Release of mechanical tension triggers apoptosis of human fibroblasts in a model of regressing granulation tissue. *Exp. Cell Res.* **248,** 608-619.

Guidry,C. (1992). Extracellular matrix contraction by fibroblasts: peptide promoters and second messengers. *Cancer Metastasis Rev.* **11,** 45-54.

Guidry,C. and Grinnell,F. (1985). Studies on the mechanism of hydrated collagen gel reorganization by human skin fibroblasts. *J. Cell Sci.* **79,** 67-81.

Guidry,C. and Grinnell,F. (1987). Contraction of hydrated collagen gels by fibroblasts: evidence for two mechanisms by which collagen fibrils are stabilized. *Coll. Relat Res.* **6,** 515-529.

Guidry,C., Hohn,S., and Hook,M. (1990). Endothelial cells secrete a factor that promotes fibroblast contraction of hydrated collagen gels. *J. Cell Biol.* **110,** 519-528.

Hall,A.C., Urban,J.P., and Gehl,K.A. (1991). The effects of hydrostatic pressure on matrix synthesis in articular cartilage. *J. Orthop. Res.* **9,** 1-10.

Hamburger,V. and Hamilton,H.L. (1992). A series of normal stages in the development of the chick embryo. 1951. *Dev. Dyn.* **195,** 231-272.

Hansen,U., Schunke,M., Domm,C., Ioannidis,N., Hassenpflug,J., Gehrke,T., and Kurz,B. (2001). Combination of reduced oxygen tension and intermittent hydrostatic pressure: a useful tool in articular cartilage tissue engineering. *J. Biomech.* **34,** 941-949.

Harris,A.K., Stopak,D., and Wild,P. (1981). Fibroblast traction as a mechanism for collagen morphogenesis. *Nature* **290,** 249-251.

Hartmann,C. and Tabin,C.J. (2000). Dual roles of Wnt signaling during chondrogenesis in the chicken limb. *Development* **127,** 3141-3159.

Henderson,J.H. and Carter,D.R. (2002). Mechanical induction in limb morphogenesis: the role of growth-generated strains and pressures. *Bone* **31,** 645-653.

Henshaw,D.R., Attia,E., Bhargava,M., and Hannafin,J.A. (2006). Canine ACL fibroblast integrin expression and cell alignment in response to cyclic tensile strain in three-dimensional collagen gels. *J. Orthop. Res.* **24,** 481-490.

Hernandez,J.A., Serrano,S., Marinoso,M.L., Aubia,J., Lloreta,J., Marrugat,J., and Diez,A. (1995). Bone growth and modeling changes induced by periosteal stripping in the rat. *Clin. Orthop. Relat Res.* 211-219.

Hinoi,E., Bialek,P., Chen,Y.T., Rached,M.T., Groner,Y., Behringer,R.R., Ornitz,D.M., and Karsenty,G. (2006). Runx2 inhibits chondrocyte proliferation and hypertrophy through its expression in the perichondrium. *Genes Dev.* **20,** 2937-2942.

Houghton,G.R. and Rooker,G.D. (1979). The role of the periosteum in the growth of long bones. An experimental study in the rabbit. *J. Bone Joint Surg. Br.* **61-B,** 218-220.

Huang,C. and Yannas,I.V. (1977). Mechanochemical studies of enzymatic degradation of insoluble collagen fibers. *J. Biomed. Mater. Res.* **11,** 137-154.

Huang,D., Chang,T.R., Aggarwal,A., Lee,R.C., and Ehrlich,H.P. (1993). Mechanisms and dynamics of mechanical strengthening in ligament-equivalent fibroblast-populated collagen matrices. *Ann. Biomed. Eng* **21,** 289-305.

Jenkins,D.H., Cheng,D.H., and Hodgson,A.R. (1975). Stimulation of bone growth by periosteal stripping. A clinical study. *J. Bone Joint Surg. Br.* **57,** 482-484.

Kim,S.G., Akaike,T., Sasagaw,T., Atomi,Y., and Kurosawa,H. (2002). Gene expression of type I and type III collagen by mechanical stretch in anterior cruciate ligament cells. *Cell Struct. Funct.* **27,** 139-144.

Krahn,K.N., Bouten,C.V.C., van Tuijl,S., van Zandvoort,M.A.M.J., and Merkx,M. (2006). Fluorescently labeled collagen binding proteins allow specific visualization of collagen in tissues and live cell culture. *Anal. Biochem.* **350,** 177-185.

Kronenberg,H.M. (2003). Developmental regulation of the growth plate. *Nature* **423,** 332-336.

Lavagnino,M. and Arnoczky,S.P. (2005). In vitro alterations in cytoskeletal tensional homeostasis control gene expression in tendon cells. *J. Orthop. Res.* **23,** 1211-1218.

Lee,E.Y., Parry,G., and Bissell,M.J. (1984). Modulation of secreted proteins of mouse mammary epithelial cells by the collagenous substrata. *J. Cell Biol.* **98,** 146-155.

Lo,C.M., Wang,H.B., Dembo,M., and Wang,Y.L. (2000). Cell movement is guided by the rigidity of the substrate. *Biophys. J.* **79,** 144-152.

Loitz,B.J., Zernicke,R.F., Vailas,A.C., Kody,M.H., and Meals,R.A. (1989). Effects of short-term immobilization versus continuous passive motion on the biomechanical and biochemical properties of the rabbit tendon. *Clin. Orthop. Relat Res.* 265-271.

Long,F. and Linsenmayer,T.F. (1998). Regulation of growth region cartilage proliferation and differentiation by perichondrium. *Development* **125,** 1067-1073.

Lovitch,D. and Christianson,M.L. (1997). Mineralization is more reliable in periosteum explants from size-selected chicken embryos. *In Vitro Cell Dev. Biol. Anim* **33,** 234-235.

Lynch,M.C. and Taylor,J.F. (1987). Periosteal division and longitudinal growth in the tibia of the rat. *J. Bone Joint Surg. Br.* **69,** 812-816.

Macfelda,K., Kapeller,B., Wilbacher,I., and Losert,U.M. (2007). Behavior of cardiomyocytes and skeletal muscle cells on different extracellular matrix components--relevance for cardiac tissue engineering. *Artif. Organs* **31,** 4-12.

Maeda,Y. and Noda,M. (2003). Coordinated development of embryonic long bone on chorioallantoic membrane in ovo prevents perichondrium-derived suppressive signals against cartilage growth. *Bone* **32,** 27-34.

Maley,M.A., Davies,M.J., and Grounds,M.D. (1995). Extracellular matrix, growth factors, genetics: their influence on cell proliferation and myotube formation in primary cultures of adult mouse skeletal muscle. *Exp. Cell Res.* **219,** 169-179.

Meshel,A.S., Wei,Q., Adelstein,R.S., and Sheetz,M.P. (2005). Basic mechanism of three-dimensional collagen fibre transport by fibroblasts. *Nat. Cell Biol.* **7,** 157-164.

Michna,H. (1984). Morphometric analysis of loading-induced changes in collagen-fibril populations in young tendons. *Cell Tissue Res.* **236,** 465-470.

Michna,H. and Hartmann,G. (1989). Adaptation of tendon collagen to exercise. *Int. Orthop.* **13,** 161-165.

Mochitate,K., Pawelek,P., and Grinnell,F. (1991). Stress relaxation of contracted collagen gels: disruption of actin filament bundles, release of cell surface fibronectin, and down-regulation of DNA and protein synthesis. *Exp. Cell Res.* **193,** 198-207.

Mosler,E., Folkhard,W., Knorzer,E., Nemetschek-Gansler,H., Nemetschek,T., and Koch,M.H. (1985). Stress-induced molecular rearrangement in tendon collagen. *J. Mol. Biol.* **182,** 589-596.

Moss,ML. (1972). The regulation of skeletal growth. In *The regulation of organ and tissue growth.* (ed. R.Gross), pp 127 - 142 (Academic Press, New York).

Nabeshima,Y., Grood,E.S., Sakurai,A., and Herman,J.H. (1996). Uniaxial tension inhibits tendon collagen degradation by collagenase in vitro. *J. Orthop. Res.* **14,** 123-130.

Nakagawa,S., Pawelek,P., and Grinnell,F. (1989). Long-term culture of fibroblasts in contracted collagen gels: effects on cell growth and biosynthetic activity. *J. Invest Dermatol.* **93,** 792-798.

Nekouzadeh,A., Pryse,K.M., Elson,E.L., and Genin,G.M. (2008). Stretch-activated force shedding, force recovery, and cytoskeletal remodeling in contractile fibroblasts. *J. Biomech.* **41,** 2964-2971.

Noonan,K.J., Hunziker,E.B., Nessler,J., and Buckwalter,J.A. (1998). Changes in cell, matrix compartment, and fibrillar collagen volumes between growth-plate zones. *J. Orthop. Res.* **16,** 500-508.

Nowlan,N.C., Murphy,P., and Prendergast,P.J. (2008). A dynamic pattern of mechanical stimulation promotes ossification in avian embryonic long bones. *J. Biomech.* **41,** 249-258.

O'Driscoll,S.W., Recklies,A.D., and Poole,A.R. (1994). Chondrogenesis in periosteal explants. An organ culture model for in vitro study. *J. Bone Joint Surg. Am.* **76,** 1042-1051.

Parkkinen,J.J., Ikonen,J., Lammi,M.J., Laakkonen,J., Tammi,M., and Helminen,H.J. (1993). Effects of cyclic hydrostatic pressure on proteoglycan synthesis in cultured chondrocytes and articular cartilage explants. *Arch. Biochem. Biophys.* **300,** 458-465.

Parsons,M., Kessler,E., Laurent,G.J., Brown,R.A., and Bishop,J.E. (1999). Mechanical load enhances procollagen processing in dermal fibroblasts by regulating levels of procollagen C-proteinase. *Exp. Cell Res.* **252,** 319-331.

Pelham,R.J., Jr. and Wang,Y. (1997). Cell locomotion and focal adhesions are regulated by substrate flexibility. *Proc. Natl. Acad. Sci. U. S. A* **94,** 13661-13665.

Petroll,W.M., Vishwanath,M., and Ma,L. (2004). Corneal fibroblasts respond rapidly to changes in local mechanical stress. *Invest Ophthalmol. Vis. Sci.* **45,** 3466-3474.

Popowics,T.E., Zhu,Z., and Herring,S.W. (2002). Mechanical properties of the periosteum in the pig, Sus scrofa. *Arch. Oral Biol.* **47,** 733-741.

Prajapati,R.T., Chavally-Mis,B., Herbage,D., Eastwood,M., and Brown,R.A. (2000). Mechanical loading regulates protease production by fibroblasts in three-dimensional collagen substrates. *Wound. Repair Regen.* **8,** 226-237.

Puxkandl,R., Zizak,I., Paris,O., Keckes,J., Tesch,W., Bernstorff,S., Purslow,P., and Fratzl,P. (2002). Viscoelastic properties of collagen: synchrotron radiation investigations and structural model. *Philos. Trans. R Soc. Lond B Biol. Sci.* **357,** 191-197.

Radhakrishnan,P., Lewis,N.T., and Mao,J.J. (2004). Zone-specific micromechanical properties of the extracellular matrices of growth plate cartilage. *Ann. Biomed. Eng* **32,** 284-291.

Rath,N.C., Huff,G.R., Huff,W.E., and Balog,J.M. (2000). Factors regulating bone maturity and strength in poultry. *Poult. Sci.* **79,** 1024-1032.

Ravetto,A., Kock,L.M., Donkelaar,C.C., and Ito,K. (2009). Mechanical stimulation enhances collagen synthesis in periosteum-derived cartilage. *Proceedings of the ASME 2009 Summer Bioengineering Conference* **SBC2009-204245**.

Roach,H.I. (1997). New aspects of endochondral ossification in the chick: chondrocyte apoptosis, bone formation by former chondrocytes, and acid phosphatase activity in the endochondral bone matrix. *J. Bone Miner. Res.* **12,** 795-805.

Robins,S.P., Duncan,A., Wilson,N., and Evans,B.J. (1996). Standardization of pyridinium crosslinks, pyridinoline and deoxypyridinoline, for use as biochemical markers of collagen degradation. *Clin. Chem.* **42,** 1621-1626.

Robling,A.G., Duijvelaar,K.M., Geevers,J.V., Ohashi,N., and Turner,C.H. (2001). Modulation of appositional and longitudinal bone growth in the rat ulna by applied static and dynamic force. *Bone* **29,** 105-113.

Rooney,P. (1984). The Cellular Basis of Cartilage Morphogenesis in Embryonic Chick Limbs. *PhD thesis, University of London*.

Rooney,P. and Archer,C.W. (1992). The development of the perichondrium in the avian ulna. *J. Anat.* **181 (Pt 3),** 393-401.

Ruberti,J.W. and Hallab,N.J. (2005). Strain-controlled enzymatic cleavage of collagen in loaded matrix. *Biochem. Biophys. Res. Commun.* **336,** 483-489.

Sawhney,R.K. and Howard,J. (2002). Slow local movements of collagen fibers by fibroblasts drive the rapid global self-organization of collagen gels. *J. Cell Biol.* **157,** 1083-1091.

Schwarz,U.S. and Bischofs,I.B. (2005). Physical determinants of cell organization in soft media. *Med. Eng Phys.* **27,** 763-772.

Serra,R., Karaplis,A., and Sohn,P. (1999). Parathyroid hormone-related peptide (PTHrP)-dependent and -independent effects of transforming growth factor beta (TGF-beta) on endochondral bone formation. *J. Cell Biol.* **145,** 783-794.

Shapiro,F., Holtrop,M.E., and Glimcher,M.J. (1977). Organization and cellular biology of the perichondrial ossification groove of ranvier: a morphological study in rabbits. *J. Bone Joint Surg. Am.* **59,** 703-723.

Shapiro,F. (2001). *Pediatric Orthopedic Deformities, Basic Science, Diagnosis, and Treatment.* San Diego: Elsevier / Academic Press.

Sharpe,J., Ahlgren,U., Perry,P., Hill,B., Ross,A., Hecksher-Sorensen,J., Baldock,R., and Davidson,D. (2002). Optical projection tomography as a tool for 3D microscopy and gene expression studies. *Science* **296,** 541-545.

Simon,T.M., Van,S., Kunishima,D.H., and Jackson,D.W. (2003). Cambium cell stimulation from surgical release of the periosteum. *J. Orthop. Res.* **21,** 470-480.

Sola,C.K., Silberman,F.S., and Cabrini,R.L. (1963). Stimulation of the longitudinal growth of long bones by periosteal stripping. An experimental study on dogs and monkeys. *J. Bone Joint Surg. Am.* **45,** 1679-1684.

Speer,D.P. (1982). Collagenous architecture of the growth plate and perichondrial ossification groove. *J. Bone Joint Surg. Am.* **64,** 399-407.

Stokes,I.A., Gwadera,J., Dimock,A., Farnum,C.E., and Aronsson,D.D. (2005). Modulation of vertebral and tibial growth by compression loading: diurnal versus full-time loading. *J. Orthop. Res.* **23,** 188-195.

Stokes,I.A.F., Aronsson,D.D., Dimock,A.N., Cortright,V., and Beck,S. (2006). Endochondral growth in growth plates of three species at two anatomical locations modulated by mechanical compression and tension. *J. Orthop. Res.* **24,** 1327-1334.

Stokes,I.A.F., Clark,K.C., Farnum,C.E., and Aronsson,D.D. (2007). Alterations in the growth plate associated with growth modulation by sustained compression or distraction. *Bone* **41,** 197-205.

Stopak,D. and Harris,A.K. (1982). Connective tissue morphogenesis by fibroblast traction. I. Tissue culture observations. *Dev. Biol.* **90,** 383-398.

Taillard,W. (1959). [Stimulation of the growth of long bones by periosteal detachment.]. *Rev. Med. Suisse Romande* **79,** 28-38.

Tanck,E., Blankevoort,L., Haaijman,A., Burger,E.H., and Huiskes,R. (2000). Influence of muscular activity on local mineralization patterns in metatarsals of the embryonic mouse. *J. Orthop. Res.* **18,** 613-619.

Tanck,E., van Donkelaar,C.C., Jepsen,K.J., Goldstein,S.A., Weinans,H., Burger,E.H., and Huiskes,R. (2004). The mechanical consequences of mineralization in embryonic bone. *Bone* **35,** 186-190.

Taylor,J.F., Warrell,E., and Evans,R.A. (1987). The response of the rat tibial growth plates to distal periosteal division. *J. Anat.* **151,** 221-231.

Tenenbaum,H.C., Palangio,K.G., Holmyard,D.P., and Pritzker,K.P. (1986). An ultrastructural study of osteogenesis in chick periosteum in vitro. *Bone* **7,** 295-302.

Thomopoulos,S., Fomovsky,G.M., and Holmes,J.W. (2005). The development of structural and mechanical anisotropy in fibroblast populated collagen gels. *J. Biomech. Eng* **127,** 742-750.

Tomasek,J.J., Haaksma,C.J., Eddy,R.J., and Vaughan,M.B. (1992). Fibroblast contraction occurs on release of tension in attached collagen lattices: dependency on an organized actin cytoskeleton and serum. *Anat. Rec.* **232,** 359-368.

Tomasek,J.J. and Hay,E.D. (1984). Analysis of the role of microfilaments and microtubules in acquisition of bipolarity and elongation of fibroblasts in hydrated collagen gels. *J. Cell Biol.* **99,** 536-549.

Vortkamp,A., Lee,K., Lanske,B., Segre,G.V., Kronenberg,H.M., and Tabin,C.J. (1996). Regulation of rate of cartilage differentiation by Indian hedgehog and PTH-related protein. *Science* **273,** 613-622.

Wakatsuki,T. and Elson,E.L. (2003). Reciprocal interactions between cells and extracellular matrix during remodeling of tissue constructs. *Biophys. Chem.* **100,** 593-605.

Wang,H.B., Dembo,M., and Wang,Y.L. (2000). Substrate flexibility regulates growth and apoptosis of normal but not transformed cells. *Am. J. Physiol Cell Physiol* **279,** C1345-C1350.

Wang,J.H.C., Jia,F., Gilbert,T.W., and Woo,S.L.Y. (2003). Cell orientation determines the alignment of cell-produced collagenous matrix. *J. Biomech.* **36,** 97-102.

Warrell,E. and Taylor,J.F. (1979). The role of periosteal tension in the growth of long bones. *J. Anat.* **128,** 179-184.

Warwick,W.T. and Wiles,P. (1934). The growth of periosteum in long bones. *British Journal of Surgery* **22,** 169-174.

Wilde,G.P. and Baker,G.C. (1987). Circumferential periosteal release in the treatment of children with leg-length inequality. *J. Bone Joint Surg. Br.* **69,** 817-821.

Wilson,W., Driessen,N.J.B., van Donkelaar,C.C., and Ito,K. (2006). Prediction of collagen orientation in articular cartilage by a collagen remodeling algorithm. *Osteoarthritis. Cartilage.* **14,** 1196-1202.

Wilson-MacDonald,J., Houghton,G.R., Bradley,J., and Morscher,E. (1990). The relationship between periosteal division and compression or distraction of the growth plate. An experimental study in the rabbit. *J. Bone Joint Surg. Br.* **72,** 303-308.

Wolpert,L. (1981). *Cartilage morphogenesis in the limb. In "Cell Behaviour".* (R. Bellairs, A.S.G. Curtis, and G. Dunn, eds.), pp. 359-372. Cambridge Univ. Press, London/New York.

Yamamoto,E., Iwanaga,W., Miyazaki,H., and Hayashi,K. (2002). Effects of static stress on the mechanical properties of cultured collagen fascicles from the rabbit patellar tendon. *J. Biomech. Eng* **124,** 85-93.

Yamamoto,N., Ohno,K., Hayashi,K., Kuriyama,H., Yasuda,K., and Kaneda,K. (1993). Effects of stress shielding on the mechanical properties of rabbit patellar tendon. *J. Biomech. Eng* **115,** 23-28.

Yang,G., Crawford,R.C., and Wang,J.H.C. (2004). Proliferation and collagen production of human patellar tendon fibroblasts in response to cyclic uniaxial stretching in serum-free conditions. *J. Biomech.* **37,** 1543-1550.

Yeung,T., Georges,P.C., Flanagan,L.A., Marg,B., Ortiz,M., Funaki,M., Zahir,N., Ming,W., Weaver,V., and Janmey,P.A. (2005). Effects of substrate stiffness on cell morphology, cytoskeletal structure, and adhesion. *Cell Motil. Cytoskeleton* **60,** 24-34.

Zhu,Y.K., Umino,T., Liu,X.D., Wang,H.J., Romberger,D.J., Spurzem,J.R., and Rennard,S.I. (2001). Contraction of fibroblast-containing collagen gels: initial collagen concentration regulates the degree of contraction and cell survival. *In Vitro Cell Dev. Biol. Anim* **37,** 10-16.

Samenvatting

De rol van periosteum tijdens botgroei

Ons skelet ontwikkelt zich door groei van kraakbeenweefsel, dat vervolgens wordt omgezet in botweefsel. Dit proces wordt gereguleerd door vele controlemechanismen. Het periosteum speelt daarbij ook een belangrijke rol, maar het mechanisme daarachter is onduidelijk. Een hypothese uit de jaren 70 beschrijft een mechanisch terugkoppelingsmechanisme tussen het groeiende kraakbeen en het omliggende periosteum. Spanning in het periosteum zou resulteren in compressie van het groeiende kraakbeen waardoor de kraakbeengroei zou worden geremd. Dit proefschrift toont aan dat de oriëntatie van collageen, de belangrijkste belastingdragende component in het periosteum, overeen komt met de richting waarin kraakbeenweefsel bij voorkeur groeit. Dit ondersteunt het idee dat spanning in het periosteum, kraakbeengroei remt. Echter, we toonden ook aan dat de spanning in het periosteum te laag is om kraakbeengroei effectief te remmen. Daarmee was bovenstaande hypothese ontkracht. Onze nieuwe hypothese was dat regulatie van kraakbeengroei gebaseerd is op een mechano-biologisch terugkoppelingsmechanisme tussen kraakbeen en periosteum, waarbij expressie van groeifactoren door periosteum-cellen afhankelijk is van de spanning in deze cellen. Deze groeifactoren remmen vervolgens de groei van het kraakbeen. We hebben deze theorie met een serie experimenten bevestigd. Er was nog één vraag over: hoe kan het zijn dat het bot, en daarmee het periosteum, zeer snel groeit, maar dat desondanks de spanning in het periosteum laag blijft? We toonden aan dat periosteum adapteert naar een evenwichtstoestand waarbij de rek op het knikpunt van de kracht-rek relatie zit; dus op de overgang van een lage stijfheid naar een hoge stijfheid. We toonden aan dat dit adaptatieproces afhankelijk is van de contractiele eigenschappen van de periosteum-cellen en gepaard gaat met structurele reorganisatie van het collageennetwerk. Deze adaptatie werd bepaald door cel-gemedieerde reorganisatie van het collageen, en verrassend genoeg niet door de hoeveelheid collageen en crosslinks in het weefsel. Dit proefschrift geeft ons inzicht in de regulatie van botgroei door het periosteum, en de belangrijke rol die de cellen in het periosteum daarbij spelen.

Een bestaande hypothese die de interactie tussen periosteum en kraakbeengroei beschrijft werd gefalsificeerd. Een nieuwe mechano-biologische hypothese waarbij periosteum-cellen een belangrijke rol spelen, werd ontwikkeld en gevalideerd. Deze cellen bleken ook bij de adaptatie van periosteum essentieel.

Dankwoord

Een promotie kun je in je eentje met gemak verknallen; succesvol afronden echter zelden zonder steun van anderen. Laten we er voor het gemak van uitgaan dat ik mijn promotie niet meer ga verknallen; en het dus gepast is mensen te bedanken die van (on)schatbare waarde zijn geweest voor de goede afloop.

René heeft daar zowel wetenschappelijk als sociaal een erg belangrijke rol in gespeeld. Ik had onze samenwerking geen andere invulling willen geven. Verder kan ik enorm waarderen dat mijn persoonlijke ontwikkeling zo goed als altijd centraal stond; en niet onbelangrijk, dat we ook erg hard hebben gelachen. Des te ironisch is het, dat ik hier nu een traantje weg zit te pinken bij de gedachte dat aan onze actieve samenwerking dan toch echt een eind gaat komen, toch? Rik Huiskes wil ik bedanken voor het aanbrengen van structuur in mijn onderzoek tijdens de eerste fase van mijn promotie en de wijze les dat onderzoek begint met een vraag, en dat een vraag eindigt met een vraagteken. I would like to thank Keita Ito for the brainstorm sessions and useful input during the last phase of my PhD, and last but not least for improving the social nature of our group. Although I was frequently searching for something I could challenge you in for a change, due to my competitive personality, I always very much appreciated our collaboration.

Ook hulp van buiten de TU/e heeft bijgedragen aan het tot stand komen van dit proefschrift. Jessica Snabel en Ruud Bank (TNO Leiden/RUG Groningen) wil ik daarom bedanken voor de mogelijkheid om keer op keer samples te sturen voor HPLC analyse. Furthermore, I am grateful to have had the opportunity to visit Trinity College in Dublin three times for performing OPT measurements. Therefore, many thanks to Paula Murphy, Niamh Nowlan and Kristen Summerhurst. Verder wil ik ook Bregtje Viegers bedanken voor het maken van de omslag en boekenlegger.

Janine, Cora, Ramon, Ana & Margarida, ondanks dat jullie werk geen onderdeel uitmaakt van dit proefschrift, heb ik in vele opzichten toch erg veel van jullie geleerd.

During my PhD, the Orthopaedic biomechanics group has grown exponentially. This resulted in more social and scientific gatherings, which I have always enjoyed. In het bijzonder heb ik erg kunnen lachen met mijn drie BBF's. Een onderzoeksgroep kan nooit functioneren zonder uitstekende secretaresses. Daarom wil ik Janneke en Alice, 2

charmante eind twintigers, bedanken voor alles wat zij hebben bijgedragen. Ook de vaste krachten uit het lab, Marcel, Moniek, Sarita, Kang Yuen, Marloes, en de knakkers van Hemolab zijn onmisbaar gebleken. Ook jullie ben ik veel dank verschuldigd.

Verder hebben natuurlijk veel (ex-)collega's van vloer 4 bijgedragen aan een zeer prettige werkomgeving, iedereen bedankt daarvoor! Vooral diegenen die altijd ten minste een glimlach wisten te ontlokken.

During my PhD, most of my time I spend in room 4.115, which was a very pleasant environment to work in. I enjoyed the discussions with Tuncay and Mohammad about issues involving the Middle East, and the lessons in what we (Dutch people) pretend to be, compared to how we really are. Verder heb ik aan Arjen en Chantal erg goede herinneringen. Veel momenten waarop we hebben gelachen, geouwehoerd; maar als het nodig was toch ook even hebben kunnen zeiken.

Chantal was natuurlijk veel meer dan een leuke kamergenoot, en maakte deel uit van de enige echte BMT vriendengroep. Ik hoop dat we de jaarlijkse tackûlevenementen met deze groep zullen voortzetten, al moet ik nog steeds leren bellen. Van deze speciale club mensen wil ik Jan bedanken voor o.a. de vele sportpsychologische gesprekken over blessures die je het fysiek onmogelijk maken goesting om te zetten in prestaties.

Ondanks de dungezaaidheid van ontmoetingen tussen 'de pauwpers', koester ik die momenten en hoop ik dat deze nog lang zullen voortduren.

Ook 'groep Vught' staat alweer voor 15 jaar goede vriendschap. Ik hoop dat deze nog lang zal voortduren, al dan niet in combinatie met een epidemische uitbraak van de buikgriep. In de loop der jaren heb ik daarbij een zeer bijzondere vriendschap opgebouwd met Hans, die ik hier dus even speciaal in de 'schijnwerpers' zet.

Albert (PaP) en Willemien (MaM); ondanks dat ik niet altijd in staat was enthousiast te vertellen over de al dan niet gemaakte wetenschappelijk vorderingen, ben ik erg dankbaar voor de onuitputtelijke interesse die jullie altijd toonde en voel ik mij bevoorrecht met jullie als mijn ouders. Net als met Floris (mijn grotere kleine broer), en Marc & Yvette (mijn kleinere grote zus), die een zeer grote indirecte rol hebben gespeeld in de totstandkoming van dit proefschrift. Ten slotte, lieve Petra; ik ben en blijf jouw allergrootste fan. Jouw bijdrage is namelijk niet met een pen te omschrijven.

Jasper, oktober 2009

Curriculum Vitae

Jasper Foolen is geboren op 30 september 1978 in Vught. In 1996 behaalde hij zijn VWO diploma aan het Maurick College in Vught. Aansluitend studeerde hij Werktuigbouwkunde aan de Fontys Hogeschool Eindhoven. Als onderdeel van deze studie liep hij stage in het Robert Jones and Agnes Hunt Orthopaedic Hospital (Engeland) en deed onderzoek naar de belastingconditie in articulaire kraakbeendefecten. Vervolgens studeerde hij Biomedische Technologie aan de Technische Universiteit Eindhoven. Zijn afstudeerwerk richtte zich op het induceren van endochondrale verbening in osteochondrale explants door mechanische belasting. In 2005 is hij begonnen met zijn promotieonderzoek aan de faculteit Biomedische Technologie van de Technische Universiteit Eindhoven in de onderzoeksgroep Orthopaedic Biomechanics, resulterend in dit proefschrift.